CAL/APT PROGRAM: TEST RESULTS FROM ACCELERATED PAVEMENT TEST ON PAVEMENT STRUCTURE CONTAINING UNTREATED AGGREGATE BASE (AB)—SECTION 501RF

Report Prepared for

CALIFORNIA DEPARTMENT OF TRANSPORTATION

by

John T. Harvey, Leonie Louw, Irwin Guada, David Hung, Jorge Prozzi, Fenella Long, Louw du Plessis

April 1999
Pavement Research Center
Institute of Transportation Studies
University of California, Berkeley

Technical Report Documentation Page

1. Report No.	2. Government Accession No.	3. Recipient's Catalog No.
FHWA/CA/PD-99/01		

4. Title and Subtitle	5. Report Date
CAL/APT Program: Test Results from Accelerated Pavement Test on Pavement Structure Containing Untreated Aggregate Base (AB)--Section 501RF	6. Performing Organization Code
7. Authors J. T. Harvey, L. Louw, I. Guada, D.Hung, J. Prozzi, F. Long, L. du Plessis	8. Performing Organization Report No.
9. Performing Organization Name and Address California Department of Transportation New Technology and Research, MS-83 P.O. Box 942873 Sacramento, CA 94273-0001	10. Work Unit No. 11. Contract or Grant No.
12. Sponsoring Agency Name and Address California Department of Transportation Sacramento, CA 95819	13. Type of Report and Period Covered 14. Sponsoring Agency Code

15. Supplementary Notes

This project was performed in cooperation with the U.S. Department of Transportation, Federal Highway Administration.

16. Abstract

This report is the third in a series that describes the results of tests on full-scale pavements at the Richmond Field Station (RFS) which were designed and constructed according to Caltrans procedures. The report contains a summary of the results and interpretation of the Heavy Vehicle Simulator (HVS) tests on the second of four pavement test sections, an asphalt-concrete section containing an untreated aggregate base, designated Section 501RF. The tests were performed as part of Goal 1 of the CAL/APT Strategic Plan.

The objectives of the test were to 1) verify existing Caltrans pavement design methodologies for asphalt treated permeable base (ATPB) pavements and conventional aggregate base pavements with regard to failure under trafficking at moderate temperatures (Goal 1), while preparing a uniform platform on which overlays (Goal 3 of the Strategic Plan) would be constructed and then trafficked; 2) quantify the effective elastic moduli of the various pavement layers, based on an ad-hoc use of layered elastic analysis; 3) quantify the stress dependence of the pavement layers; 4) determine the failure mechanisms of the various layers; and 5) determine and compare the fatigue lives of two types of pavement structure.

17. Key Words	18. Distribution Statement
Accelerated Pavement Testing, asphalt, aggregate base, fatigue, cracking, rutting, permanent deformation	No restrictions. This document is available to the public through the National Technical Information Service, Springfield, VA 22161

19. Security Classif. (of this report)	20. Security Classif. (of this page)	21. No. of Pages	22. Price
Unclassified	Unclassified	168	

Form DOT F 1700.7 (8-72)

DISCLAIMER

The contents of this report reflect the views of the authors who are responsible for the information and the accuracy of the data presented herein. The contents do not necessarily reflect the official views of policies of the California Department of Transportation or the Federal Highway Administration. The report does not constitute a standard, specification, or regulation.

FINANCIAL DISCLOSURE STATEMENT

This research has been funded by the Division of New Technology and Research of the State of California Department of Transportation (contract No. RTA-65W485). The total contract amount for the five year period (1 July 1994 through 30 June 1999) was $5,751,159 at the time this study was performed. The contract was later ammended to extend an additional year to 30 June 2000 with additional funding to a total of $12,804,824. This report presents the results of the second HVS test completed in February 1996 on a pavement section containing untreated aggregate base. The report provides an analysis of the test results and conclusions which contain implications for Caltrans pavement design and pavement construction practices.

IMPLEMENTATION STATEMENT

Results of this HVS test like that on the previously tested section—500RF, demonstrate the importance of mix compaction on pavement performance (both fatigue and permanent

deformation) and that improved pavement performance which results from improved compacting can result in large, quantifiable savings to the State.

As in the first section, 500RF, a weak bond was observed between the asphalt-concrete lifts in the section and was found to significantly degrade pavement performance. The recommendations contained in the first report relative to the use of a tack are confirmed by the results of this test as well.

ACKNOWLEDGMENTS

Financial support for this project was provided by the State of California Department of Transportation as part of the CAL/APT Project. Mr. Wesley Lum of the Division of New Technology and Research is the CAL/APT Project Manager and Mr. William Nokes, Office of Project Planning and Design, is the Contract Monitor for the University of California, Berkeley contact.

TABLE OF CONTENTS

LIST OF FIGURES

LIST OF TABLES

EXECUTIVE SUMMARY

This report is the **third** in a series which describe the results of tests on full-scale pavements constructed an the Richmond Field Station (RFS) which have been designed and constructed according to Caltrans procedures. It contains a summary of the results of their interpretation of the Heavy Vehicle Simulator (HVS) tests on the *second* of *four* pavements test sections, and asphalt-concrete sections containing an untreated aggregate base designated Section 501RF. The tests on the four test sections have been performed as part of Goal 1 of the CAL/APT Strategic Plan *(1)*.

One objective of the test program is to develop data to quantitatively verify existing Caltrans pavement design methodologies for asphalt treated permeable base (ATPB) pavements and conventional aggregate base pavements with regard to failure under trafficking at moderate temperatures (Goal 1), while preparing a uniform platform on which overlays (Goal 3 of the Strategic Plan) will be constructed which also will be trafficked. Other objectives are:

- to quantify the effective elastic moduli of the various pavement layers, based on an ad-hoc use of layered elastic analysis;
- to quantify the stress dependence of the pavement layers;
- to determine the failure mechanisms of the various layers; and
- to determine and compare the fatigue lives of the two types of pavement structure.

HVS loading on this pavement section began in November 1995 and was completed in February 1996 after the application of more than 1.4×10^6 load repetitions. At the end of the

test, cracking had reached a level which, according to Caltrans pavement management criteria, resembled a newer pavement that had failed by alligator cracking.

Chapter 2 describes the test program for Section 501RF. Design thicknesses for the pavement components for a Traffic Index of 9.0 (1.0 million ESALs) are: aggregate subbase—137 mm (0.75 ft); aggregate base—274 mm (0.90 ft); and asphalt concrete—137 mm (0.45 ft). Actual thicknesses at the loading site are: aggregate subbase—215 mm (0.70 ft); aggregate base—274 mm (0.90 ft); and asphalt concrete—150 mm (0.49 ft).

Table 2.1 summarizes the data collection program for Section 501RF. Loading, applied by dual bias-ply tires inflated to a pressure of 690 kPa (100 psi), consisted of 150,000 repetitions of a 40 kN (9,000 lb) load followed by 50,000 repetitions of a 80 kN (18,000 lb) and then by about 1.23 million repetitions of a 100 kN (22,500 lb) load. At the termination of loading, fatigue cracking was visible throughout the test section. Lateral wander of the wheels over the one meter (3.3 ft) width of the section was the same as for Test Section 500RF.

Pavement response measurements were obtained using the Multi-Depth Deflectometers (MDDs), the Road Surface Deflectometer (RSD), the laser prolifometer, and a straight edge. Fatigue crack development was monitored using photographs and analyzed using a digital image analysis procedure. Thermocouples were used to measure the air temperature and pavement temperatures at various depths in the asphalt concrete. To maintain a reasonably consistent temperature of about 20°C, a temperature control cabinet (“cold box”) was installed. Chapter 3 summarizes the data obtained suring the course of loading.

As with Section 500RF, cracking appears to have occurred in only the top lift of the aggregate concrete layer. Moreover, it was observed from a limited coring program that there appeared to be little or no bond between the two lifts used to achieve the constructed thickness

of the aggregate concrete layer. In addition, measurements indicate that the lower asphalt concrete lift was compacted to an average air void content of 5.6 percent while the upper lift was not well compacted, i.e. to an average air void content of about 7.2 percent.

The 1.43 million repetitions actually applied to Test Section 501RF corresponds to about 60 million ESALs (based on the Caltrans load equivalency factor of 4.2). Chapter 3 provides a detailed analysis of the test results using multilayered elastic analysis to explain the observed behavior.

Results of the analysis reported in Chapter 4 indicate a reasonable correspondence between the Caltrans design estimate of approximately 1,000,000 ESALs and the HVS test measurement of approximately 60,000,000 ESALs. The major impediment to reconciling these two estimates seems to be the inability to accurately quantify effects of the layer interface condition. The following findings of this aspect of the study are considered to have been reasonably well demonstrated and to represent appropriate hypotheses for future inquiry and validation:

1. Fatigue life measurements under full-scale accelerated loading are typically expected to exceed design estimates because design estimates must incorporate a safety factor to minimize the risk of premature failure while accommodating, at the same time, expected variability in testing, in construction, in traffic, and in mix design. For a design reliability level of 90 percent, the computed ration of simulated HVS ESALs to design ESALs estimated using the fatigue analysis and design system was approximately 3.7.

2. The mix fatigue analysis and design system proved to be an effective tool for explaining fatigue performance of the HVS pavement. The relatively good agreement between

the simulation estimate and actual HVS measurement suggests that the analysis and design system may eventually prove more useful for structural design as well as for mix design.

3. According to Asphalt Institute's subgrade strain criterion, severe subgrade rutting in the HVS pavement would not be expected. Testing of HVS Section 501RF generally confirmed this.

4. The analysis reported herein corroborates prior work showing the importance of good compaction of the asphalt concrete surface to superior fatigue performance. Good compaction of the mix also reduces the magnitude of subgrade rutting.

5. Loss of bonding at the interface between asphalt-concrete lifts can cause a significant degradation in fatigue life and an increase in subgrade rutting.

6. Different mixes, even with similar binders, can result in significantly different fatigue performance. The importance and effectiveness of laboratory fatigue testing and simulation to quantitatively estimate differences in fatigue performance in situ was demonstrated by analyses presented in this chaper.

Chapter 5 contains the conclusions which are as follows:

1. The fatigue analysis and design system developed during the SHRP program and refined within the CAL/APT program has been used to explain the different between the design estimate for Section 501RF of approximately one million ESALs and the HVS measurement of approximately 60 million ESALs. Although some of the discrepancy remains unaccounted for (possibly as a result of difficulties in modeling the bonding between the two lifts of asphalt concrete), the overall agreement helps to validate both the analysis and design system as a mechanism for structural design and the current Caltrans design mehtodology.

2. As with Section 500RF, results of this HVS test suggest that the Asphalt Institute's subgrade strain criterion for controlling subgrade rutting would be a reasonable design parameter. Accordingly, this criterion is suitable for use in mechanistic/empirical analyses of subgrade rutting to supplement routine Caltrans design procedures in special investigations.

3. Results of the 501RF test suggest that the Caltrans structural design procedure may not be sufficiently conservative for pavements with aggregate base, typical compaction, and certain asphalt concrete mixes. The analysis and design system used herein and being refined, in part, through the CAL/APT program, should provide an improved methodology for structural pavement design permitting.

4. The recommendations regarding mix compaction and tack coat application resulting from the 500RF test are supported by the results on test 501RF.

CHAPTER 1

INTRODUCTION

This report is the third in a series of reports which describe the results of accelerated pavement testing with the Heavy Vehicle Simulator (HVS) on full-scale pavements designed and constructed according to Caltrans's procedures at the Richmond Field Station (RFS). It contains a summary of the results of HVS tests and their interpretation on the second of four pavement test sections: an asphalt-concrete section containing a conventional aggregate base designated Section 501RF. The HVS tests on the four test sections are being performed as part of Goal 1 of the CAL/APT Strategic Plan *(1)*.

The first report in this series, entitled *Initial CAL/APT Program: Site Information, Test Pavements Construction, Pavement Materials Characterizations, Initial CAL/HVS Test Results, and Performance Estimates* contains detailed information on the construction of the test pavements, as well as results of tests to define the properties of the various pavement components of the four pavement test sections *(2)*. The second report in this series entitled: *CAL/APT Program: Test Results from Accelerated Pavement Test on Pavement Structure Containing Asphalt-Treated Permeable Base (ATPB) — Section 500RF* contains detailed information on the HVS test of the ATPB Section 500RF *(3)*. [1]

The information and findings presented herein support the recommendations regarding changes in Caltrans construction and construction control procedures presented in Reference *(3)*.

---

[1]A separate report describing the performance of ATPB under saturated conditions in laboratory repeated load tests; performance estimates of pavements containing saturated ATPB through simulation; and a review of Caltrans experience ATPB has also been prepared *(4)*.

1.1 OBJECTIVES

The main objective of this test plan, described in Reference *(2)*, is to develop data to quantitatively verify existing design methodologies for asphalt treated permeable base (ATPB) pavements and conventional aggregate base pavements with regard to failure under trafficking at moderate temperatures. The other objectives are:

- to quantify the effective elastic moduli of the various pavement layers, based on an ad-hoc use of layered elastic analysis;
- to quantify the stress dependence of the pavement layers;
- to determine the failure mechanisms of the various layers; and
- to determine and compare the fatigue lives of the two types of pavement structure.

This report together with the reports on each of the four sections, associated special reports, and a final report will complete this test plan objective and the work included in Goal 1 of the CAL/APT Strategic Plan.

1.2 PURPOSE AND SCOPE

The scheduled sequence of HVS testing of the four test sections has been: 1) drained ATPB site (500RF); 2) undrained aggregate base site (501RF); 3) drained ATPB site (502CT); and 4) undrained aggregate base site (503RF). This report presents the results of tests on Section 501RF.

1.3 ORGANIZATION OF REPORT

Chapter 2 of the report contains a complete description of the test program performed on Section 501RF, including the loading sequence, instrumentation, and data collection scheme. Chapter 3 presents a summary and discussion of the data collected during the test, including pavement performance and temperatures. Chapter 4 compares the actual pavement performance with the fatigue life predicted for the test section using the Caltrans thickness design procedure. Analyses are presented which evaluate how the fatigue life was affected by construction variables, mix characteristics and temperature environment and permit extrapolation of the HVS test results to Caltrans in-service pavements. The HVS results are shown to validate the analyses. Chapter 5 contains a summary of the results and conclusions drawn from them.

CHAPTER 2

TEST PROGRAM

2.1 TEST SECTION LAYOUT

Test site 501RF is one of the undrained sections built for Goal 1 of the HVS test program. This section is one of two, containing one conventional aggregate base. The locations of the four Goal 1 test sections are shown in Figure 2.1. Details of the layout of the other undrained section (503RF) and the two drained sections (500RF and 502CT) are included in the Goal 1 Interim Report *(2)* and the report on Section 500RF *(3)*.

The pavement structure (Figure 2.2) was designed according to Caltrans procedures *(5)* and consists of a clay subgrade (classified by the AASHTO method as an A-7-6), aggregate subbase, aggregate base, and asphalt concrete. A summary of the construction control data for this section is contained in Reference *(2)*.

The design thicknesses of the pavement components are: aggregate subbase, 229 mm, aggregate base, 274 mm; and asphalt concrete, 137 mm. The as-built thickness of the aggregate subbase varies transversely because of a 2 percent slope transverse in the aggregate subbase layer *(2)*. Estimated as-built thicknesses of the pavement layer are: aggregate subbase, 215 mm; aggregate base, 274 mm; asphalt concrete, 150 mm. Exact layer thicknesses of each of the HVS test sections will be determined from direct measurement of cores and in test pits after the completion of Goal 3 overlay testing *(6)*. Construction measurements and data from several cores immediately adjacent to 501RF suggest that the aggregate base thickness does not vary more than about 15 mm from the design thickness.

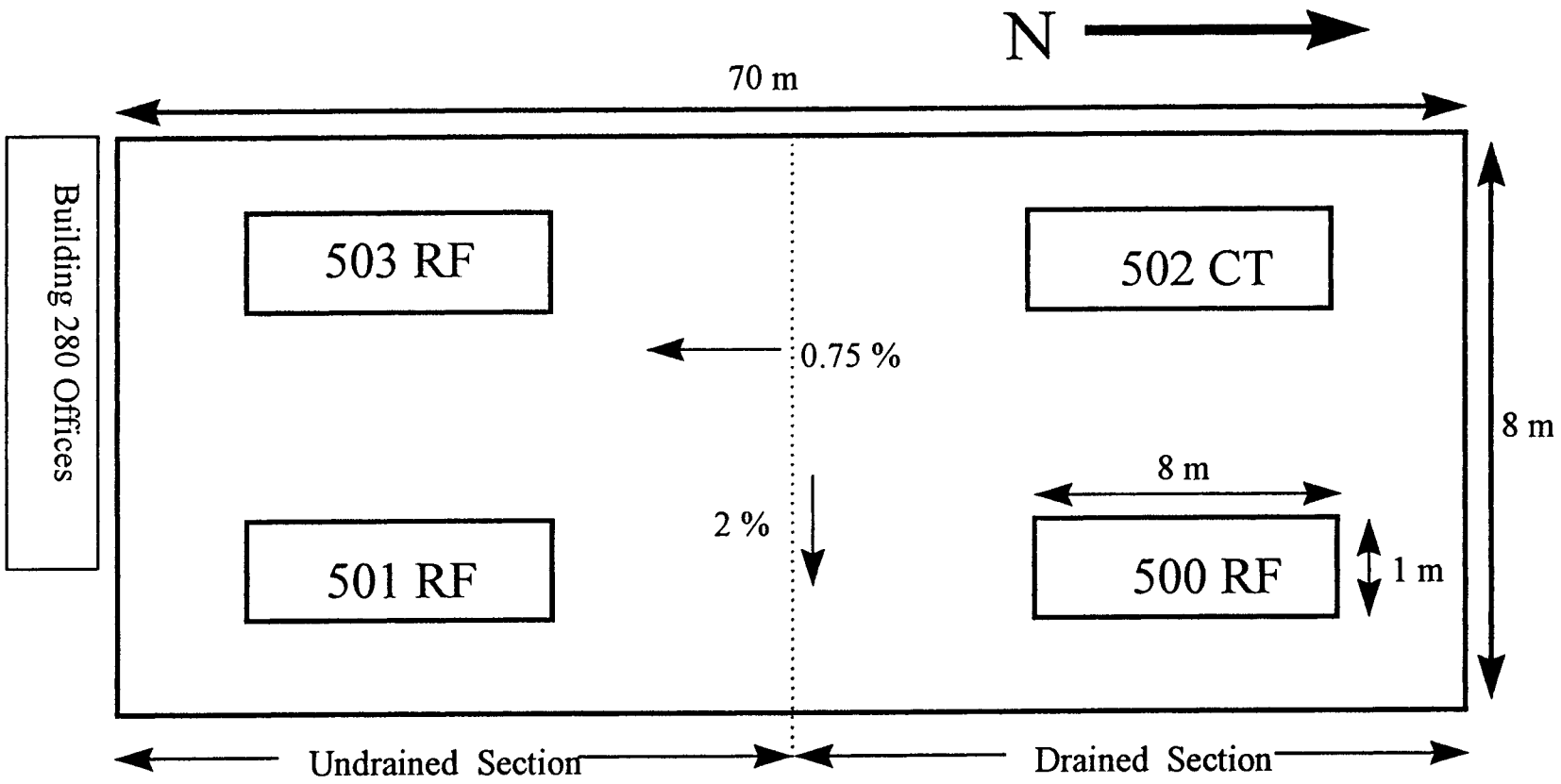

Figure 2.1 Test pavement at Richmond Field Station with test sections

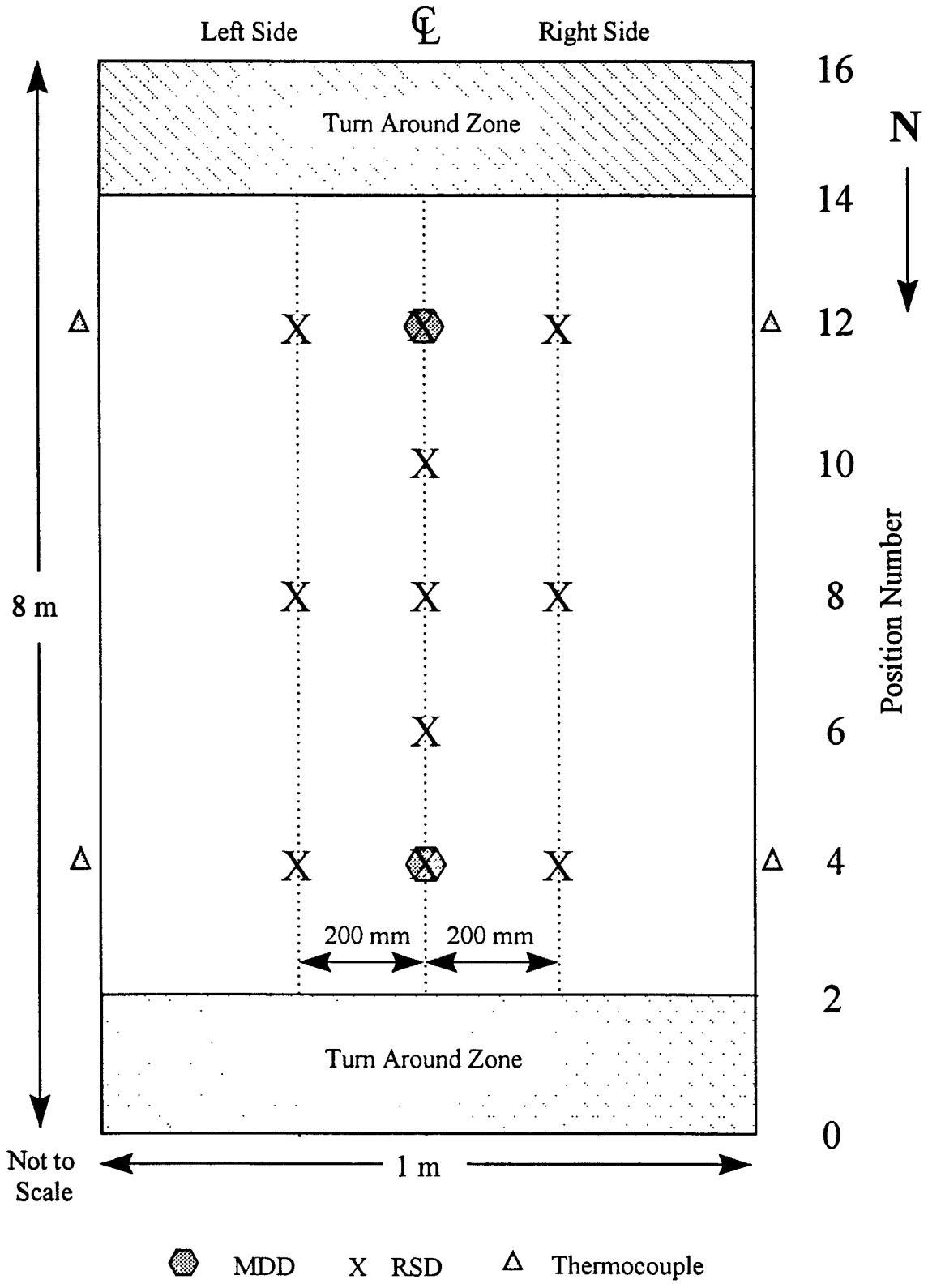

Figure 2.2 Plan view of test section and location of instruments for data collection

2.2 TEST PROGRAM

2.2.1 Loading Program

HVS loading on Section 501RF began in November 1995 and was completed in February 1996 after the application of more than 1.43×10^6 load repetitions. At the end of the test, cracking had reached a level which, according to Caltrans pavement management criteria, resembled a newer pavement that had failed by alligator cracking. The HVS test program for Section 501RF, including the loading and data collection schedules, is summarized in Table 2.1. The loading applied to Section 501RF is similar to that applied to Section 500RF as described in Reference *(3)*. As shown in Table 2.1, a load of 40 kN was used to traffic the section for the first 150,000 repetitions. After 150,000 repetitions, the load was increased to 80 kN for 50,000 repetitions. At 200,000 repetitions the trafficking load was increased to 100 kN and was maintained at this level for the remainder of the test to accelerate pavement cracking.

The gradual increase in loading is intended to permit densification of the asphalt concrete under loads it was designed to carry and to reduce the chance of early and excessive rutting under the 100 kN wheel loads. The HVS was equipped with dual bias-ply truck tires inflated to a pressure of 690 kPa. Lateral wander over the 1 m width of the test section is programmed to simulate traffic wander on a typical highway lane [3.7 m wide][2].

---

[2] Reference *3* contains a discussion of the lateral load distribution (wander) used in this test.

Table 2.1 Data collection program for Test Section 501RF

Repetitions	Trafficking Load kN	Rut Profiles	MDD				RSD											
							Centerline				200 mm Left[1]				200 mm Right[1]			
			Test Wheel Load, kN				Test Wheel Load, kN				Test Wheel Load, kN				Test Wheel Load, kN			
			40	60	80	100	40	60	80	100	40	60	80	100	40	60	80	100
10	40	X	X				X				X				X			
10,000 to 50,000 (10,000 incr)	40	X	X				X				X				X			
100,000	40	X	X				X				X				X			
125,000	40	X	X				X				X				X			
150,000	40 to 80	X	X	X	X		X		X		X		X		X		X	
175,000	80	X	X		X		X		X		X		X		X		X	
200,000	80 to 100	X	X	X	X	X	X		X	X	X		X	X	X		X	X
225,000	100	X	X			X	X			X								
250,000	100	X	X			X	X			X								
300,000 to 800,000 (50,000 incr)	100	X	X			X	X			X	X			X	X			X
Crack Appearance (540,215)	100	X	X		X	X	X		X	X	X		X	X	X		X	X
800,000 to final (50,000 incr)	100	X	X			X	X			X								
800,000 to final (100,000 incr)	100	X	X			X												
850,000 to final (100,000 incr)	100	X	X			X	X			X								
Final (1,426,467)	100	X	X	X	X	X	X	X	X	X	X	X	X	X	X	X	X	X

[1]Looking in direction of increasing longitudinal reference points (0-16)

2.2.2 Measurements

To evaluate pavement response during HVS testing of Section 501RF, measurements were obtained using:

- Multi-Depth Deflectometer (MDD);
- Road Surface Deflectometer (RSD);
- Laser Profilometer; and
- Straight edge.

Fatigue crack development was monitored visually and recorded using photographs. Thermocouples were used to measure the air temperature and pavement temperatures at various depths in the asphalt concrete. Detailed descriptions of the instrumentation and the various measuring equipment are included in References *(2)* and *(7)*.

RSD surface deflection data were obtained at the reference points, as shown in Figure 2.2, along the centerline of the section and at locations 200 mm on each side of the centerline. The latter measurements are taken slightly off the centerline where the wander pattern results in fewer load applications and assist in characterizing the effects of the traffic loading pattern on pavement performance across the entire test section. Measurements of transverse surface rut depth using the laser profilometer permit determination of:

- the location and magnitude of the maximum rut;
- the average rut which occurred throughout the test section, and
- the rate of permanent deformation, or rut rate.

Permanent deformation occurring at various depths in the different layers during the course of loading are measured using the MDDs. The MDDs are installed at two locations, as

shown in Figure 2.2. The surface deflection measured using the MDD at Station 4 of the test section provides a check on the RSD deflection measured at the same location.

All pavement temperature measurements using the thermocouples, at the locations shown in Figures 2.2 and 2.3, were obtained at one-hour intervals during HVS loading. Air temperatures near the test section were recorded at the same times.

Visual observation of surface distress was primarily directed to the identification of surface cracks and crack length measurement. It should be noted that at the conclusion of testing of the overlaid Section 501RF, a trench will be dug to allow visual inspection and measurement of all the layers.

Depths at which the Multi-Depth Deflectometers (MDDs) and thermocouples were placed are shown in Figure 2.3, while their locations on the surface of the test section are shown in Figure 2.2. Positions at which deflections were measured using the Road Surface Deflectometer (RSD) are also shown in Figure 2.2. Intervals between measurements (Table 2.1), in terms of load repetitions, were selected to insure adequate characterization of the pavement as damage developed.

2.3 ENVIRONMENTAL CONDITIONS

Temperature has an important influence on the fatigue performance of a pavement. Laboratory tests and pavement simulations have indicated that maximum fatigue damage per load repetition typically occurs at temperatures between 25°C and 35°C depending on pavement structure and binder source. However, rutting of the asphalt concrete layer increases with increased temperature, and fatigue cracking was the focus of the HVS test, not rutting.

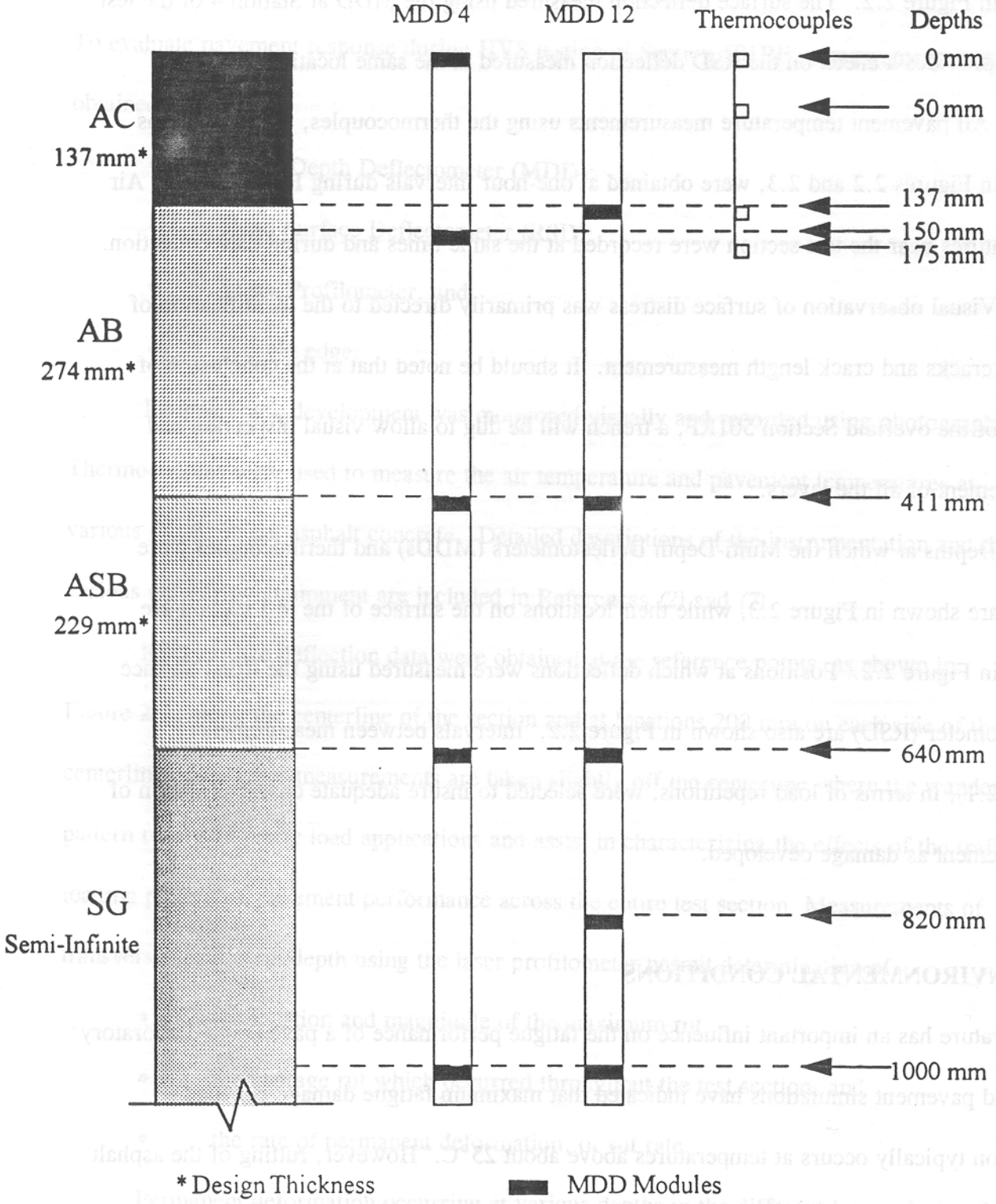

Figure 2.3 501RF pavement structure with MDD and thermocouple positioning

Accordingly, the test plan stipulated that the pavement surface temperature not exceed about 24°C to minimize rutting in the AC, and not drop below about 16°C in order accelerate damage from load repetitions. To maintain a fairly constant temperature, a temperature control cabin, or "cold box," was installed on the HVS.

Except for the lack of direct rainfall on the surface (the test sections are located within Building 280), the pavement test sections at the RFS are subjected to water conditions much like actual roads. Water can accumulate underneath the pavement due to lateral movement of water from outside the building and fluctuations in the ground water table. Initially, during the rainy season of 1994-95 and before construction of the first test pavements, large quantities of water entered the aggregate subbase from surface runoff outside the building housing the test sections. The subbase was subsequently allowed to dry before construction. To eliminate this problem, a drainage system was installed around the perimeter of the building to capture surface runoff outside the building. Additionally, a standard Caltrans drainage system had been built into the test pavements as described in Reference *(2)*. Outflow from the system has not been observed because of the lack of surface water and a depth of the water table at about 4 m.

CHAPTER 3

DATA SUMMARY: TEMPERATURES, PERMANENT DEFORMATIONS, ELASTIC DEFLECTIONS, CRACKING

This chapter provides a summary of the data obtained as well as a brief discussion of the results. Interpretation of the data in terms of pavement performance is discussed in Chapter 4.

3.1 TEMPERATURES

Pavement temperatures in Section 501RF were better controlled than during testing of Section 500RF. The improved temperature control was possible due to the installation of the "cold box" shown in Figure 3.1. The target air temperature inside the temperature control box for both sections was 20°C ± 4°C. The air temperature during testing of Section 501RF was mostly at the lower end of this range.

In addition to air temperatures, pavement temperatures were monitored and recorded regularly for the entire test duration on Section 501RF. Temperature was monitored at several locations around the test section and at several depths in the pavement as noted in Chapter 2. Temperature measurements at various depths and locations is important for analyzing the performance of the HVS test sections and translating results to field conditions. For evaluation of fatigue cracking, temperature at the bottom of the asphalt concrete (in this case about 150 mm below the pavement surface) and temperature gradient are the controlling temperature parameters *(8,9)*.

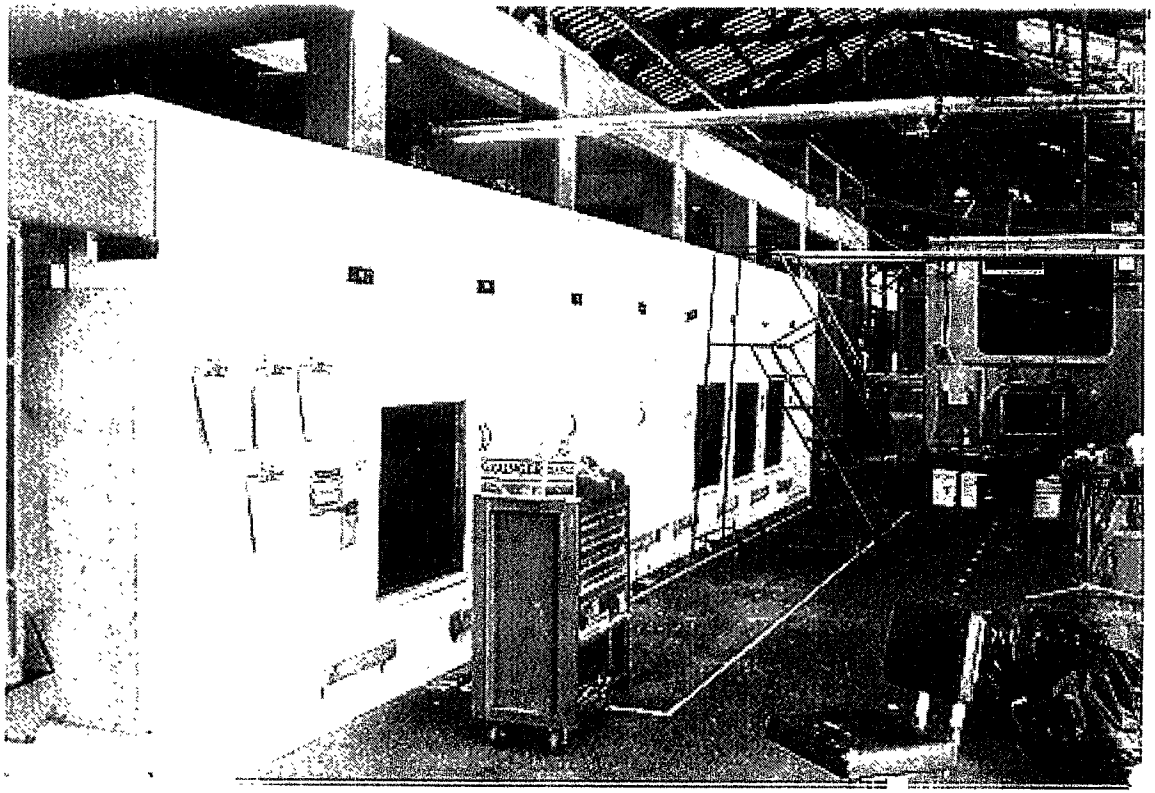

Figure 3.1 HVS with cold box and chiller

3.1.1 Air Temperature Outside Temperature Control Box

The average daily air temperatures inside the building and outside the temperature control box throughout the test are summarized in Figure 3.2. The daily averages were calculated from the hourly temperatures taken during HVS operation. It will be noted that the average ambient temperature varied from 12°C to 20°C.

Air temperature data from within the temperature control box were divided into four 6-hour periods with relatively uniform temperatures to illustrate the ability of the system to control temperature. Temperatures collected at the end of each hour, 0100 to 0600, were averaged. Similarly, temperatures from the other periods, 0700 to 1200, 1300 to 1800, and 1900 to 2400 hours, were averaged the same way. Average air temperatures for each of the periods for the duration of the entire test are summarized in Table 3.1. The lowest ambient temperatures occurred during 0100 hours to 0600 hours (15°C average) and the highest during 1300 hours to 1800 hours (18°C average). The average air temperatures during test 501RF are significantly lower than those which occurred during test 500RF.

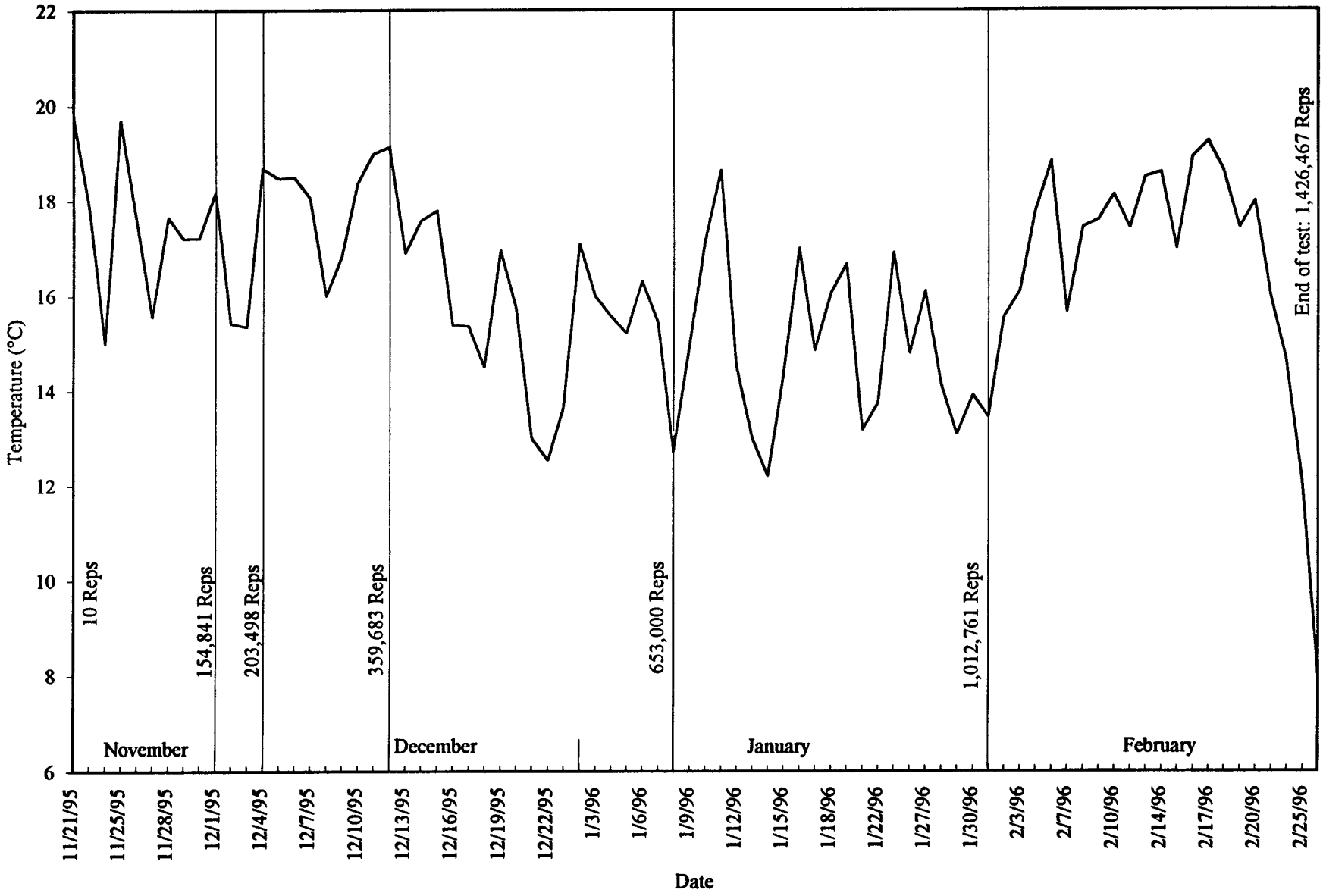

Figure 3.2 Daily average air temperature for the entire testing period of Section 501RF

Table 3.1 Average temperature (°C) over 6-hour periods for air outside box, surface, and in-depth levels

TIME PERIOD	Air Temp outside box (°C)		Pavement Surface Temp inside box (°C)		In-depth temperatures (°C)					
					50 mm		137 mm		175 mm	
	Avg	Std	Avg	Std	Avg	Std	Avg	Std	Avg	Std
0100-0600	15	2.3	18.6	1.3	18.8	1.2	19	1.1	19.1	1.1
0700-1200	16.5	2.5	18.1	1.6	17.9	1.7	18.1	1.7	18.1	1.8
1300-1800	18.1	2.5	19.6	1.3	19.6	1.2	19.4	1.2	19.6	1.2
1900-2400	16.2	2.3	19.2	1.2	19.4	1.2	19.5	1.1	19.5	1.1
Maximum* Difference	3.1		1.5		1.7		1.4		1.5	

*difference between minimum and maximum 6-hour interval averages

The "Maximum Difference" data in Table 3.1 show that pavement temperatures did not fluctuate as much as air temperatures throughout each day. The maximum variation in the pavement was only 1.7°C at a depth of 50 mm while the air temperature experienced a larger maximum variation of 3.1°C. The morning periods (0100 hours to 1200 hours) experienced somewhat lower temperatures than did the afternoon periods (1300 hours to 1800 hours). Table 3.1 also shows that the cycle of variation in pavement temperatures lagged behind the air temperature. Air temperatures start to increase after the early morning hours (0100-0600 hours), while pavement temperatures continue to decrease during that same period. This trend is similar to the situation experienced during test 500RF.

Average temperatures in the pavement at depths of 50 mm, 137 mm, and 175 mm are higher than at the surface and are close to 20°C.

3.1.2 Surface Temperature

Daily averages of surface temperature are shown in Figure 3.3. These temperatures have a less pronounced warming and cooling trend than the daily average air temperatures, and the surface temperatures were greater on average than were air temperatures.

Table 3.2 presents the average temperatures for four periods during the test. It can be seen that regardless of the trend in temperature, the average temperature at the surface of the pavement is higher than the average air temperature.

Table 3.2 Average daily temperature

Dates and Repetitions	**11/21–12/12/95** 10 to 359,683	**12/13/95–1/8/96** 359,683 to 653,000	**1/9–1/31/96** 653,000 to 1,012,761	**2/1–2/20/96** 1,012,761 to 1,426,467
Level	**Avg Temp (°C)**			
Air inside box	17.6	15.43	14.93	16.75
Surface	18.91	18.43	19.07	19.56
50 mm	18.95	18.53	19.7	19.89
137 mm	18.99	18.83	19.42	20.13
175 mm	18.98	18.71	19.45	20.11

3.1.3 50 mm Depth

The temperature occurring in the pavement at 50 mm depth is used to evaluate rutting in the asphalt concrete, as this is the approximate location of maximum shear stresses *(10)*. Figure 3.3 and Tables 3.1 and 3.2 show that the daily average temperature for the 50 mm depth is similar to that of the daily average surface temperature. The variation among the 6-hour intervals is much like the surface temperature data, as summarized in Table 3.1.

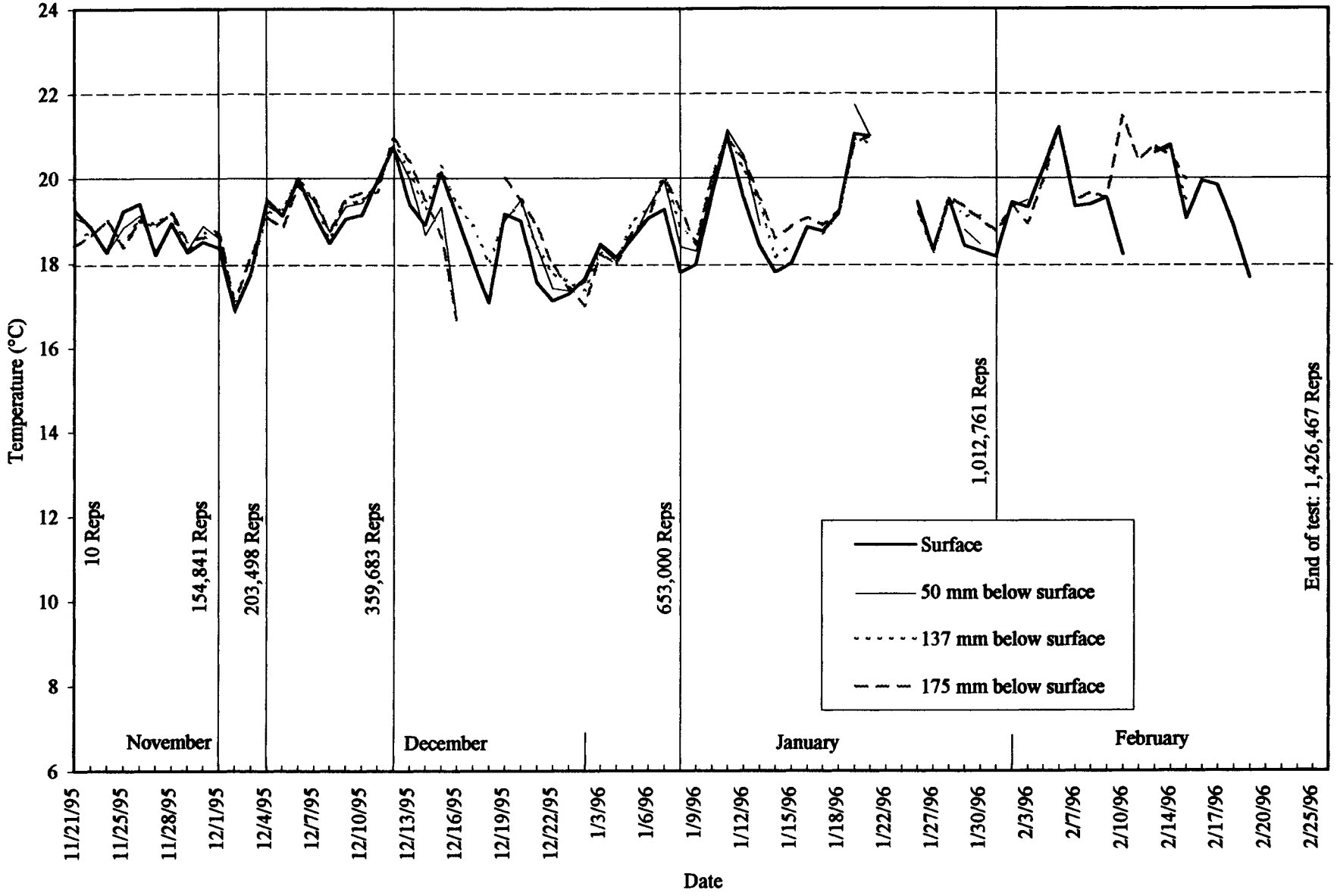

Figure 3.3 Daily average temperature at surface, 50 mm, 137 mm, and 175 mm below surface for the entire testing period

3.1.4 137 mm Depth

Temperatures 137 mm below the surface are important for fatigue cracking since this is near the bottom of the asphalt concrete where maximum tensile strains typically occur. Average temperatures 137 mm below the surface divided into 6-hours intervals are more uniform throughout the day than at shallower depths (Table 3.1).

3.1.5 175 mm Depth

Temperatures 175 mm below the pavement surface, located in the aggregate base are shown in Tables 3.1 and 3.2.

3.1.6 Gradients

Temperature gradients (°C per mm) within the asphalt layer are illustrated in Figures 3.4a-d. The figures show that the temperature gradients are small over the four periods of test 501RF.

3.1.7 Comparison with Section 500RF

A comparison of the pavement temperatures at depths of 50 mm (important for rutting in the asphalt concrete) and 137 mm (important for fatigue cracking) in Sections 500RF and 501RF is shown in Table 3.3:

Table 3.3 Comparison of in-depth pavement temperatures (daily average)

DEPTH	SECTION 500RF	SECTION 501RF
50 mm	24.8	18.9
137 mm	24.9	19.0

From Table 3.3 it can be concluded that the likelihood of fatigue cracking is greater in Section 500RF than in Section 501RF due to the higher pavement temperatures, which are closer to the

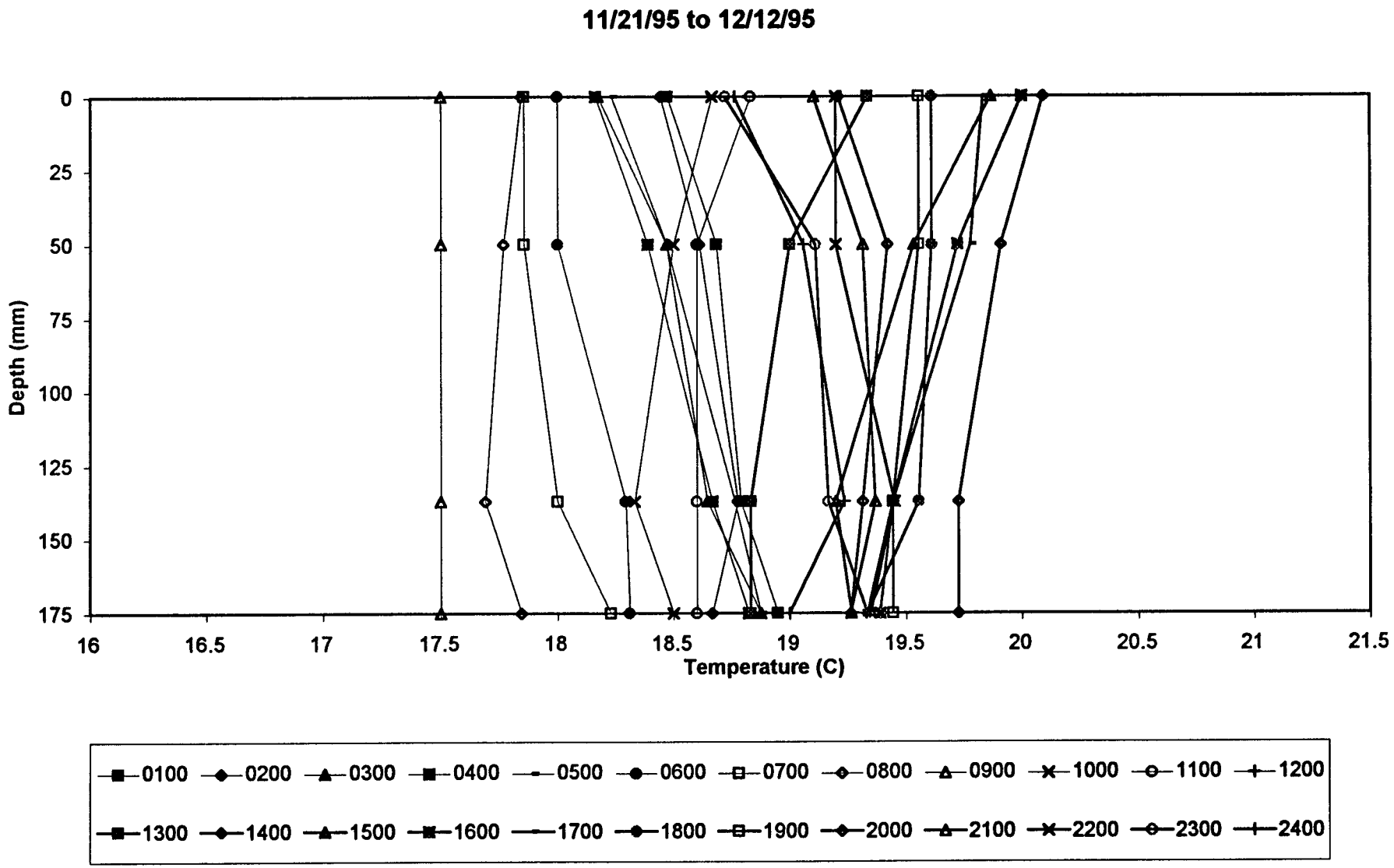

Figure 3.4a Temperature gradient from November 21 to December 12, 1995

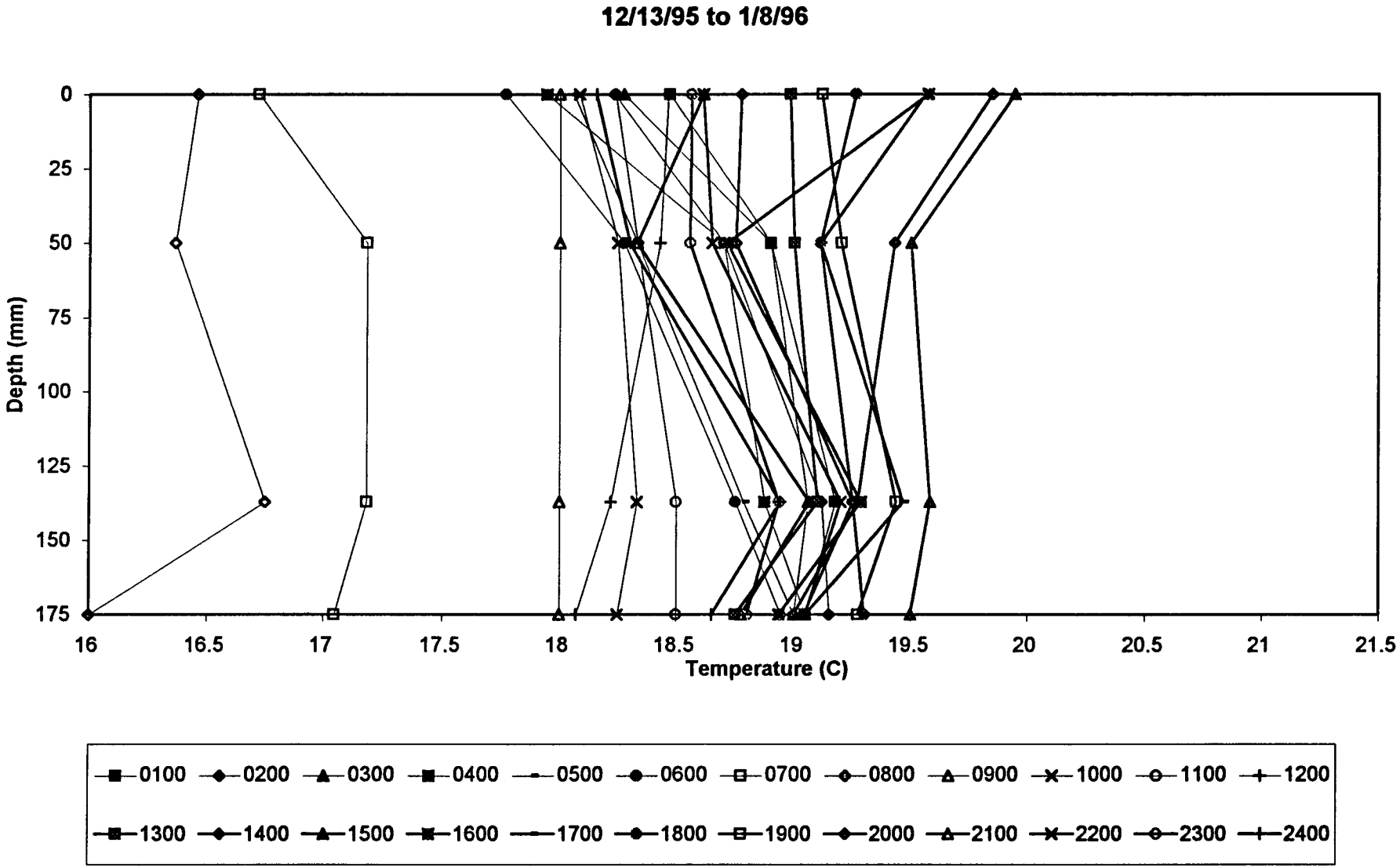

Figure 3.4b Temperature gradient from December 13, 1995 to January 8, 1996

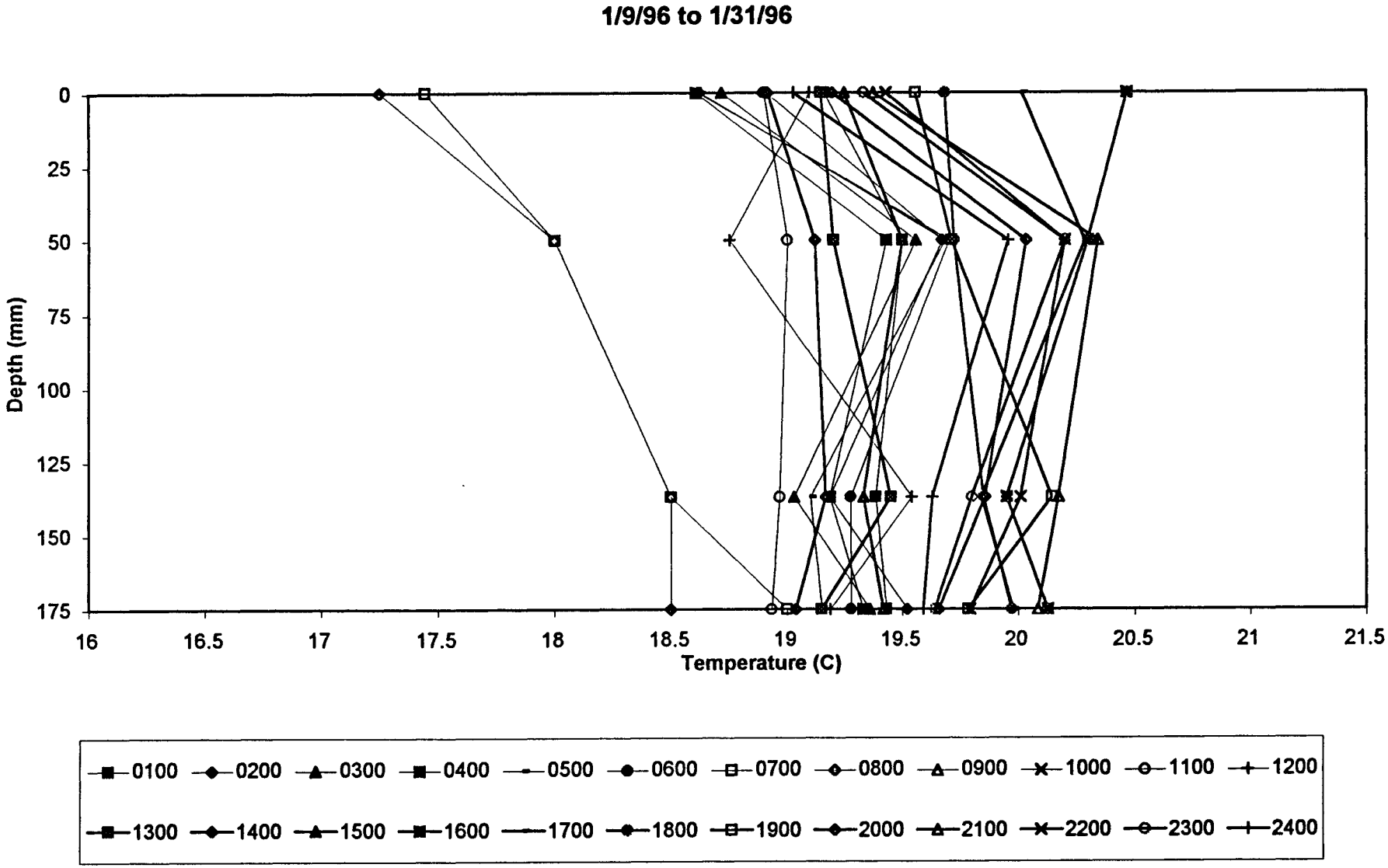

Figure 3.4c Temperature gradient from January 9 to January 31, 1996

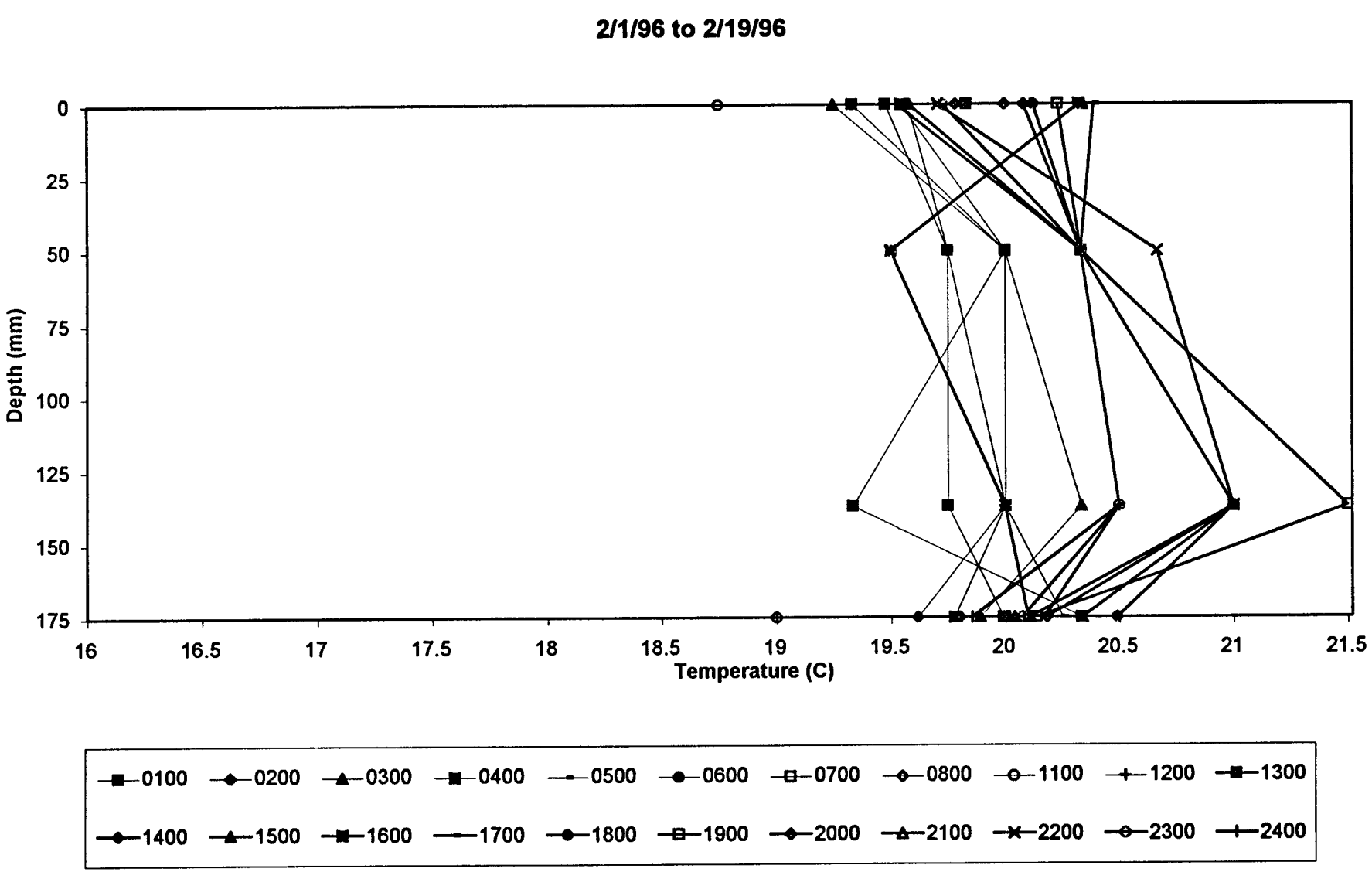

Figure 3.4d Temperature gradient from February 1 to February 19, 1996

critical range (greater than 25°C to 35°C) as explained in reference *(3, 8)*. However, the temperature in Section 500RF will not only increase the likelihood of traffic-associated cracking, but also increase the likelihood of permanent deformation in the asphalt bound layers as well. The different temperature regimes in the two tests result from the different periods during the year (winter versus summer) and temperature control (control box versus no control box) when the two tests were conducted.

3.2 RAINFALL AND WATER CONTENTS OF UNTREATED MATERIALS

During the trafficking of Section 501RF, in the period of 21 November 1995 to 20 February 1996 the average rainfall was about 190 mm per month. While the average rainfall during the period of testing for Section 500RF, 3 May 1995 to 9 November 1995, was approximately 7 mm per month.

Figure 3.5 shows the monthly rainfall from July 1994 to April 1996 as recorded by the National Weather Service in Richmond, California (near the Richmond Field Station). Large amounts of rain fell during the period from November 1994 through March 1995 prior to construction of the test sections. Construction of the test sections started at the end of March 1995, when little or no rain fell, and finished near the end of April 1995. Section 501RF then had seven months of relatively dry weather while Section 500RF was tested. However, no tests were done to measure in-situ moisture contents of the untreated materials to determine differences during testing of Sections 501RF and 500RF.

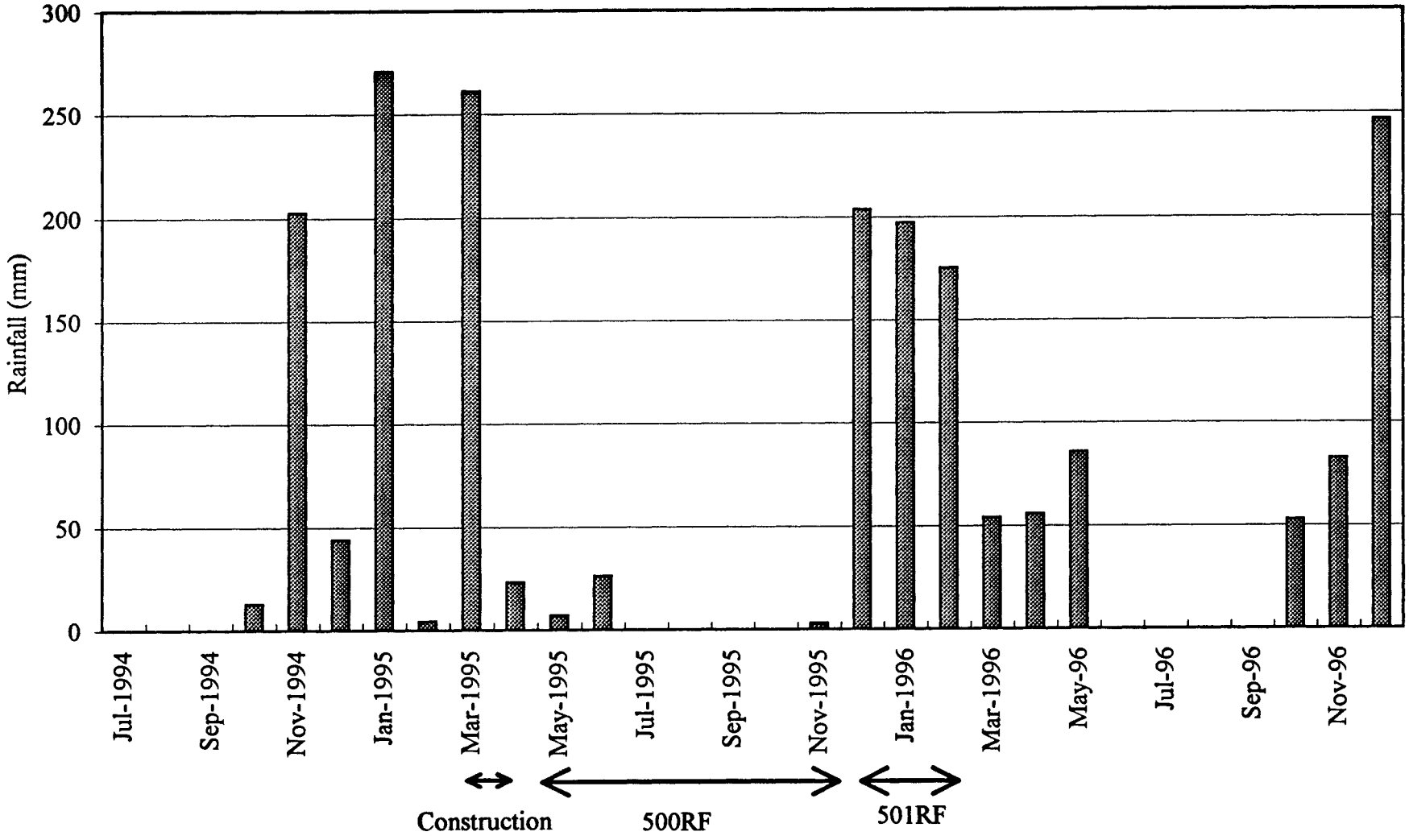

Figure 3.5 Monthly rainfall data in Richmond from the National Weather Service

Water contents of the unbound materials were measured after construction of the Goal 1 test sections and again prior to the construction of the overlays in February 1997 as indicated in Table 3.4. Both groups of samples were taken at the end of the winter, which is the same period when Section 501RF was tested, and the moisture contents at the completion of testing Section 501RF were expected to be in the same range. Because no water contents were measured during the testing of Section 500RF, the role of moisture in the relative performance of the two sections cannot be determined. It is interesting to note, however, that the data presented in Table 3.4 indicate a reduction in the range of water contents in the untreated materials from March 1995 to February 1997.

Table 3.4 Water contents

LOCATION	IN-SITU WATER CONTENT	
	March / April 1995[a]	**February 1997[b]**
aggregate base	4.2 - 6.0 %	4.6 - 4.9 %
aggregate subbase	4.0 - 7.9 %	5.3 - 6.0 %
subgrade	13.6 - 23.9 %	14.4 - 16.3 %

[a]moisture tests conducted on twelve samples per layer
[b]moisture tests conducted on four samples per layer

3.3 PERMANENT DEFORMATION

Permanent deformation of the pavement was monitored with a laser profilometer to determine changes in the surface profile, and with multidepth deflectometers (MDDs) at two locations to determine the permanent deformation at the surface and at various depths within the pavement. Judicial placement of the LVDTs in the MDDs permit determination of permanent deformation

within each of the pavement layers as well. The following two sections discuss the surface and in-depth permanent deformation determinations.

3.3.1 Permanent Deformation at the Surface

Figure 3.6 shows the development of permanent deformation on the pavement surface versus number of load repetitions as determined with the laser profilometer. Transverse surface profile measurements are taken at each longitudinal station (every half meter). From these measurements the following response characteristics were determined and are plotted in Figure 3.6:

- average rut at each station averaged across the entire transverse profile;
- average rut (excluding the transverse profiles at the two stations where MDD top caps are located); and
- average maximum rut, the average across all stations of the maximum rut from each transverse profile.

The laser profilometer measurements permit the development of a three dimensional representation of rutting with successive land applications. Figures 3.7 through 3.11 depict the change in the pavement surface at specific numbers of load repetitions (i.e. 50,000; 150,000; 200,000; 550,000; 1,430,000).

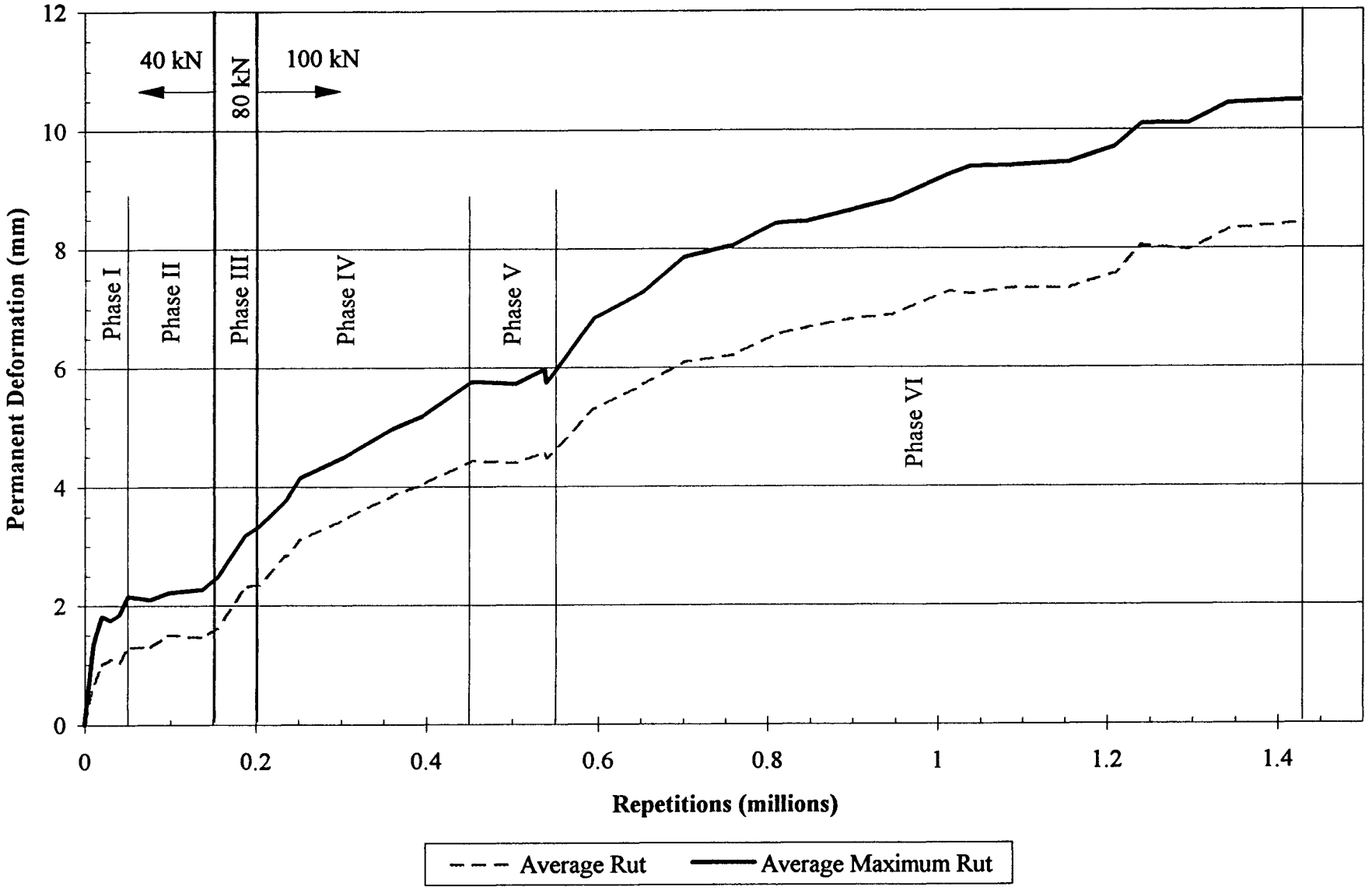

Figure 3.6 Permanent deformation from laser profilometer

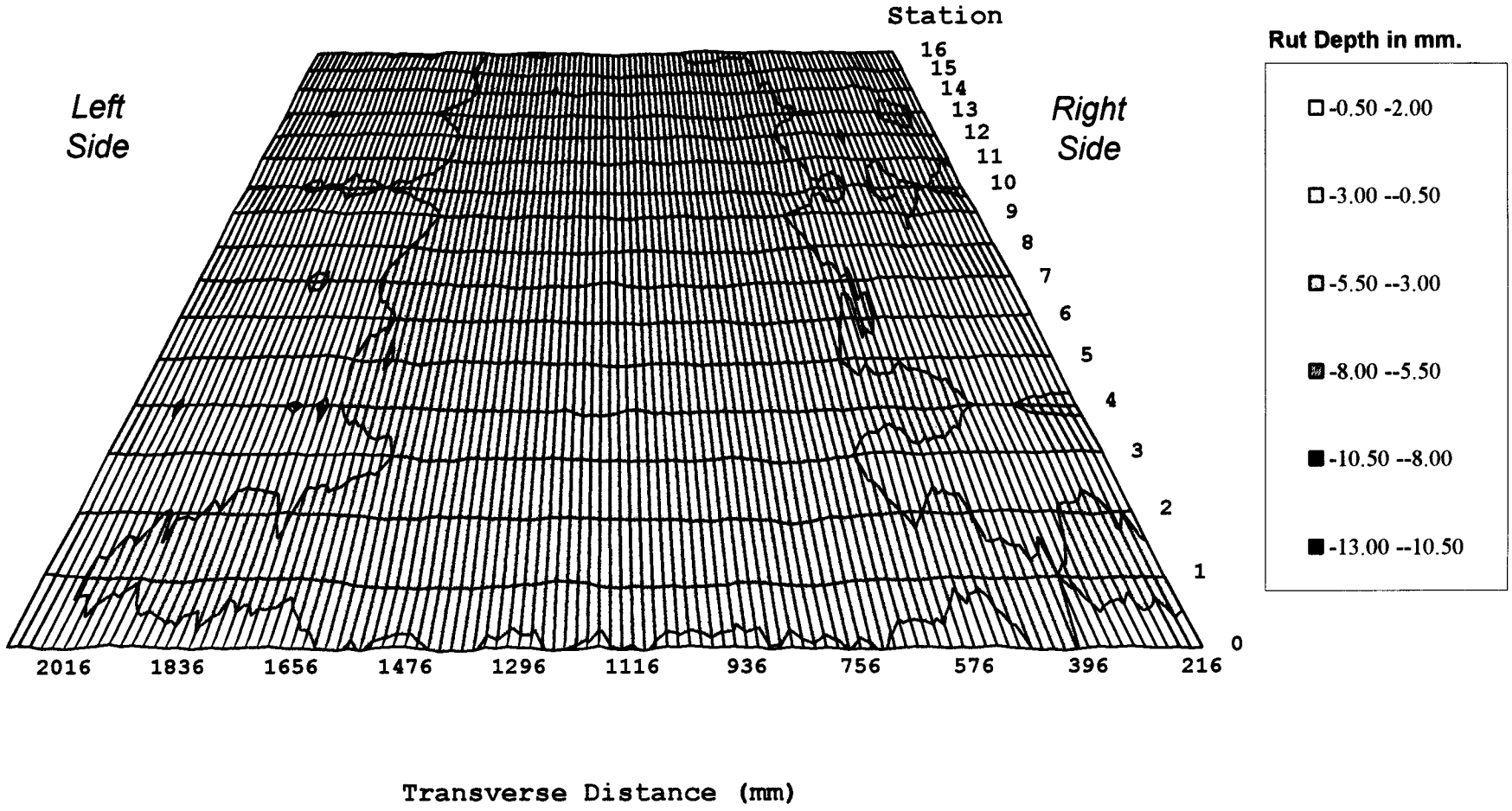

Figure 3.7 Deformed test section surface at 50,000 repetitions

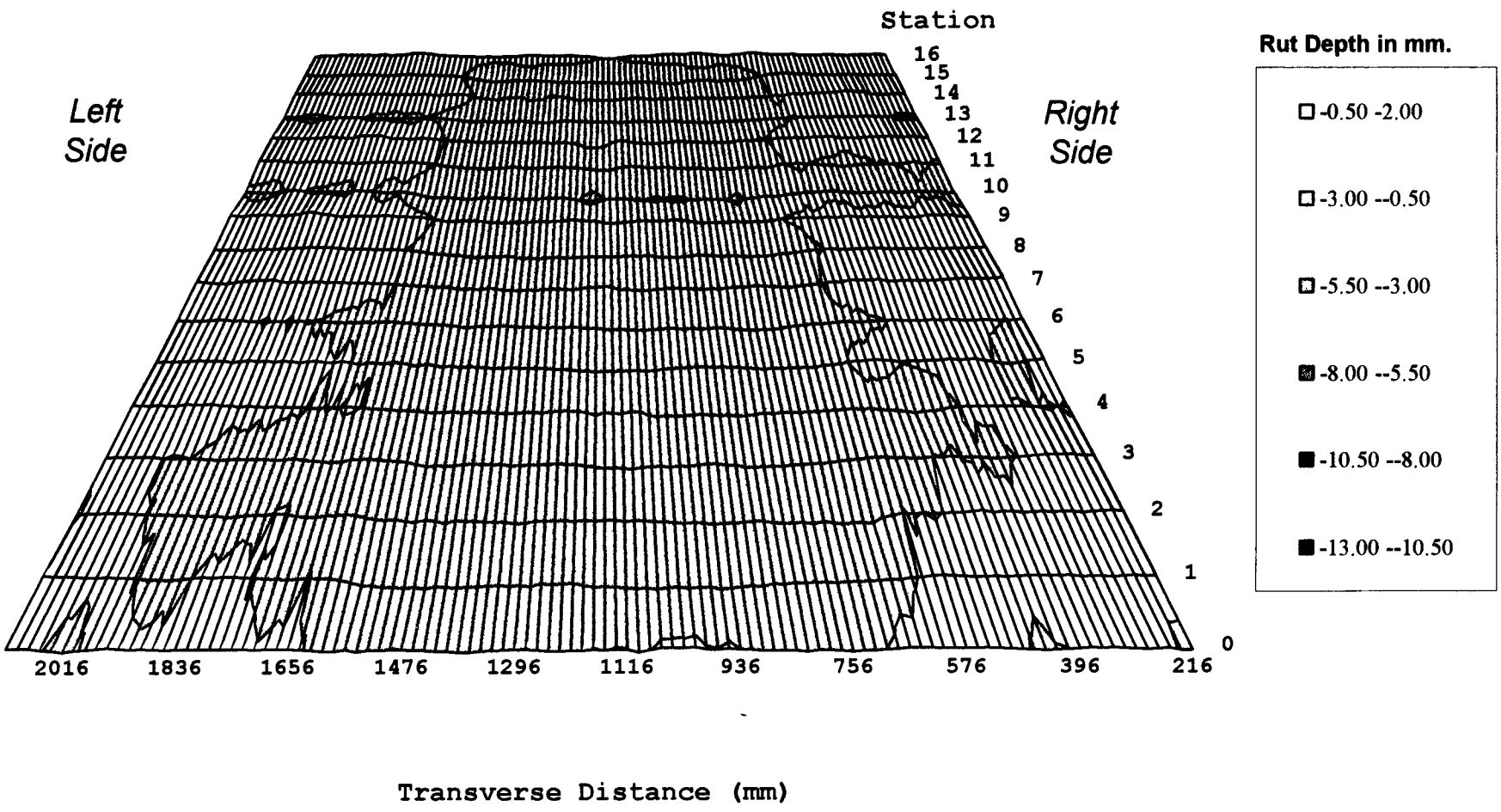

Figure 3.8 Deformed test section surface at 150,000 repetitions

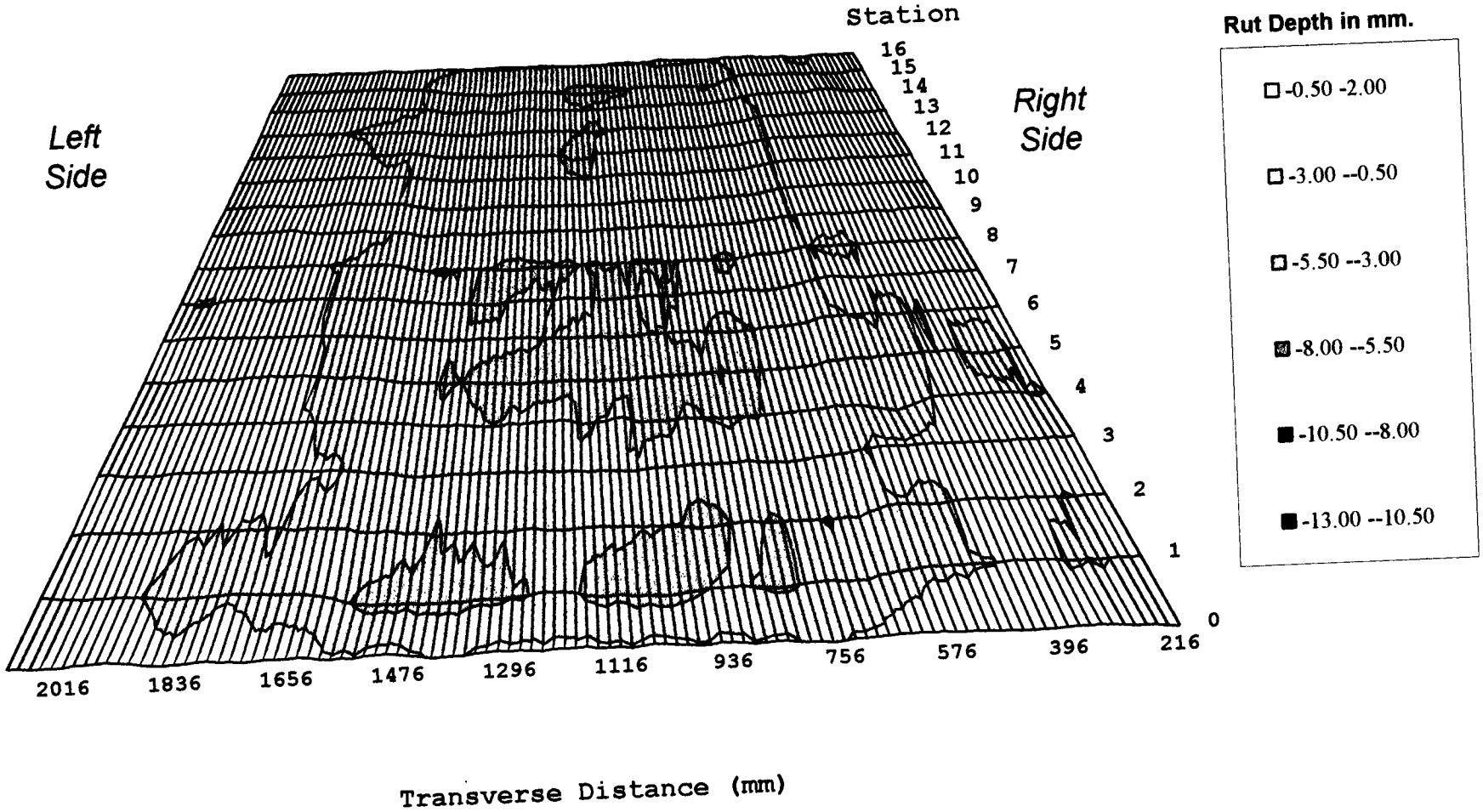

Figure 3.9 Deformed test section surface at 200,000 repetitions

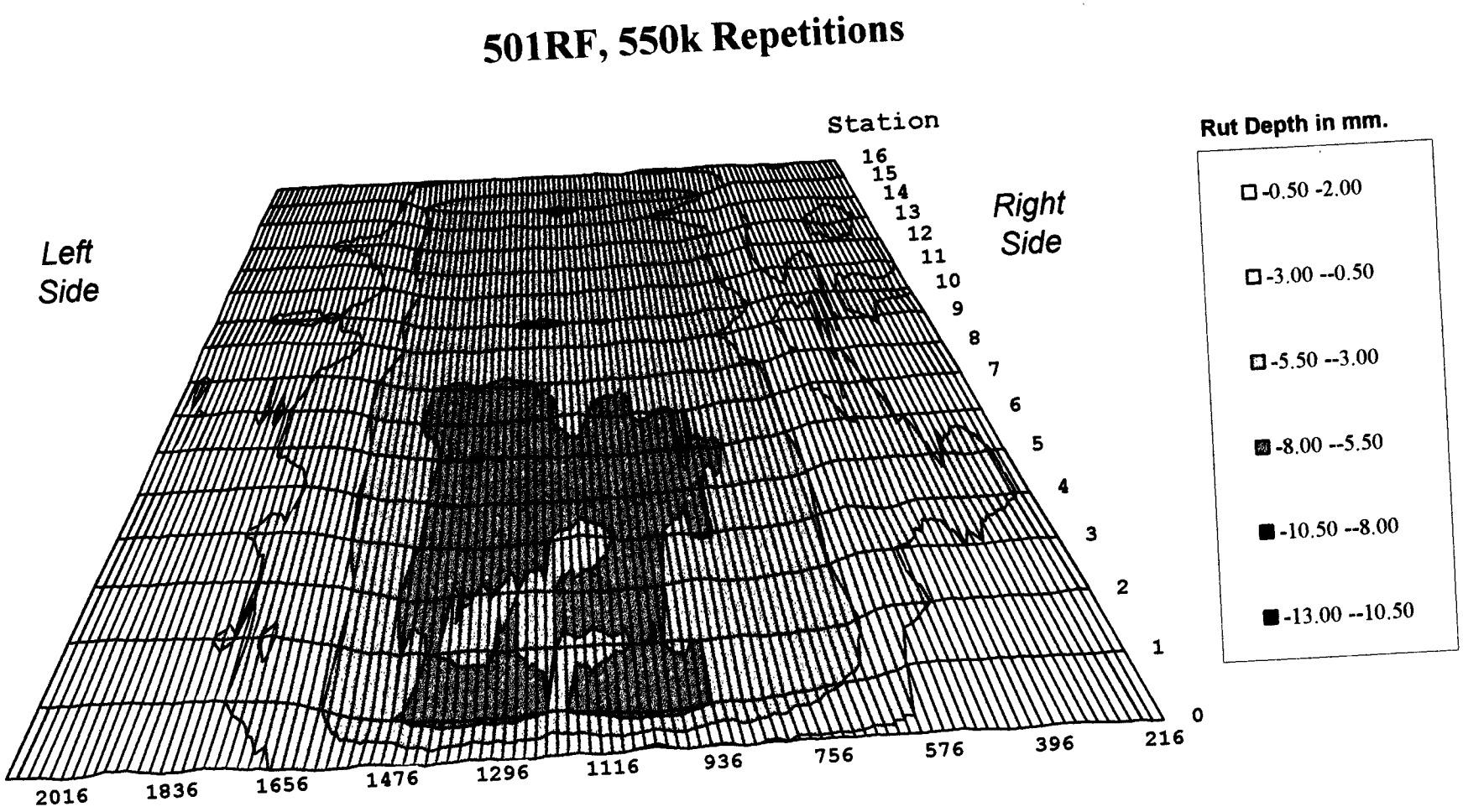

Figure 3.10 Deformed test section surface at 550,000 repetitions

501RF, 1.43M Repetitions

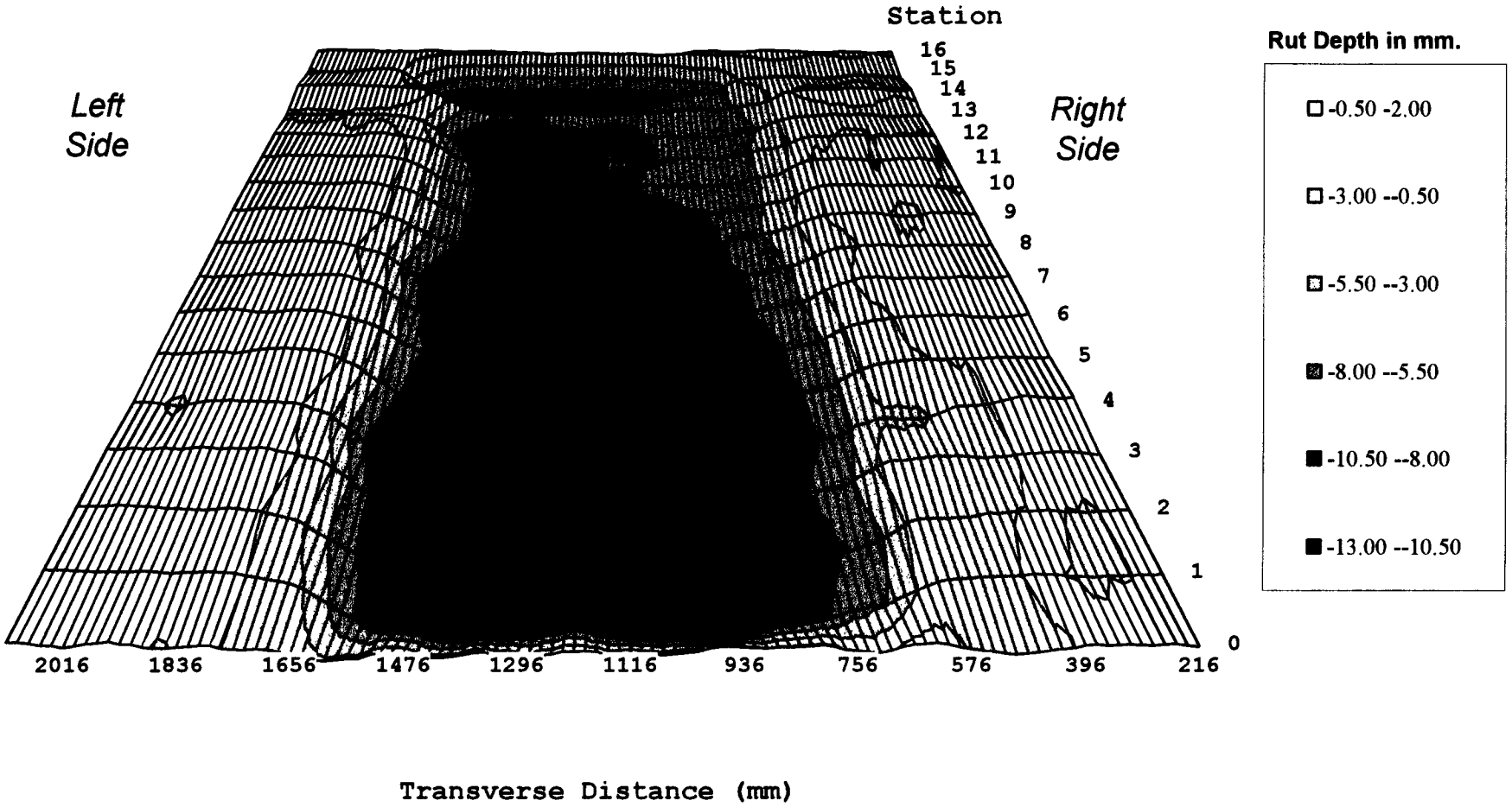

Figure 3.11 Deformed test section surface at 1,430,000 repetitions

Figure 3.7 illustrates the pavement surface at 50,000 repetitions with a minimal amount of rutting. Figures 3.8 to 3.11 show the surface at 150,000 up to 1.43 million load repetitions respectively, as rutting increases. At the conclusion of trafficking (1.43×10^6 repetitions), the average rut was just over 8 mm and the average maximum rut had reached 10.5 mm. The maximum rut (15 mm) was at Point 4, near the MDD location. Slight disturbance around the MDD during installation may have influenced the location of the maximum rut. The data for Point 6 is more typical, and is presented in Figure 3.12.

At 550,000 repetitions, the approximate time at which cracking began, approximately 60 percent of the total permanent deformation had already occurred. The remaining 40 percent of total pavement deformation occurred in the final 800,000 repetitions.

At the conclusion of the test, rut depth measurements were taken both with the laser profilometer and with a straight edge at each station. Excellent correspondence between the two measurement methods was noted, e.g Figure 3.12.

Figure 3.6 shows the variations that occurred in the rate of rut development throughout the test. To characterize stages with different rates of rut development during the life of the pavement, the data presented in Figure 3.6 were subjectively divided into phases. Differences in the rate of rut development in each phase were caused by changes in the load, and changes in permanent deformation resistance of the pavement. The phases being applied are summarized in Table 3.5 with calculated rutting rate expressed in millimeters of rut per million load applications (mm/MiLA).

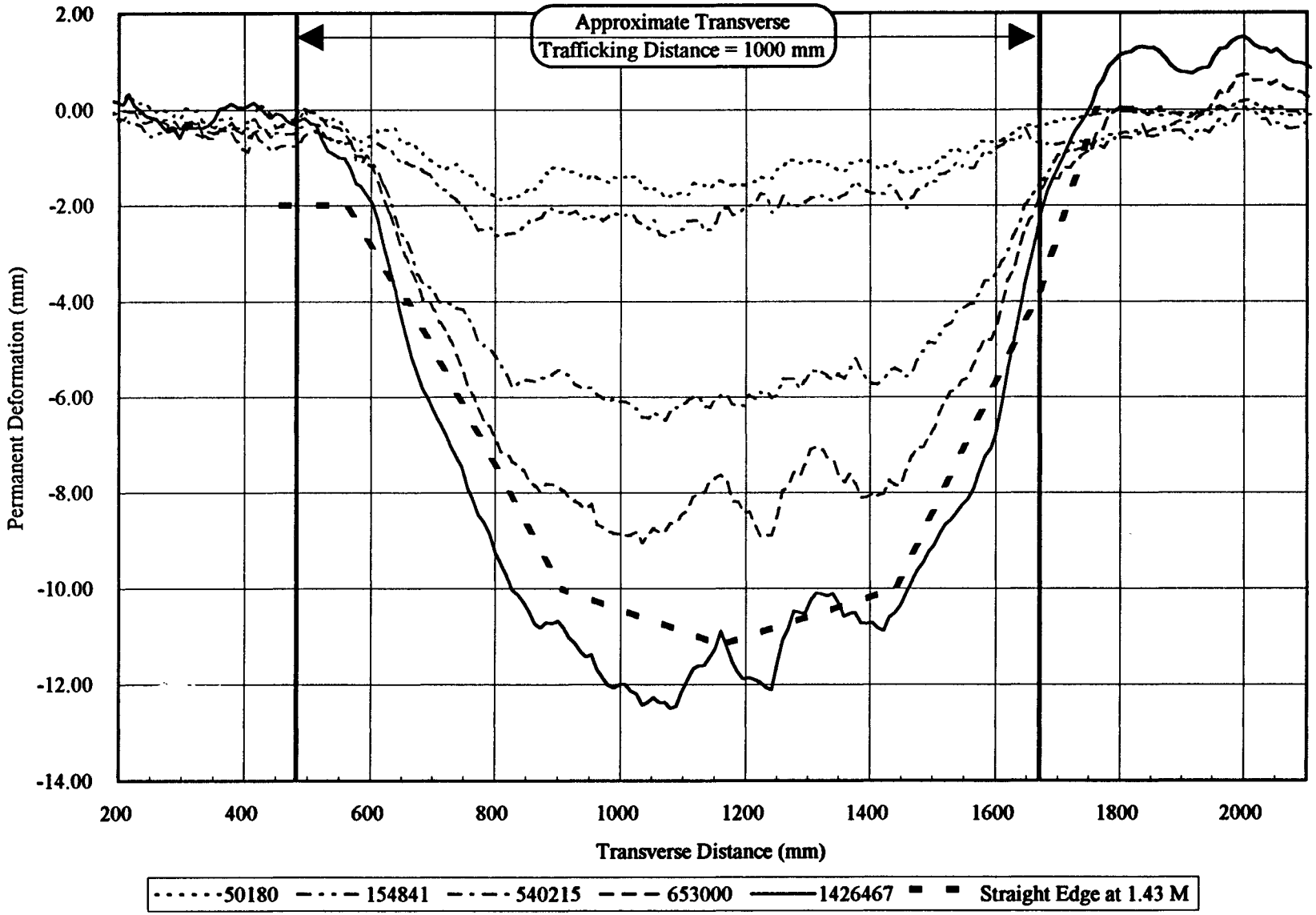

Figure 3.12 Profilometer cross section at Point 6 and final straight edge measurement

Table 3.5 Rutting rates during HVS loading on Section 501RF

Phase	Repetitions ($\times 10^3$)	Load (kN)	Condition	Average Rut (mm)	Average Maximum Rut (mm)	Rut Rate * (mm/MiLA) (Average Rut)
I	0 – 50	40	Embedding	1.3	2.2	25.8
II	50 – 150	40	Steady-State	1.6	2.5	3.3
III	150 – 200	80	Embedding	2.4	3.3	14.6
IV	200 – 450	100	Embedding	4.4	5.8	8.3
V	450 – 540	100	Transition	4.5	5.7	0.6
	550	100	Cracking	x	x	-
VI	540 – end	100	Steady-State	8.4	10.5	4.4

*MiLA=Million Load Application

The first phase, zero to 50,000 repetitions, is considered an embedding phase in which the asphalt pavement undergoes post-construction compaction as the result of the 40 kN traffic loading. The 40 kN load is representative of the design traffic for both the asphalt concrete mix and the pavement structural section. Figure 3.6 shows that the embedding under 40 kN loading appears complete at approximately 50,000 load repetitions. The test plan required that the 40 kN load be maintained to 150,000 repetitions to ensure that this initial embedding phase was accomplished so that the asphalt concrete would be reasonably compacted and thus better able to withstand the higher wheel loads (80 kN and 100 kN) without excessive rutting. At 154,841 repetitions the load was increased to 80 kN and a rapid increase in rutting per load repetition was observed (Figure 3.6). The load was further increased to 100 kN at 203,498 repetitions and the rut depth per load repetition increased significantly.

Each time the load is increased a new embedding phase is observed. The 150,000 to 200,000 repetitions period represents the embedding phase resulting from the increase in load

from 40 kN to 80 kN; and the embedding phase when the load was increased to 100 kN at 200,000 repetitions was completed by 250,000 repetitions.

Cracking occurred at approximately 550,000 repetitions. However, this did not result in an increased rut rate as seen in Figure 3.6. The rut rate remained at a relatively constant rate until the end of the test. In the field it might be expected that rutting of the unbound soils layers would accelerate if cracking resulted in surface water entering the pavement. For Section 501RF there was no surface water; accordingly the observed behavior was to be expected.

Rutting rates during the embedding phases for Section 501RF were less than those for Section 500RF (25.8, 14.6, and 8.3 mm/MiLA versus 27.0, 24.6, and 26.0 mm/MiLA). This is likely due to the difference in temperatures during the two tests, although changes (drying) in water content of the untreated materials may have also contributed. On the other hand steady rut rates were similar for the two tests.

Comparison of surface maximum rut depth measured using the laser profilometer and the MDD at Point 4 shows similar results for both devices, as can be seen in Figure 3.13.

3.3.2 In-Depth Permanent Deformation

The MDD measurements permitted the determination of the accumulation of vertical permanent deformation at various depths in the pavement during the course of HVS loading. From the MDD data obtained at Points 4 and 12 and shown in Figures 3.14a and 3.14b, it is possible to estimate the permanent deformation occurring in each layer. Table 3.6 shows the results of this analysis.

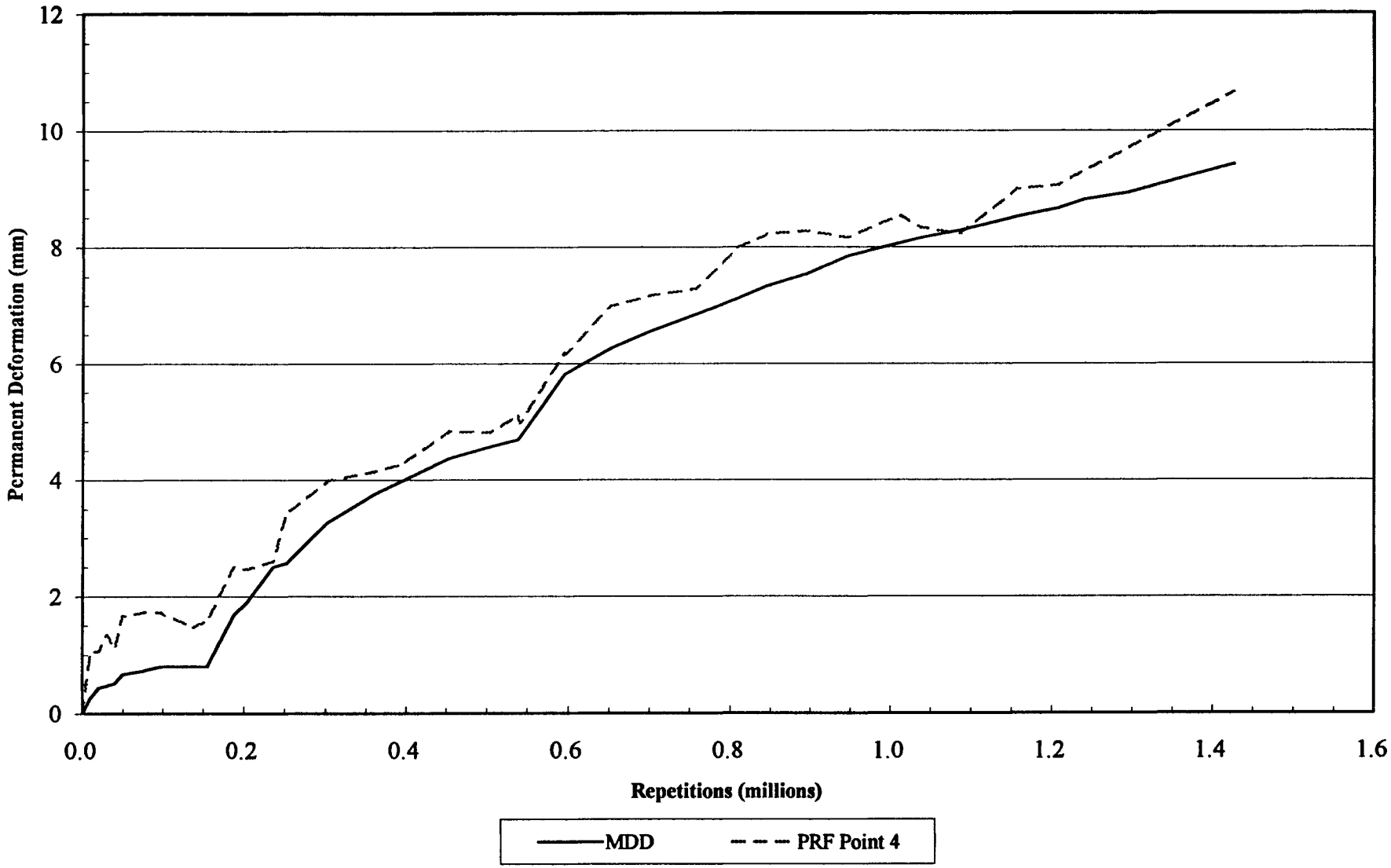

Figure 3.13 Permanent deformation comparison of MDD at Point 4 and the laser profilometer

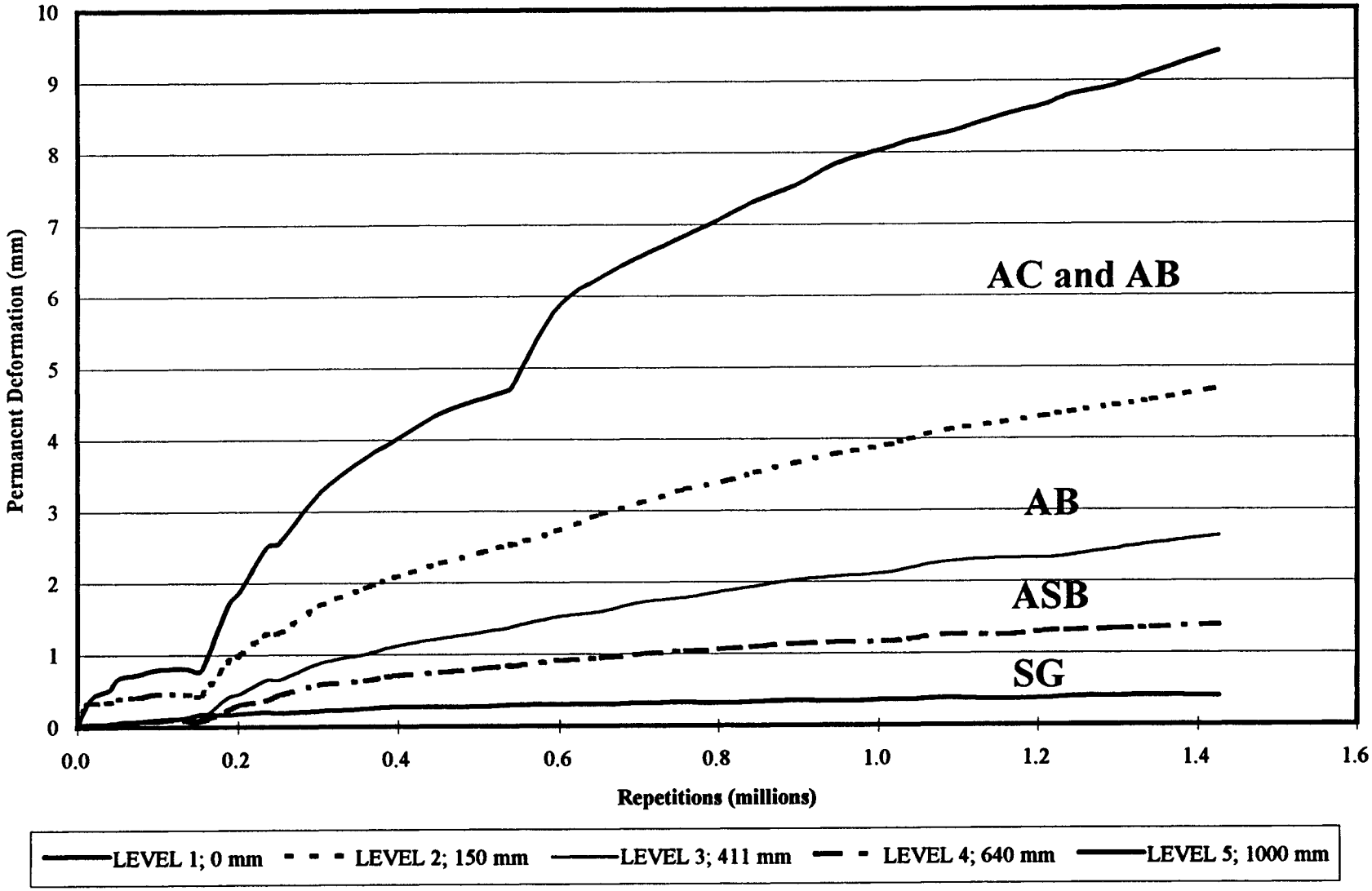

Figure 3.14a MDD at Point 4 permanent deformation

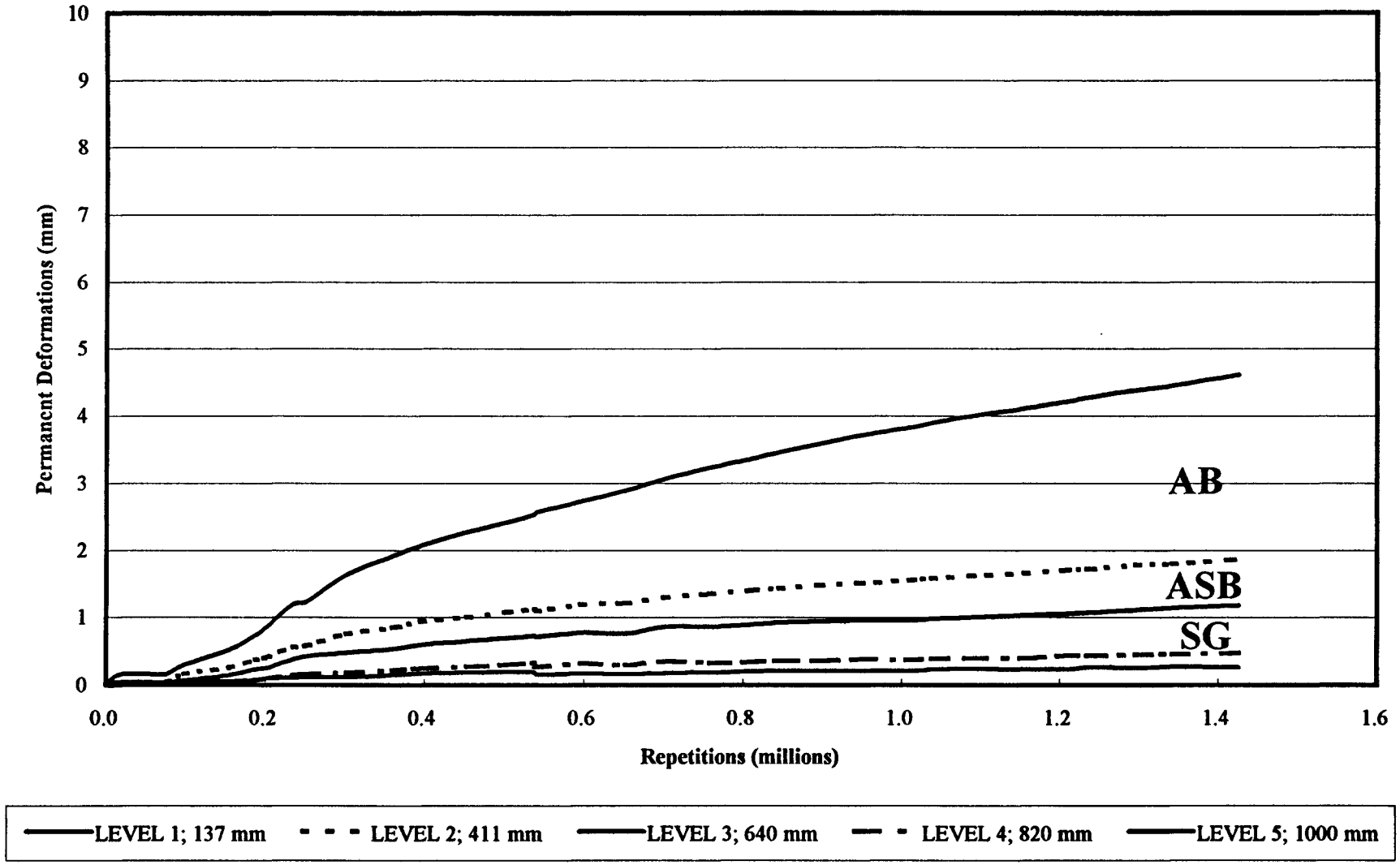

Figure 3.14b MDD at Point 12 permanent deformation

Table 3.6 Permanent deformation as measured by MDD modules

Layer	Approximate Thickness (mm)	Vertical Permanent Deformation (mm)	Percentage of Total Deformation
AC	137	4.73	52.5
Aggregate Base	274	2.4	26.2
Aggregate Subbase	229	1.0	10.7
Subgrade	infinite	1.0	10.6
Total		9.0	100

3.3.2.1 Asphalt Concrete. As seen in Table 3.6 slightly more than 50 percent of the total observed vertical permanent deformation occurred in the asphalt concrete layers. Figures 3.7 through 3.12 show little upheaval adjacent to the ruts. In order to estimate what proportion of the measured rutting was attributable to volume decrease and what proportion was attributable to deviatoric (shear) distortions, four 150 mm diameter cores were extracted and their air void contents measured. Two of the cores were taken from outside the trafficked area, and the other two from inside the test section at Stations 9 and 14. Results of the air voids determinations are presented in Table 3.7.

Table 3.7 Air void contents of cores from the dense graded asphalt concrete layer

	Specimen	% Air-voids Top Lift	Height (mm) Top Lift	% Air-Voids Bottom Lift	Height (mm) Bottom Lift
Outside Trafficked Area	15	7.1	63	5.6	84
	Sta 0+44	6.6	88*	N/A	N/A
	Sta 0+23	7.9	66*		
	Average	7.2	63	5.6	84
Inside Trafficked Area	9.75	6.2	63	5.8	83
	14.25	7.6	65	6.9	77
	Average	6.9	64	6.4	80

* Not included in average height calculation

The change in air voids with trafficking is relatively small suggesting that the majority of permanent deformation is due to shear deformations. The data of Table 3.7 also suggest most if not all densification occurred in the less compacted top lift, as also occurred on Section 500RF. The air voids measurement results also show that the bottom lift (average air voids content of 6.1 percent) was better compacted than the top lift during construction (average air voids content of 7.7 percent). However, this difference is not as marked as that observed in test Section 500RF, where the bottom lift was compacted to about 4 percent air voids and the top lift to about 8 percent.

3.3.2.2 Unbound Soil Layers. Permanent deformation in the aggregate base was estimated from data obtained at MDD at Point 12. It is estimated that 26 percent of the total calculated deformation occurred in the aggregate base, as shown in Table 3.6.

The proportion of permanent deformation in the aggregate base of Section 501RF is about equal to that measured in the combined asphalt treated permeable base (ATPB) and aggregate base layers for Section 500RF, i.e. 24 percent.

The remaining permanent deformation, 22 percent, occurred in the subbase (11 percent) and subgrade (11 percent). These percentages of permanent deformation are nearly the same as those measured in Section 500RF, which were both 12 percent. The amount of rutting observed in the subgrade suggests that the Caltrans design procedure provides an adequate pavement thickness to minimize permanent deformation in the subgrade, even under the 100 kN loading used for the test program.

3.4 ELASTIC (RECOVERABLE) DEFLECTIONS

Elastic (recoverable) deflections provide an indication of the overall stiffness of the pavement structure and, therefore, a measure of load carrying capacity. As damage occurs, the stiffness of a structure decreases, resulting in larger strains, which in turn result in fatigue cracking and rutting. In the HVS tests elastic deflections are measured with the multi-depth deflectometer (MDD) and the road surface deflectometer (RSD). The RSD measures surface deflections at any point whereas the MDDs measure in-depth deflections. At Point 4 the MDD has an added module to measure deflections at the surface. The RSD is very similar to the Benkelman Beam, and produces comparable measurements for most highway applications.

3.4.1 Surface Deflections

Elastic surface deflections as measured by the RSD and the MDD module at Point 4 are summarized in this section. Since pavement temperatures did not vary significantly during the test, influence of temperature on the deflections measured by the RSD or MDD was not investigated.

3.4.1.1 RSD Surface Deflection Results. Figures 3.15 and 3.16 show the individual RSD deflections for centerline measuring Points 4, 6, 8, 10, and 12 under 40 kN and 100 kN loads respectively. These deflections are all within a narrow range indicating that structural capacity across the section was reasonably uniform. The maximum difference between centerline deflections at Points 4, 6, 8, and 10 is approximately 20 percent throughout the whole testing period.

A marked increase in deflection resulted after cracking was observed at the surface at approximately 550,000 repetitions. Deflections from the 40 kN load increased from approximately 600 microns just before cracking to approximately 750 microns just after cracking, an increase of 25 percent. Deflections under the 100 kN load increased from approximately 1300 microns (average) to 1500 microns, an increase of approximately 15 percent. The measured deflections remained relatively uniform after cracking. Average 40 kN load RSD deflection data measured on the test section before HVS loading commenced and the average after 1.43×10^6 load applications are shown in Table 3.8. The average 100 kN deflection at the end of the test (1.43×10^6 repetitions) ranged between 1400 and 1600 microns.

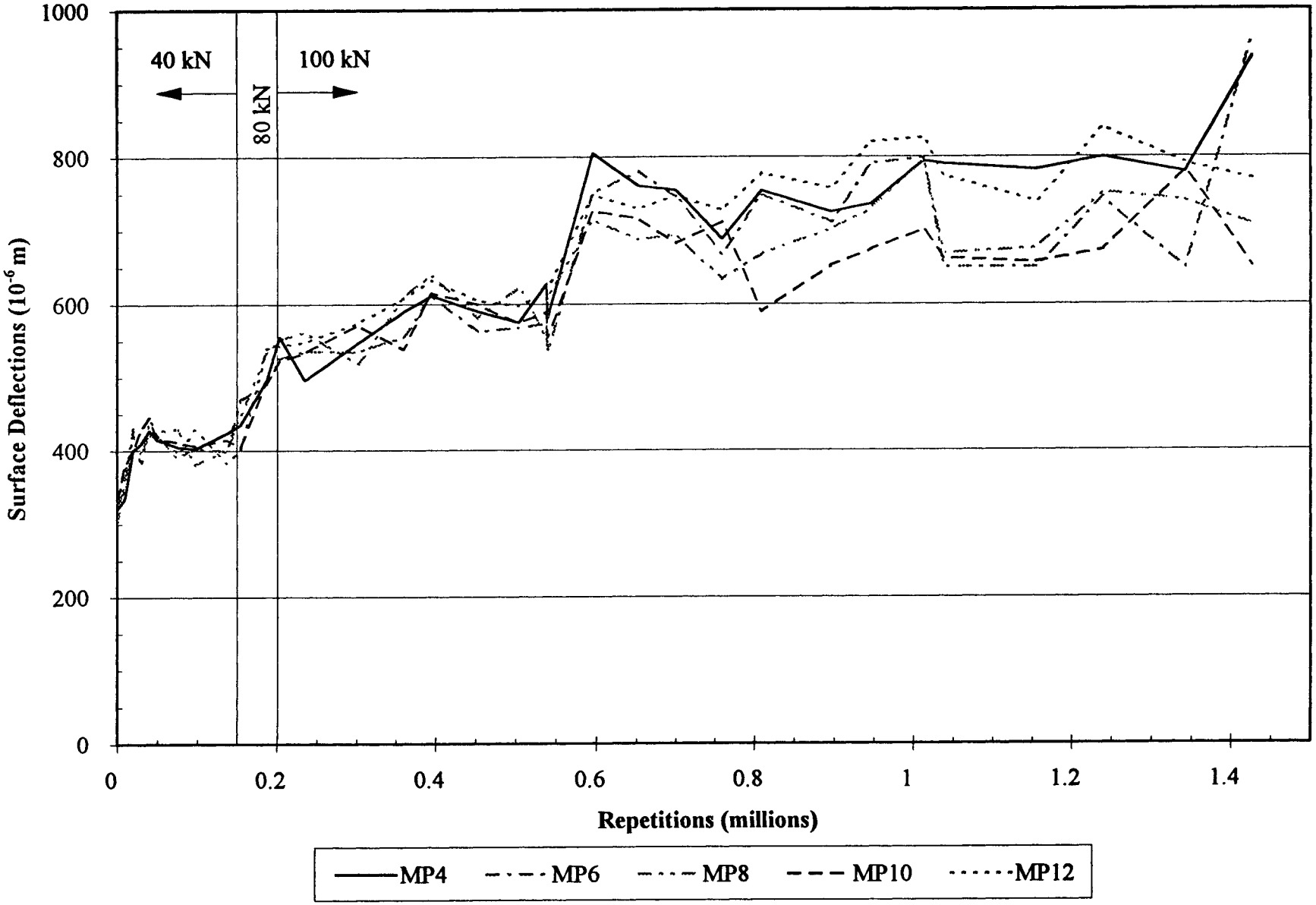

Figure 3.15 Road surface deflections, 40 kN test load

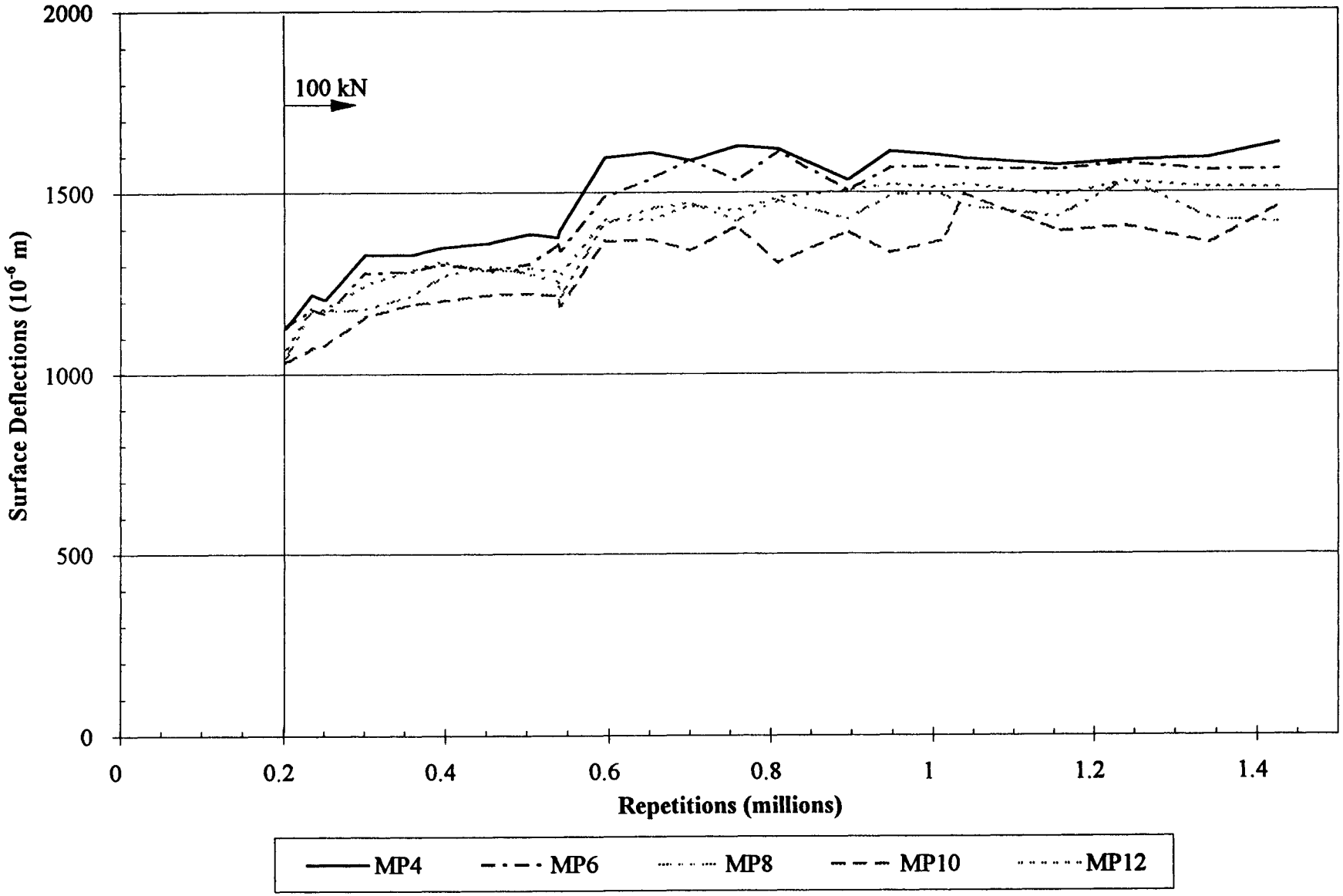

Figure 3.16 Road surface deflections, 100 kN test load

Table 3.8 Average of RSD deflections under 40 kN load

	Before HVS testing	After 1.43×10^6 HVS Load applications
Average Deflection (microns)	322	805
Standard deviation	12	123

The average RSD deflections are illustrated in Figures 3.17 and 3.18 for 40 kN and 100 kN loads respectively. Phases with similar trends in the rate of increase in elastic deflection are indicated on these figures by Roman numerals. Deflections in phases I, II, III, and IV occurred during the first 50,000 repetitions of the 40 kN load, the next 100,000 repetitions at 40 kN, as the load was increased from 40 kN to 80 kN, and from 80 kN to 100 kN respectively, and indicate increased damage rates each time as loading was increased. Phase II indicates a slower rate of deflection increase than Phase I although both have under 40 kN loading. Phase V (approximately 550,000 to 600,000 repetitions) indicates the increase in deflection as cracks appeared at the surface. The rate of deflection increase appears to slow substantially thereafter under continued 100 kN loading in Phase VI (600,000 to 1,430,000 repetitions). In Phase VI cracking of the top lift was essentially complete and gradual damage of the uncracked bottom lift, which was better compacted, likely continued.

3.4.1.2 MDD Surface Deflection Results. Figures 3.19 and 3.20 summarize the surface deflections measured with the MDD at Point 4 under the 40 kN and 100 kN loads respectively. Figures 3.19 and 3.20 also show the results of the RSD deflections measured at Point 4 at the same time. Similar trends are visible between the two instruments. However, the data do not show the same level of agreement between the two devices observed earlier in the results from test Section 500RF.

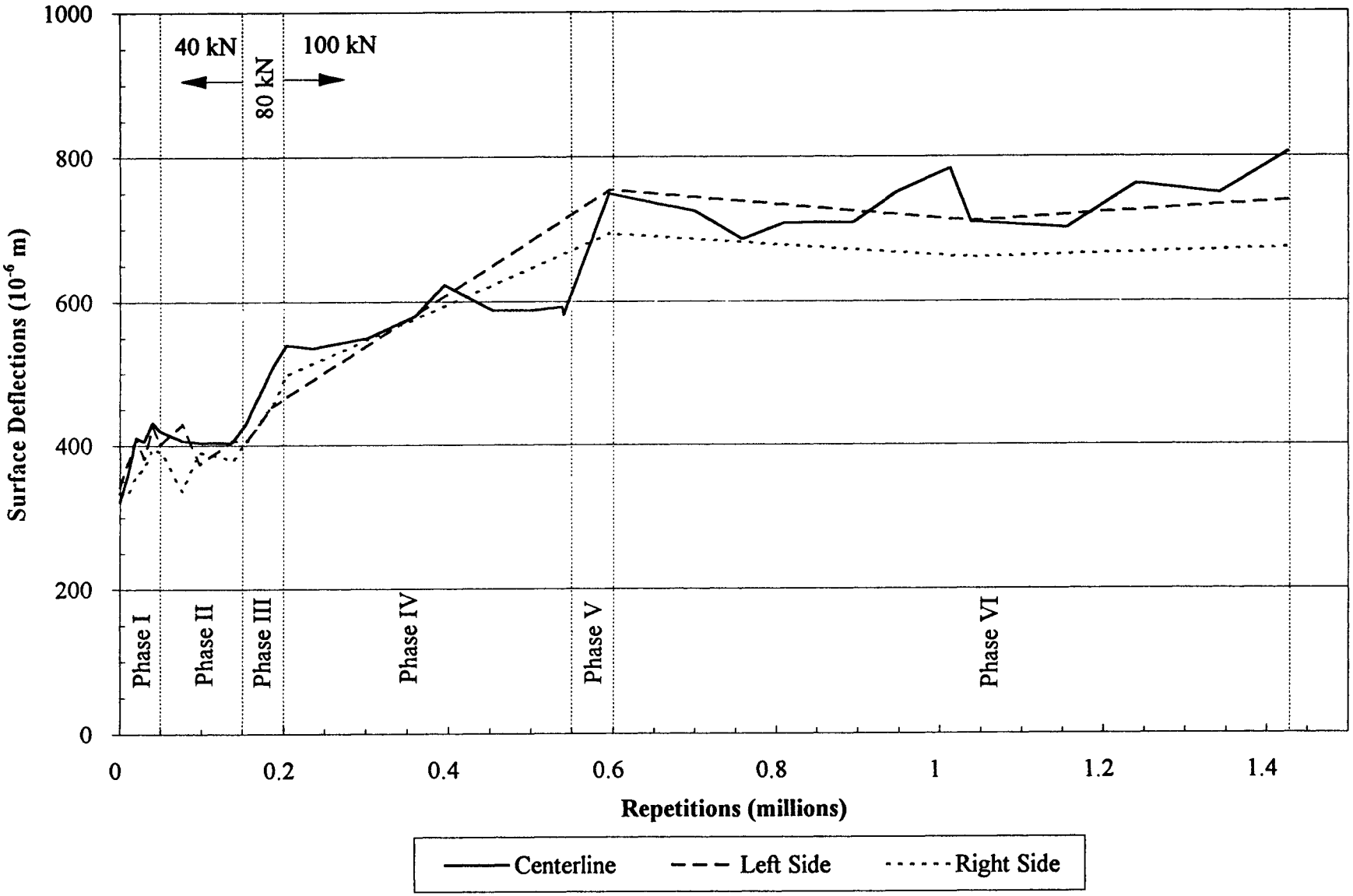

Figure 3.17 Average road surface deflections, 40 kN test load

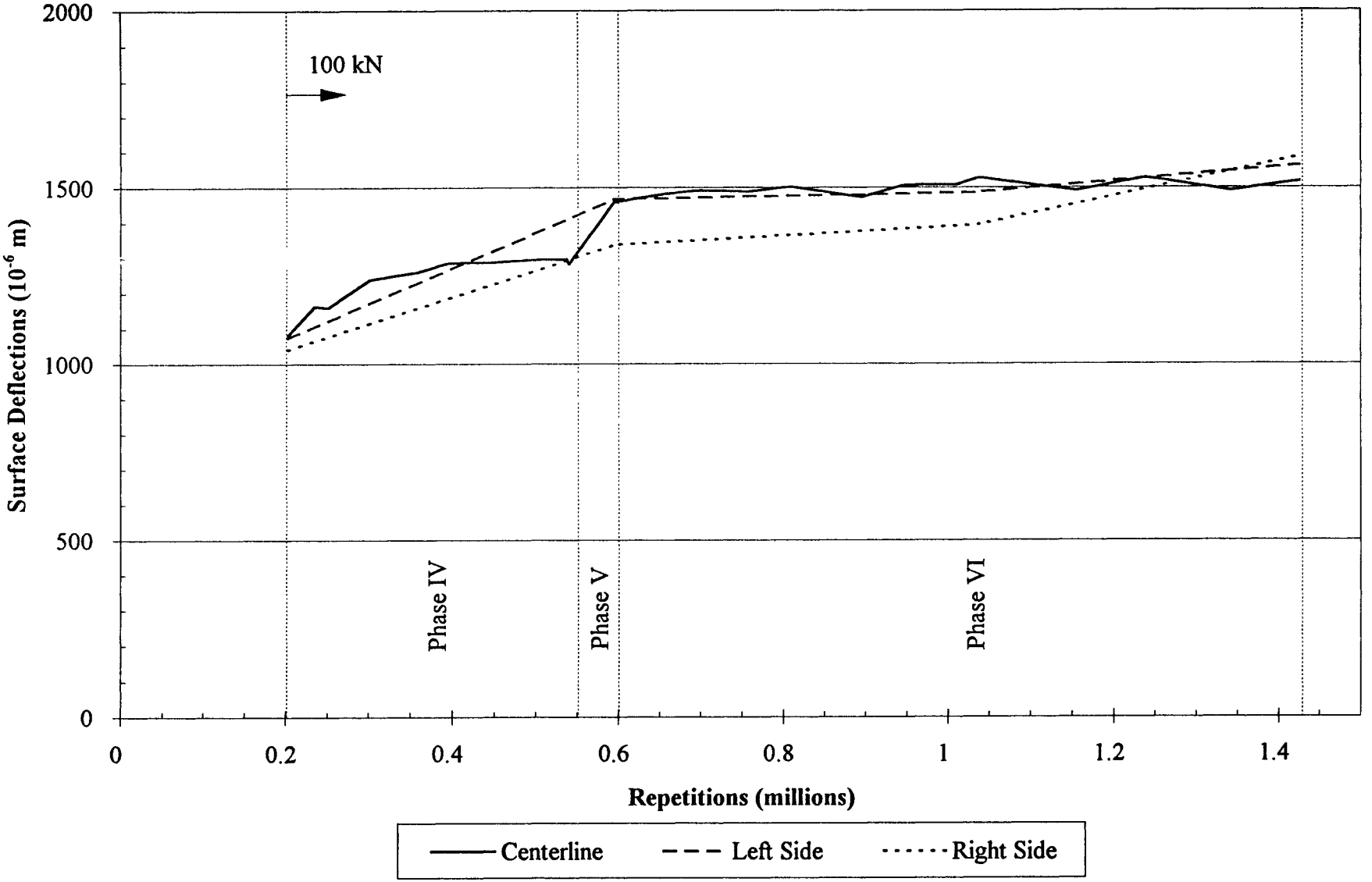

Figure 3.18 Average road surface deflections, 100 kN test load

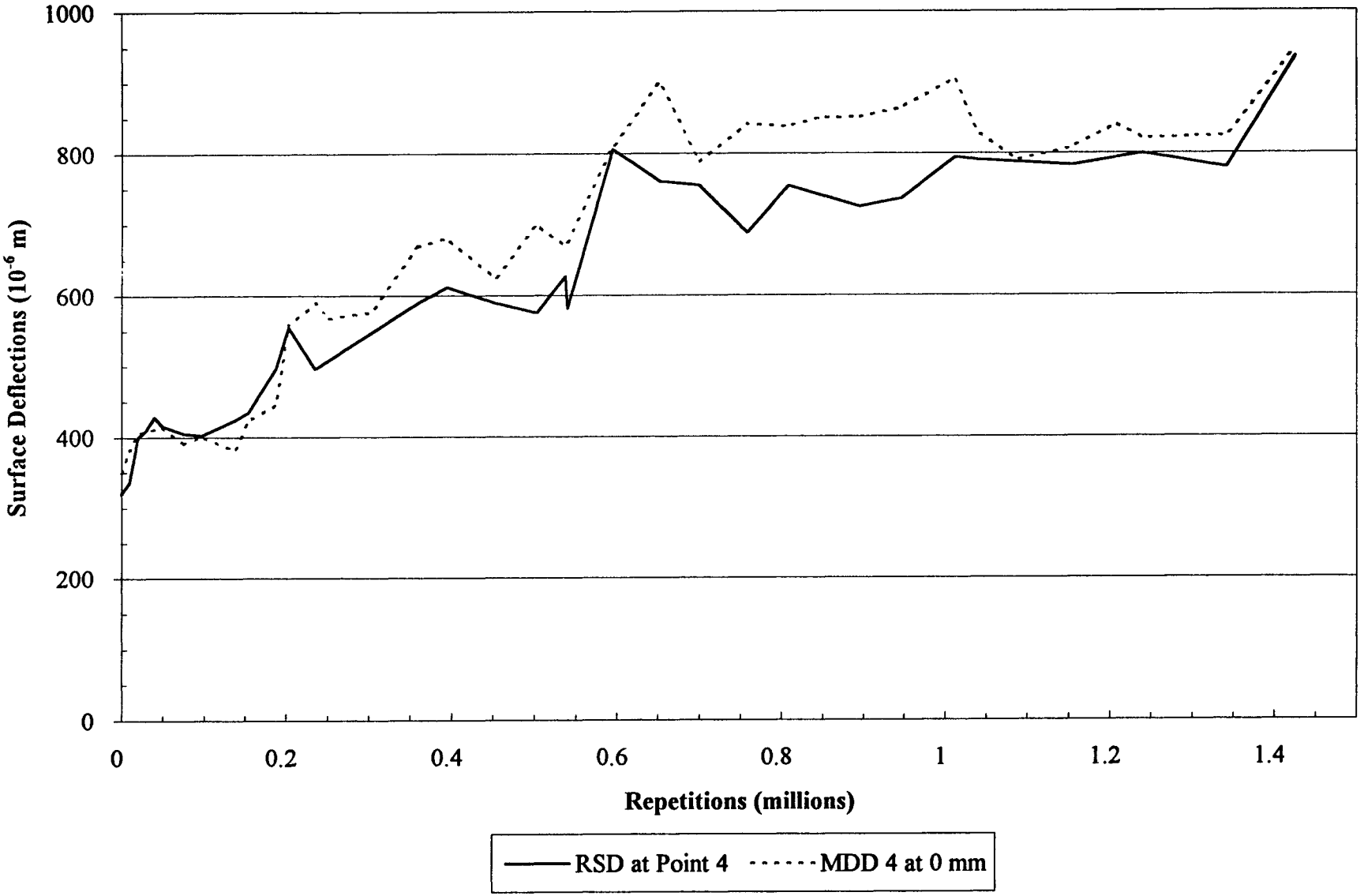

Figure 3.19 Comparison of elastic deflections determined by the RSD and by the MDD at Point 4 with a 40 kN load

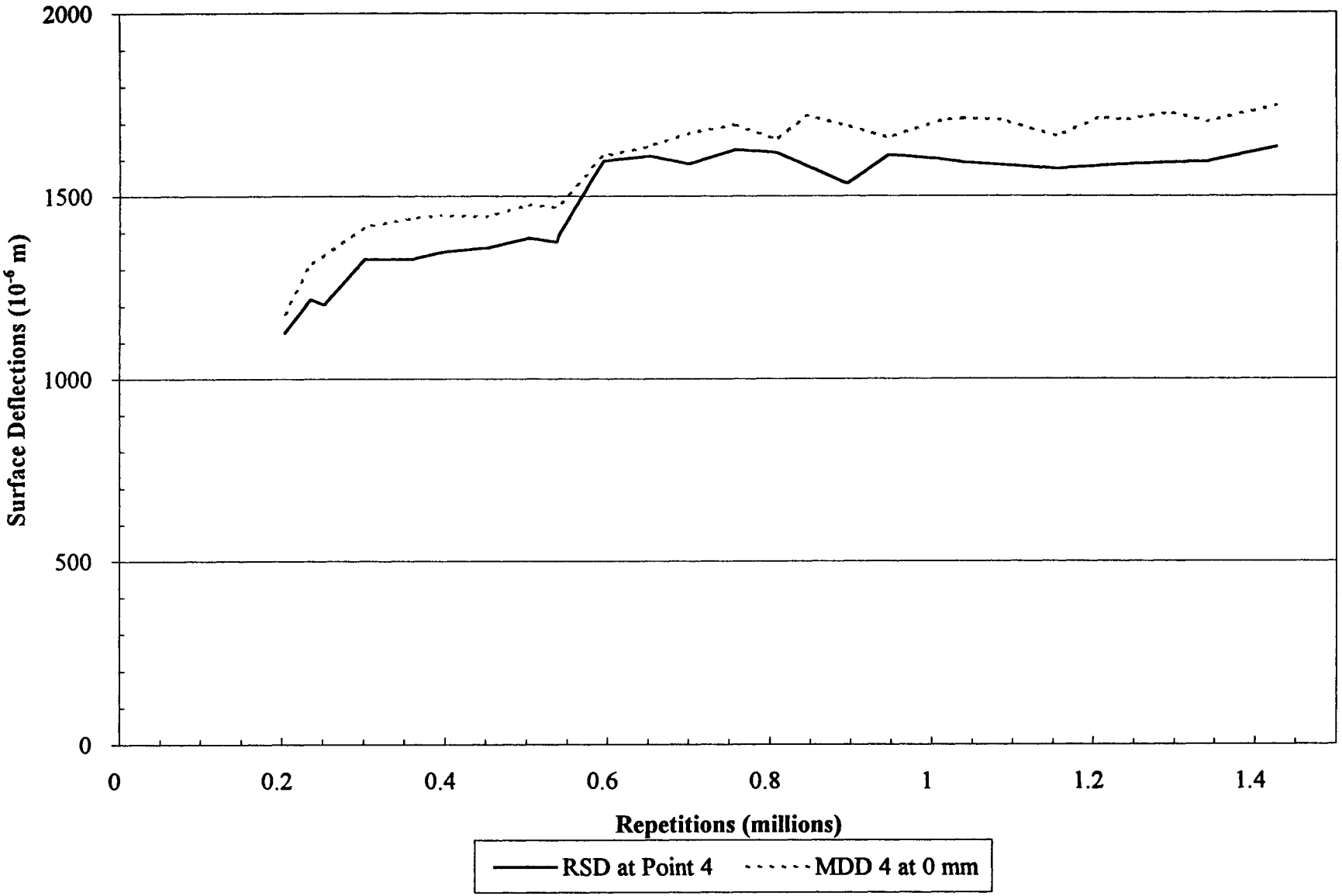

Figure 3.20 Comparison of elastic deflections determined by the RSD and by the MDD at Point 4 with a 100 kN load

3.4.2 In-Depth Elastic Deformations

Figures 3.21 and 3.22 summarize the in-depth deflections measured at various numbers of load applications at the MDDs both at Point 4 and Point 12. The deflections are reported separately for the measurements under the 40 kN and 100 kN loads.

Averages of all 40 kN and 100 kN MDD elastic deflection data measured on Section 501RF are summarized in Tables 3.9 and 3.10. The tables show deflections at the time HVS loading commenced and those obtained after 1.43 million load applications for 40 kN (Table 3.9) and 100 kN test loads (Table 3.10). It will be noted that the 100 kN test load deflections were measured *only* after the HVS had reached 200,000 load repetitions at which point the traffic load had been increased to 100 kN (Table 2.1). The data contained in Tables 3.9 and 3.10 represent the average of 3 deflection measurements per measuring point.

The damage which took place in the asphalt concrete layer with load repetitions (as manifested by surface cracking) is likely responsible for the increase in surface deflection. Due to the decrease in stiffness in the surface layer from cracking, the deflections in the other layers also increased.

The proportion of total surface deflection contributed by each layer can be determined from the deflection results presented in Tables 3.9 and 3.10. These results are summarized in Tables 3.11 and 3.12 for the 40 kN and 100 kN test loads respectively.

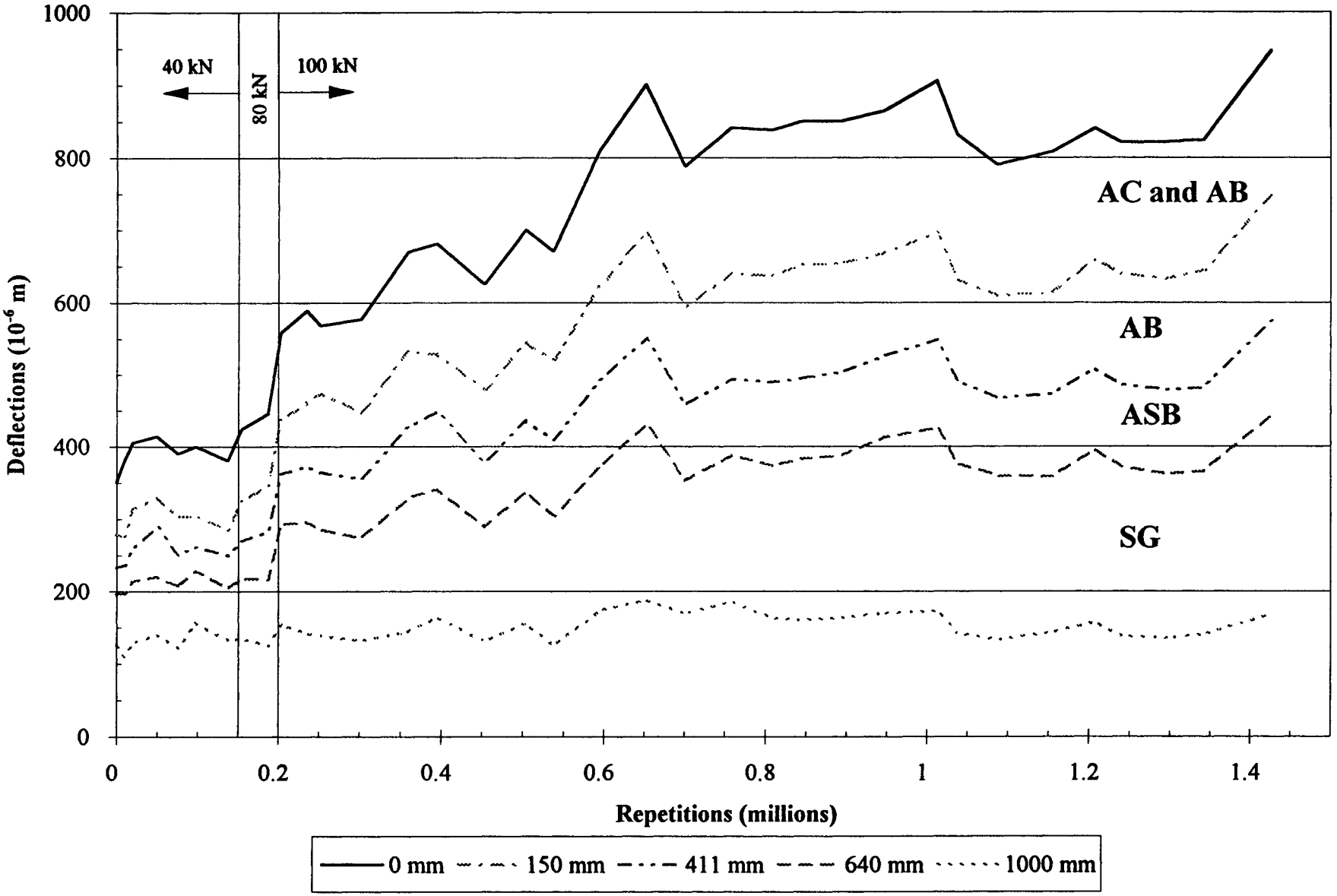

Figure 3.21a Measured MDD deflections at Point 4 versus load repetitions at various depths below pavement surface, 40 kN load

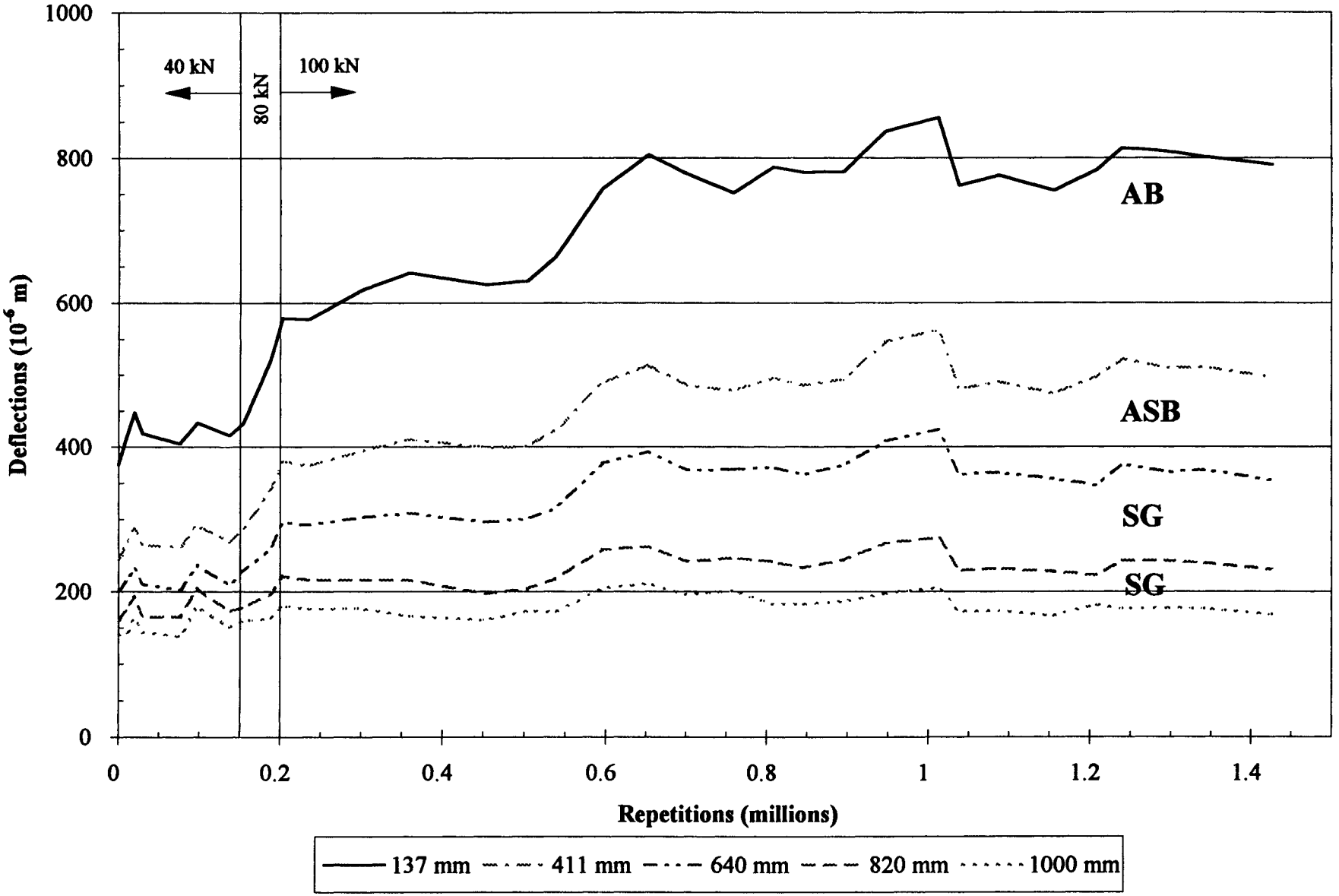

Figure 3.21b Measured MDD deflections at Point 12 versus load repetitions at various depths below pavement surface, 40 kN load

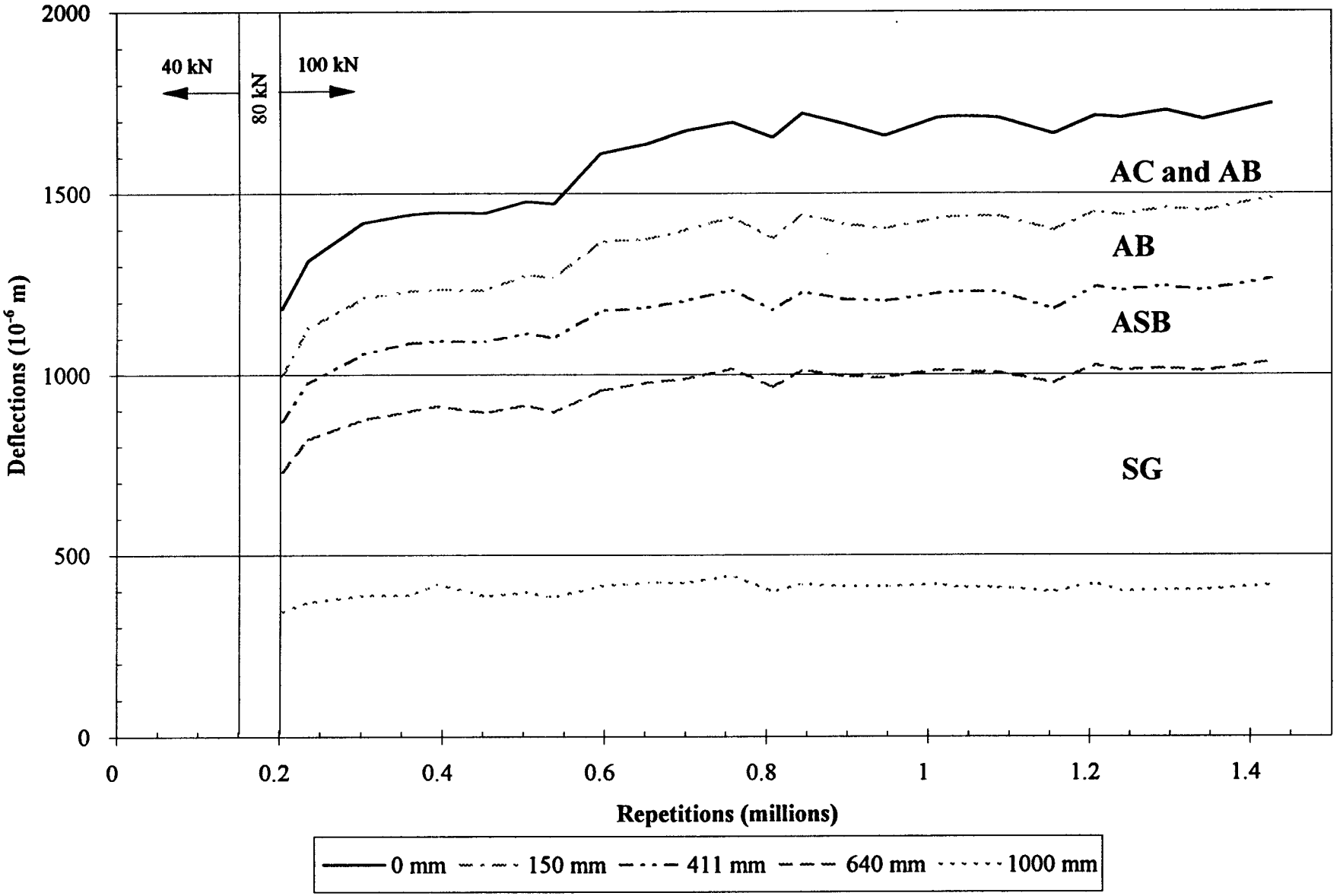

Figure 3.22a Measured MDD at Point 4 deflections versus load repetitions at various depths below pavement surface, 100 kN load

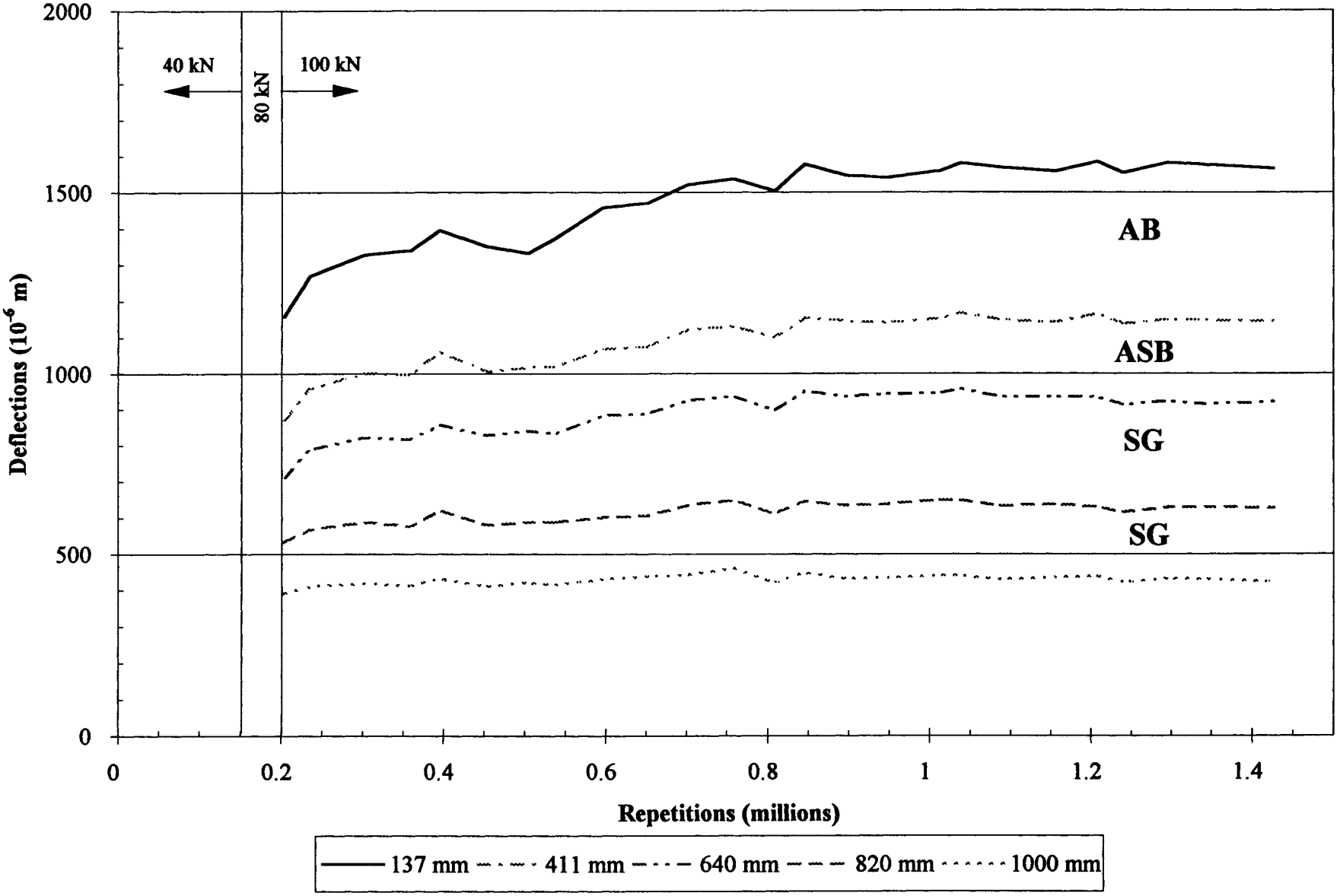

Figure 3.22b Measured MDD at Point 12 deflections versus load repetitions at various depths below pavement surface, 100 kN load

Table 3.9 Summary of 40 kN MDD elastic deflections

Level (mm)	Pavement Layer	Elastic in-depth Deflections (microns): Test Load = 40 kN			
		MDD at Point 4		MDD at Point 12	
		Before HVS loading	After 1.43 M load applications	Before HVS loading	After 1.43 M load applications
0	Asphalt Concrete	350	947	N/A	N/A
137	Ashpalt Concrete	N/A	N/A	375	791
150	Aggregate Base	279	746	N/A	N/A
411	Aggregate Subbase	233	575	246	497
640	Subgrade	196	443	202	354
820	Subgrade	N/A	N/A	160	231
1000	Subgrade	125	168	141	169

N/A MDD modules were not placed at these locations (see Figure 2.2)

Table 3.10 Summary of 100 kN MDD elastic deflections

Level (mm)	Layer	Elastic in-depth Deflections (microns): Test Load = 100 kN			
		MDD at Point 4		MDD at Point 12	
		After 200k load repetitions	After 1.43 M load repetitions	After 200k load repetitions	After 1.43 M load repetitions
0	Asphalt Concrete	1180	1747	N/A	N/A
137	Asphalt Concrete	N/A	N/A	1154	1565
150	Aggregate Base	998	1487	N/A	N/A
411	Aggregate Subbase	870	1264	873	1144
640	Subgrade	732	1034	713	921
820	Subgrade	N/A	N/A	532	628
1000	Subgrade	342	417	391	423

N/A MDD modules were not placed at these locations (see Figure 2.2)

Table 3.11 Percentage elastic deflection contributed by each layer, 40 kN test load

Pavement Layer	Percentage of total elastic deflection			
	MDD at Point 4		MDD at Point 12	
	Before HVS loading	After 1.43 M load applications	Before HVS loading	After 1.43 M load applications
Asphalt Concrete	20.1	22.9	N/A	16.5
Aggregate Base + Asphalt Concrete	33.6	39.2	----	47.5
Aggregate Base	N/A	N/A	N/A	31
Aggregate Subbase	10.6	13.9	N/A	15.2
Subgrade	56.0	46.8	N/A	37.4

N/A MDD modules were not placed at these locations (see Figure 2.2)
Note: Calculated from Table 3.9

Table 3.12 Percentage elastic deflection contributed by each layer, 100 kN test load

Pavement Layer	Percentage elastic deflection			
	MDD at Point 4		MDD at Point 12	
	After 200k load applications	After 1.43 M load applications	After 200k load applications	After 1.43 M load applications
Asphalt Concrete	15.4	14.9	2	10.4
Aggregate Base + Asphalt Concrete	26.2	27.6	26	34.5
Aggregate Base	$\pm 10.8^{*}$	$\pm 12.8^{*}$	24	24.1
Aggregate Subbase	11.5	13.1	13.8	12.7
Subgrade	62.0	59.2	60.5	52.7

N/A MDD modules were not placed at these locations (see Figure 2.2)
Note: Calculated from Table 3.10
* 95% of Aggregate Base

It will be noted in both Tables 3.11 and 3.12 that the elastic deflections increased in both the base and subbase layers with increased trafficking. This may be due in part to the higher stresses transmitted to the base as the asphalt concrete surface was damaged and in part due to a potential increase in water content of the untreated materials as noted earlier because of the time of testing. It is also interesting to compare the proportion of elastic deformations exhibited by the subgrade under the 40 kN and 100 kN loads. As would be anticipated the proportion of elastic deflections in the subgrade is larger for the 100 kN load.

3.5 VISUAL INSPECTIONS

Crack monitoring was an essential part of data collection for test Section 501RF because fatigue distress in an asphalt pavement manifests itself in the form of surface cracks. As with Section 500RF, crack monitoring included visual inspection of the test pavement, direct measurement of crack length, photographic documentation of the cracking progress, and coring to examine the propagation of cracks with depth. In addition to these methods, a new system of digital image analysis was employed to further explore the process of cracking in asphalt pavements.

This section presents the results of surface cracking measurements (both extent and severity) together with the methodology used to obtain this information. A detailed description of the digital image analysis procedure, used for the first time for test Section 501RF, is included. It should be noted that one set of photographs was incomplete and therefore digital image analysis of the test section could only be employed from Point 3 to Point 14 instead of the desired Point 2 to Point 14.

3.5.1 Visual Inspection of Cracks

The first surface cracks were observed at approximately 550,000 repetitions and regular inspection of crack development was made from that point through the end of the test. To obtain crack length data, the pavement was illuminated with high-power lights followed by the marking of the cracks with lumber crayon in order to make them easily visible. A small chain was then laid out on each crack along its course and then stretched out and measured with a ruler. The observed crack length obtained by this method as a function of load repetitions is shown in Figure 3.23.

With this method of crack detection operator error is possible; such error was particularly evident for the data shown in Figure 3.25 of the report on Section 500RF *(3)*, which displayed a high degree of fluctuation in the total measured crack length, contrary to the expected trend of monotonic crack growth with respect to accumulated load repetitions.

As with Section 500RF, the observed cracks were hairline cracks and at times difficult to detect visually. It is presumed therefore that operator error will result in fewer cracks being detected than actually exist. However, the influence of operator error is greatly diminished with the implementation of a digital method of crack observation and analysis method described in detail in Section 3.5.2.

The lack of expansion, spalling and other deterioration of the hair line cracks observed on the pavement surface can likely be attributed to two factors:

- lack of rainfall and mineral particles on the surface of the test pavement, and
- lack of cracking in the bottom lift of asphalt concrete.

A detailed discussion of these factors is in the Section 500RF report *(3)*.

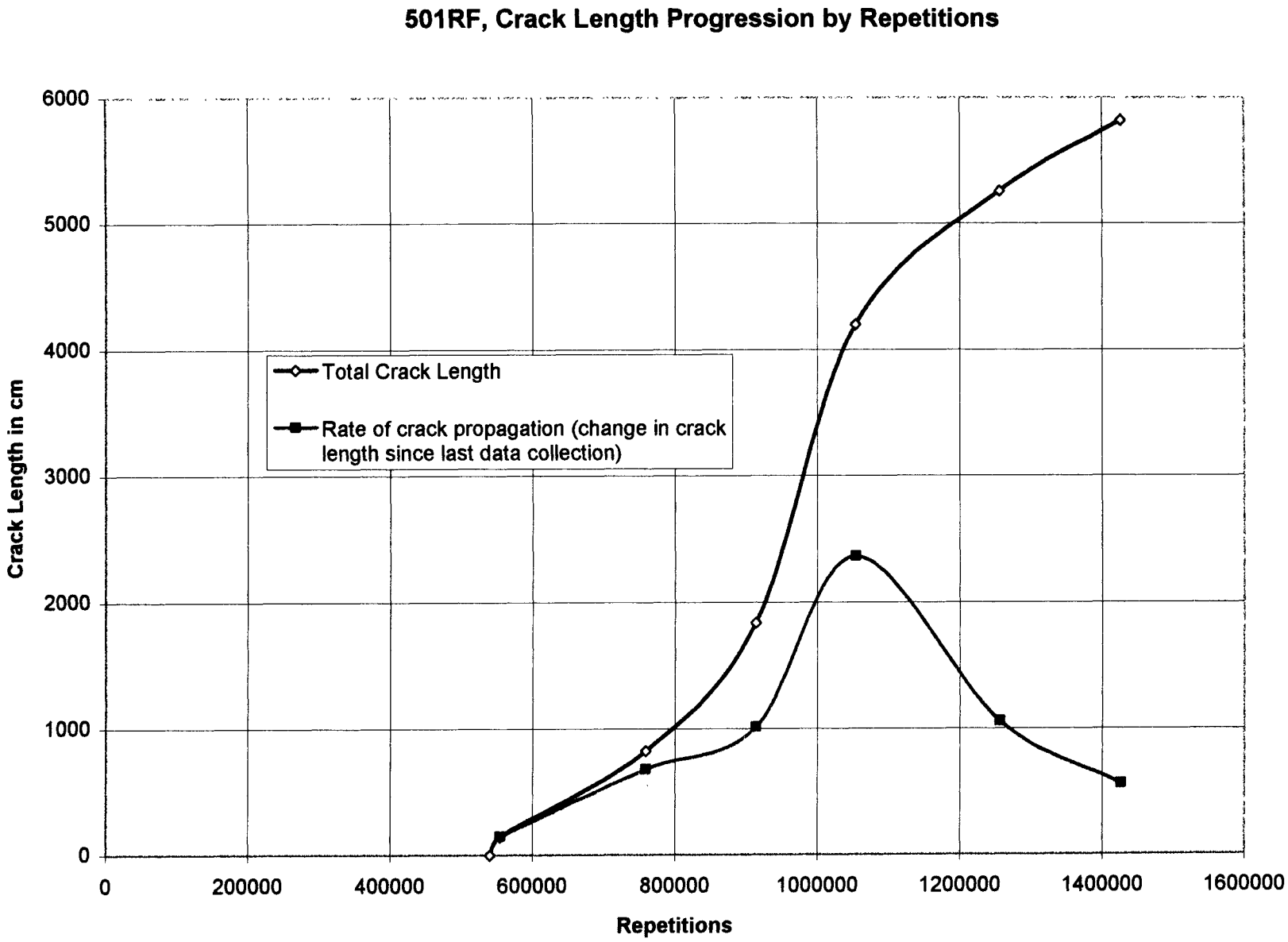

Figure 3.23 Average crack length versus load repetitions

3.5.2 Digital Image Analysis of Cracks

Figures 3.24a, b, and c show crack length as determined by digital image analysis for the final three crack data sets at 1.05 million, 1.26 million, and 1.43 million repetitions. The process for digitally analyzing crack length was not available before Section 501RF had already reached 1.05 million repetitions and therefore the method was not employed for all crack monitoring.

A variety of quantitative information is available from images of cracks through digital image analysis. The software employed is a personal computer software package called Optimas® *(11)*. A description of the process follows.

The test section is marked with a lumber crayon as with visual inspection, and then photographed in sections with a medium-format (60 mm x 70 mm negative) camera. The photographs are then digitized, adjusted to remove camera perspective and distortion, and then recombined to create a composite 2-dimensional image of the test section. Examples of such composite images are shown in Figures 3.25a, b, and c. The cracks from these composite images are then traced in Optimas and the images are calibrated to the real-life dimensions of the test section. Crack statistics can then be calculated and the analysis introduced to a spreadsheet for analysis.

The first real advantage of this method is the elimination of some operator error. In the Section 500RF report, the plot showing total crack length on the test section displayed a great deal of fluctuation due to operator error in detecting cracks. With the digital method, starting with the first crack photos, an overlay is created from the traced cracks. This overlay is then placed over the next set of crack photos. Then, when the crack image of the second set is

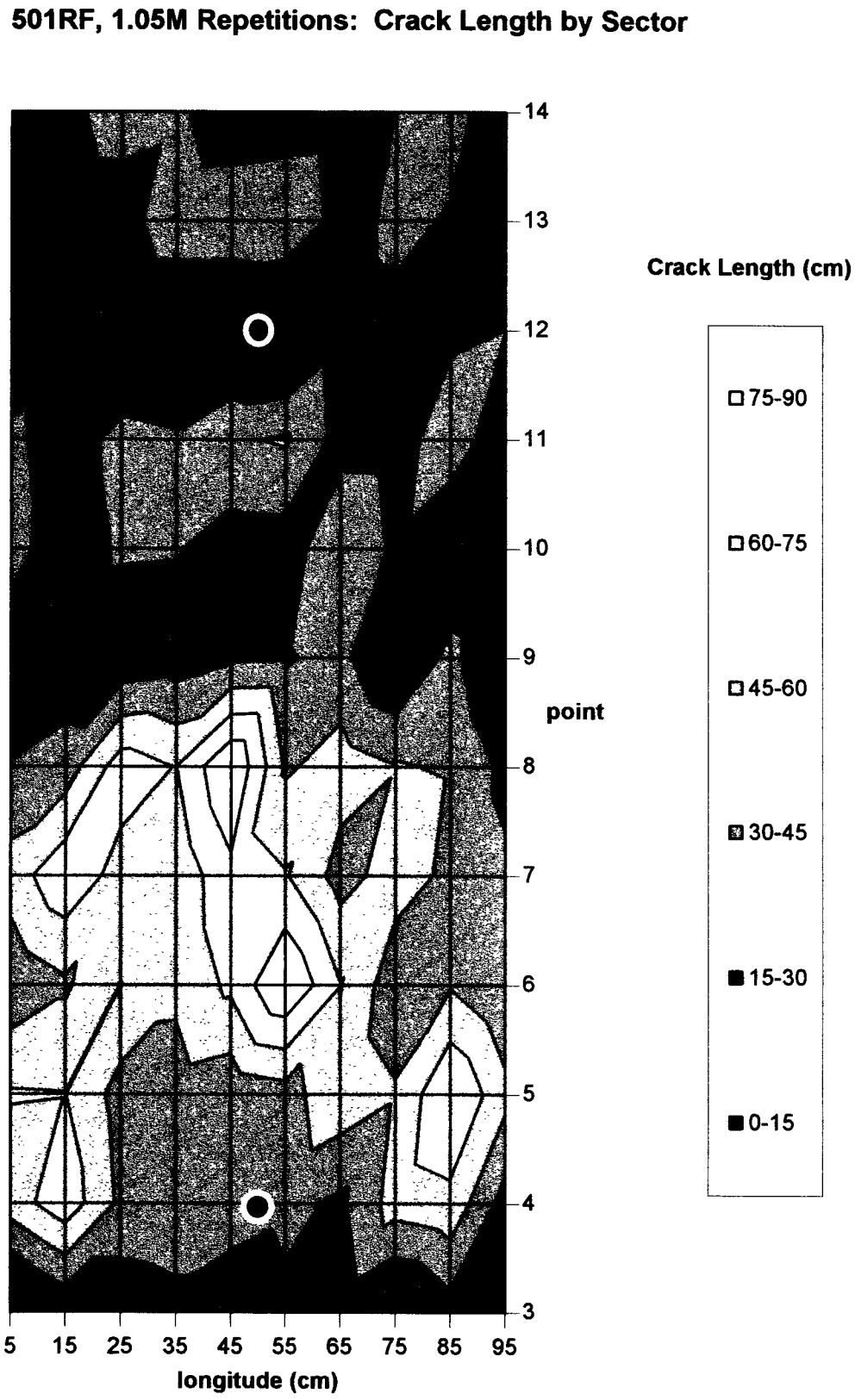

Figure 3.24a Average crack lengths by sector at 1,050,000 repetitions

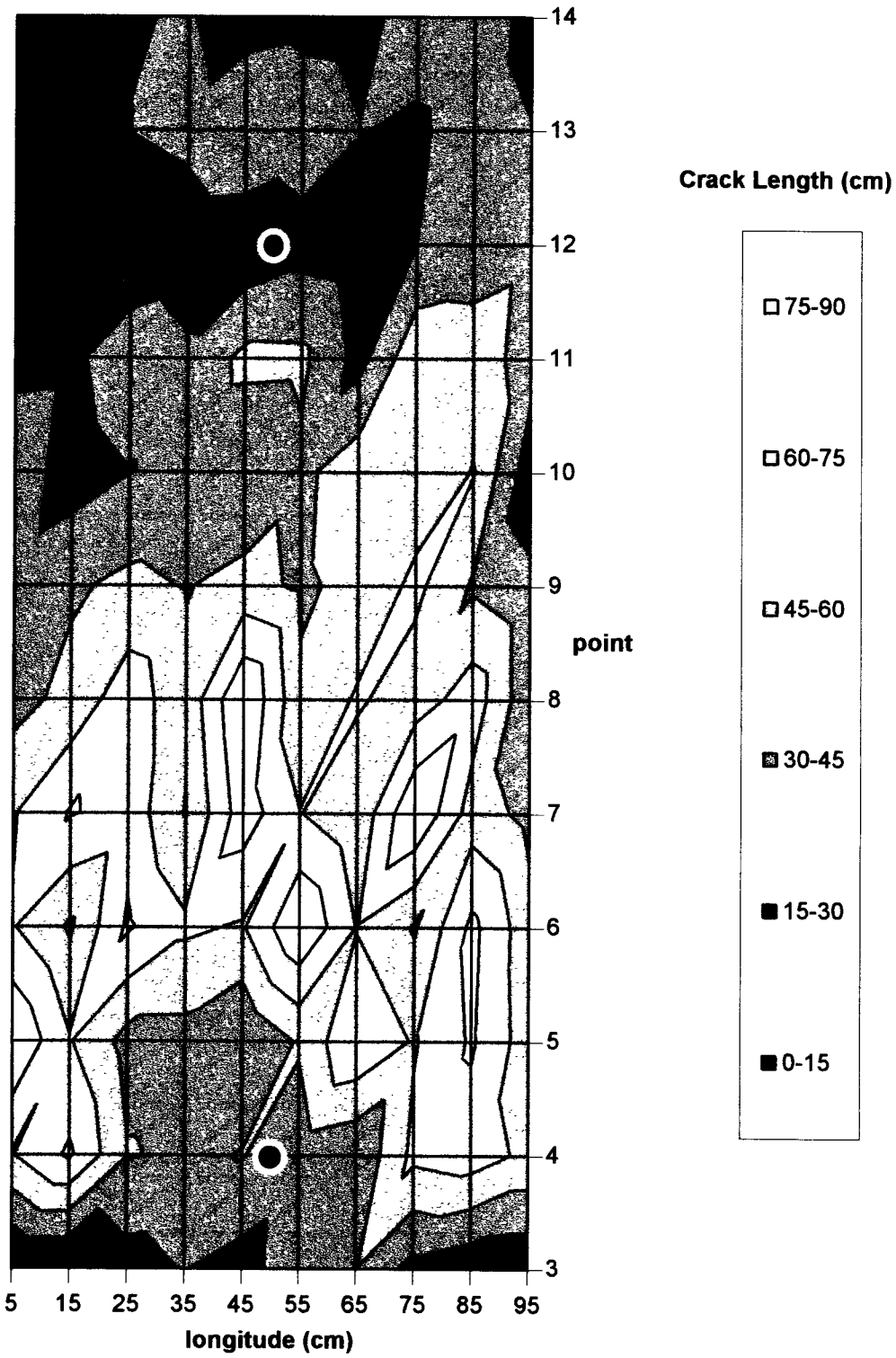

Figure 3.24b Average crack length by sector at 1,260,000 repetitions

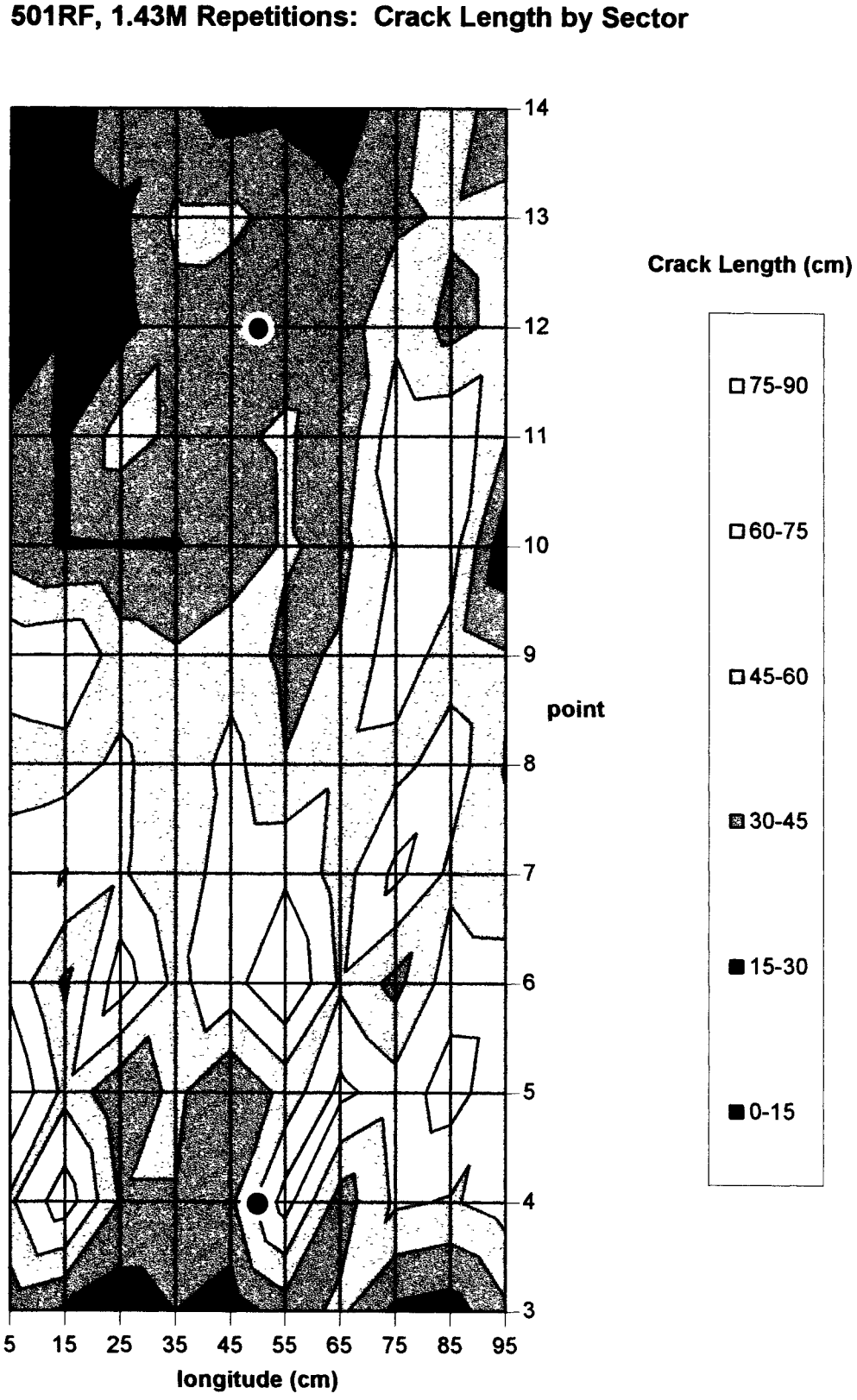

Figure 3.24c Average crack length by sector at 1,430,000 repetitions

501RF, 1.05M Repetitions: Schematic of Cracking Pattern

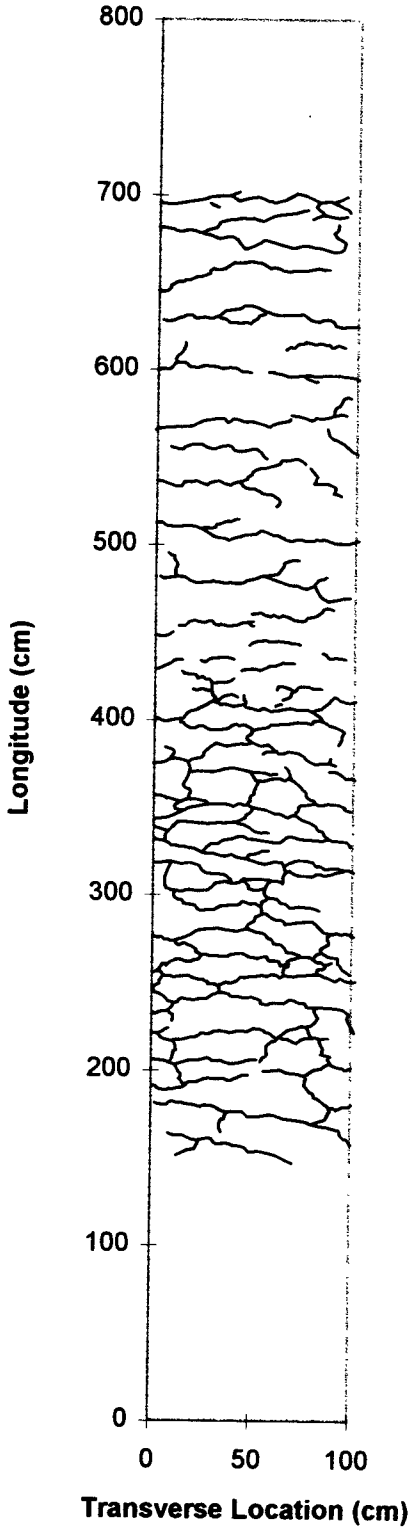

Figure 3.25a Crack schematic at 1,050,000 repetitions

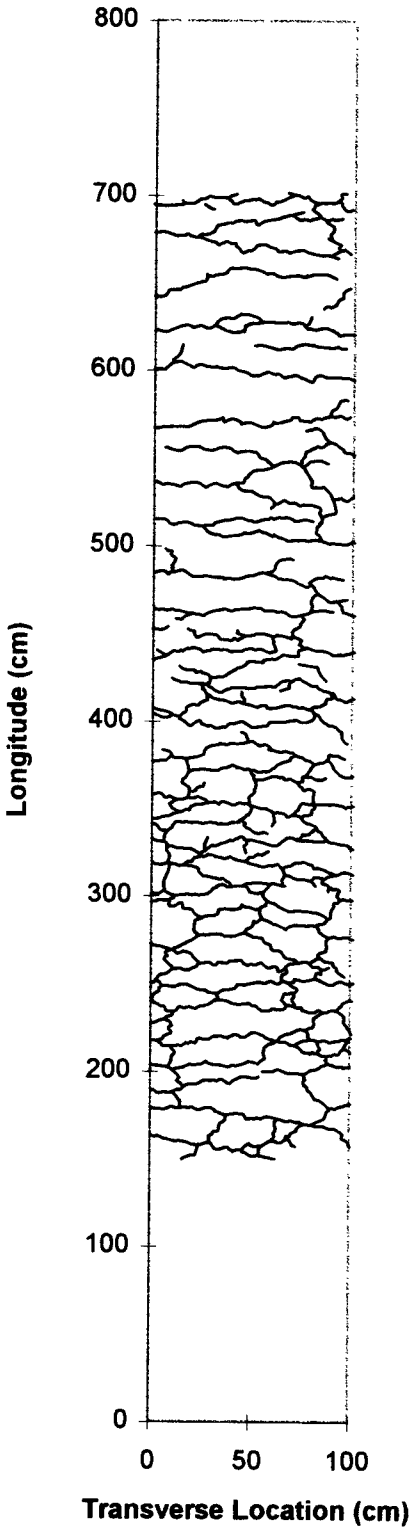

Figure 3.25b Crack schematic at 1,260,000 repetitions

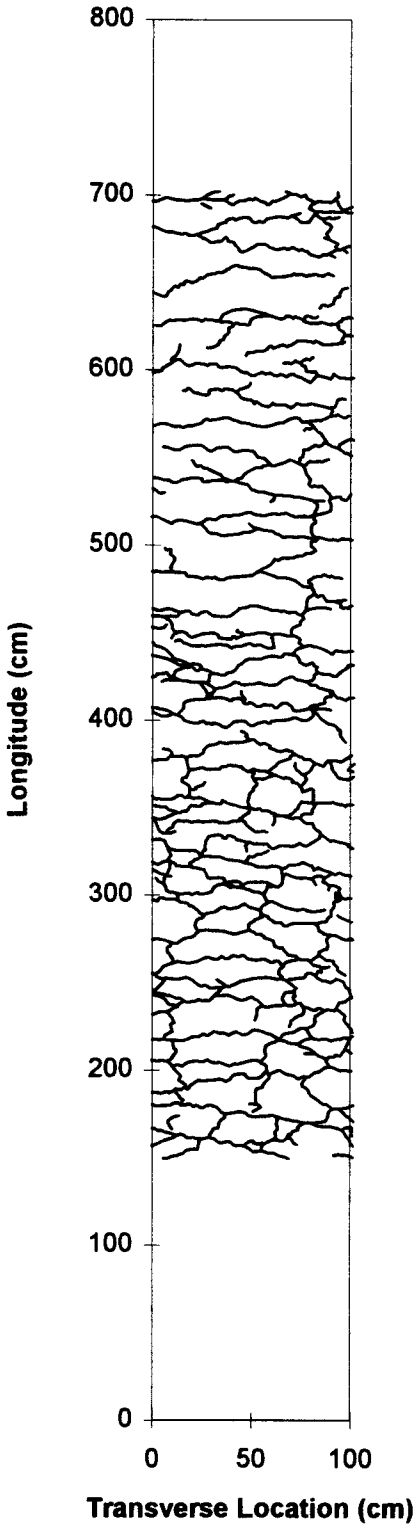

Figure 3.25c Crack schematic at 1,430,000 repetitions

traced, cracks which appear to have decreased in length, or with portions missing or undetected by the technicians performing crack monitoring, can be traced via the overlay along with the new cracks which were detected. The crack trace from this image is then used as an overlay for the next set of crack photos creating a cumulative assessment of crack progress. This process is then repeated through all the sets of crack photos until the end of the test.

It was found that all the cracks which may have "disappeared" and "reappeared" later, or which shortened and then lengthened again, were doing so in exactly the same locations and would without exception progress over the duration of the test though they may have been undetected during some crack inspections. Verification of this phenomenon is only possible through the use of digital techniques. Most often, the overlays matched successive crack photos exactly. On occasion, camera perspective could cause some uncorrectable distortion which would offset the overlays slightly. However, this offset was never more than 2 cm in the calibrated image, an error of 0.25 percent.

3.5.3 Assessment of Cracking on Section 501RF

From Figure 3.23 it can be seen that the pavement cracked much like Section 500RF. Soon after cracks were first detected at approximately 550,000 repetitions, a period of rapid crack growth ensued followed by a tapering off at about 1.2 million repetitions. Had the test been run longer, it can be assumed that new crack growth would at some time cease due to the fact that at some point, the pavement behaves more like a series of individual blocks separated by cracks from each other and rocking in place as the wheel passes over instead of a single material which is undergoing fatigue stress with every pass of the test wheel. A look at the crack schematic in Figure 3.25e provides an indication of the severity of cracking experienced on

Section 501RF during the last stages of the test. The section at this point is fairly well cracked, exhibiting the condition referred to as “alligator cracking.”

Figure 3.24 show the crack length as a distribution function. These figures illustrate that cracking was somewhat focussed in the center of the test pavement, as would be expected given the loading pattern of the HVS test wheel. However, these figures also show a slightly higher degree of cracking between Points 3 and 8 than is seen between Points 8 and 14. The crack data correlated well with RSD, MDD, and profilometer data as discussed earlier.

3.5.4 Cores Taken from Section 501RF

In the Goal 1 Interim Report *(2)* it is observed that inspection of some cores taken after construction for mix evaluation showed little or no bond between the two asphalt concrete lifts. No tack coat was placed between the lifts because it was not required by Caltrans specifications, and would not have been used in typical Caltrans practice. It is likely, however, that a tack coat would have contributed to an improved bond between the lifts.

After completion of testing of Section 501RF, a few cores were taken from observed crack locations to determine whether both asphalt concrete lifts were cracked. From the cores it was evident that the cracks went completely through the top lift and there was no evidence of cracking in the bottom asphalt concrete lift. More cores will be necessary to fully assess the cracking condition of the pavement. Further investigative coring is not possible, however, until Goal 3 testing is completed.

As is explained in Chapter 4, the absence of a tack coat and resultant weak bond between the two asphalt concrete lifts resulted in the critical horizontal tensile strain occurring

at the underside of the top asphalt concrete lift. As a result, crack formation started in this location rather than on the underside of the bottom asphalt concrete lift.

Another factor which can influence fatigue performance of asphalt concrete is the degree of compaction. In this instance, the top asphalt concrete lift exhibited an average air void content after construction of about 7.2 percent while that of the bottom lift was about 5.6 percent.

The effects of construction compaction and bonding between the asphalt conrete lifts on fatigue life and subgrade rutting are examined in Chapter 4.

CHAPTER 4

SECTION 501RF PERFORMANCE EVALUATION

At the end of the accelerated pavement testing using the Heavy Vehicle Simulator (HVS), Section 501RF had been subjected to 150,000 applications of 40 kN loading, 50,000 applications of 80 kN loading, and 1,230,000 applications of 100 kN loading. Using an exponent of 4.2 in calculating load equivalency factors according to the Caltrans procedure[3], Section 501RF experienced approximately 60,000,000 ESALs during its useful life, much greater than its design life of approximately 1,000,000 ESALs. The primary purpose of this chapter is to investigate this large difference between the predicted Caltrans design loading and the performance of the test section.

As stated in Reference *(3)*, the Caltrans flexible pavement design procedure does not identify and distinguish among various modes of pavement distress and does not enable detailed examination of many of the factors that can affect pavement performance. As a result, the methodology described in Reference *(3)* for Section 500RF will be used to analyze Section 501RF since the predominant distress mode was surface cracking due to fatigue. The surface cracking was visible throughout the test section, averaging 9.7 m in length for each square meter of area.

Some surface rutting was also observed in Section 501RF. The average rut depth at the surface was approximately 8.4 mm. MDD measurements indicated that the asphalt concrete surface layers contributed approximately 53 percent to this average followed by 26 percent for the aggregate base, 11 percent for the subbase, and 11 percent for the subgrade. As was done

---

[3]Load equivalency factor = (wheel load in kN/40)$^{4.2}$.

for Section 500RF, an examination of subgrade rutting is made herein based on the Asphalt Institute's subgrade strain criterion.

4.1 FATIGUE ANALYSIS AND DESIGN SYSTEM

The fatigue analysis and design system used herein is the same as that used to analyze Section 500RF *(3)*, and illustrated in Figure 4.1. It considers not only fundamental mix properties but also the level of design traffic, the temperature environment at the site, the pavement structural section, laboratory testing and construction variabilities, and the acceptable level of risk. It has the necessary capabilities for assessing the impact of the structural section on pavement performance in fatigue.

4.1.1 System Description

The fatigue analysis and design system is used herein to estimate the number of ESALs that can be sustained either in a design setting or in the HVS enclosure at the Richmond Field Station. The parameters used to determine ESALs has already been described in Reference *(8)*. The critical strain, determined using CIRCLY*(12)*, permitted determination of the shift factor, SF, according to the equation (Figure 4.1).

$$SF = 3.1833 \times 10^{-5}\varepsilon^{-1.3759}$$

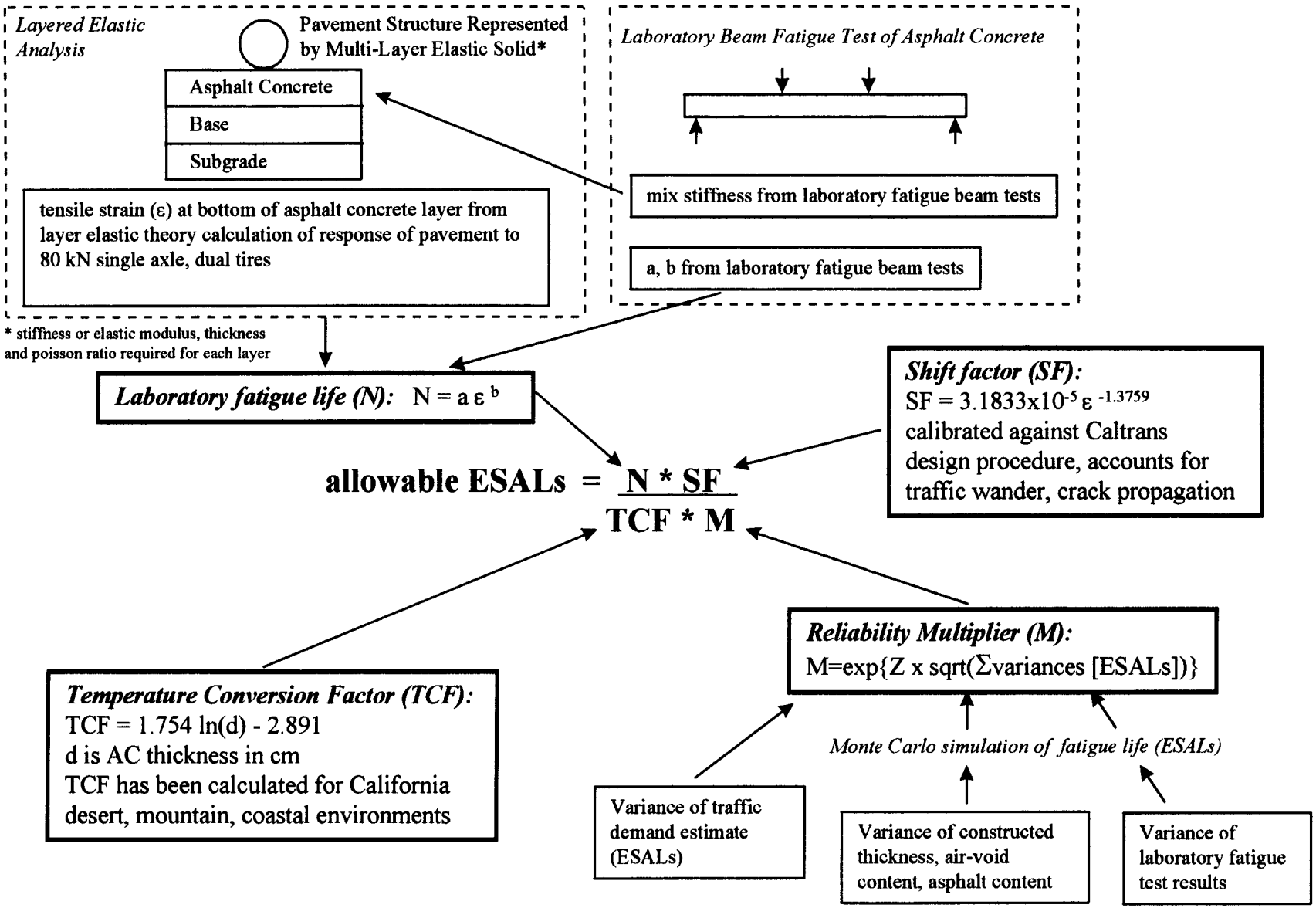

Figure 4.1 Methodology followed in the fatigue analysis system to determine ESALs

The temperature conversion factor, TCF, used for in-situ performance simulations is that derived earlier for a coastal environment *(8)* (Figure 4.1):

$$TCF = 1.754\ln(d) - 2891$$

The reliability multiplier, M, determined from the expression (Figure 4.1):

$$M = e^{z\sqrt{var(lnN) + var(lnESALs)}}$$

The factor Z varies from 0 at a design reliability of 50 percent to 2.05 at a design reliability of 98 percent *(8)*.

The variance in the logarithm of the laboratory fatigue life, var(ln N), has been calculated using a Monte Carlo simulation procedure. This procedure accounts for the inherent variability in fatigue measurements; the nature of the laboratory testing program (principally the number of test specimens and the strain levels); the extent of extrapolation necessary for estimating fatigue life at the design, in-situ strain level; mix variability due to construction (namely asphalt and air-void contents); and structural variability due to construction (namely thickness of the asphalt concrete surface and the equivalent stiffness or modulus of supporting layers). Variances for these parameters considered representative of prevailing California construction practice have been used herein *(14)*. A var(ln ESALs) of 0.3, the variance associated with uncertainty in the traffic estimate, has also been used in the calculations.

4.1.2 Important Differences Between Pavement Design and HVS Testing

Summarized in this section are some of the important factors that help to explain the difference between the Caltrans design estimate of approximately 1,000,000 ESALs and the HVS measurement of approximately 60,000,000 ESALs. Recognized and emphasized at the outset is the unknown error that results from assuming that the Caltrans design estimate is dictated primarily by the prevention of premature fatigue cracking and not other distress modes.

One fundamental difference between a pavement design estimate and the corresponding test measurement is that design must accommodate a range of mixes of varying performance characteristics and must incorporate a safety factor to prevent premature failure as a result of testing, construction, and traffic variability. A direct measurement in the HVS test, on the other hand, reflects the performance characteristics of a specific mix, it is independent of laboratory testing and traffic variability; and, because the test section is limited to a relatively small area, 1 m. × 8 m. in plan, the influence of construction variability is minimal. The design estimate is always expected to be much smaller in magnitude than the test measurement with the difference between the two increasing as the design reliability increases. The fatigue design and analysis system has the ability to distinguish between design estimates and test measurements and to assess the impact of reliability on design estimates. No reliability factor is associated with simulations of HVS test ESALs for the reasons described above.

The next type of difference between design and testing relates primarily to pavement structural effects. In the current case, four notable differences distinguished Section 501RF from its design scenario including a top asphalt concrete lift thickness of 63 mm instead of 61 mm, a bottom asphalt concrete lift thickness of 88 mm instead of 76 mm, a thickness of subbase of 215 mm instead of 229 mm, a distinct difference in the air voids within the two

asphalt concrete lifts instead of uniform air voids, and a largely unbonded interface between the lifts instead of a fully bonded one *(2)*.

Important differences are also found between the standard mix used for calibrating the fatigue analysis and design system and that used in HVS Section 501RF. Asphalt and air-void contents for the standard mix were set at 5 and 8 percent, respectively representing the approximate asphalt content found from the Caltrans mix design procedure and relative compaction of about 97.3 percent. The asphalt content for the mix used in Section 501RF averaged 4.8 percent, also based on the Caltrans procedure. Air-void contents averaged 7.2 percent in the upper lift and 5.6 percent in the lower lift corresponding to about 96.7 percent and 98.3 percent relative compaction respectively for mix.

In addition to differences in degree of compaction, there were other differences between the standard mix and the mix used in the HVS test section. That is:

1. The aggregates for the two mixes came from different sources and did not have the exactly same gradations, although both constructed gradations met Caltrans's standard specifications for 19 mm coarse Type A mixes;
2. The asphalt binders in both mixes were identified as being from California Valley sources and exhibited similar rheological and aging behavior in laboratory tests performed at TransLab *(15)*. However, the binders were produced 6 years apart and not necessarily at the same refinery or using the same processes; and
3. Laboratory test results for the mix from the HVS test were obtained from beams cut from the test pavement soon after construction, while laboratory test results

for the standard mix were obtained from laboratory mixed and compacted specimens.

In all likelihood, however, specimen compaction is not a source of the differences; comparison of laboratory test results on beam sawed from the test pavement and obtained by laboratory rolling wheel compaction exhibited little difference in stiffness and fatigue properties *(2)*. Moreover large differences in mix properties caused by laboratory mixing and short-term oven aging (STOA) versus plant mixing are also considered unlikely at this time although they have only been evaluated in terms of mix and binder stiffness and not in terms of fatigue properties. More data will be obtained from future CAL/APT test pavements to compare differences in fatigue properties between laboratory mixed and plant–mixed, laboratory compacted specimens.

As reported elsewhere *(10)*, laboratory testing of the standard mix yielded the following expressions:

$$\ln N = -22.0012 - 0.164566AV + 0.575199AC - 3.71763 \ln \varepsilon$$

and

$$\ln S = 10.282 - 0.076AV - 0.172AC$$

where N = laboratory fatigue life in a third-point loading controlled-strain flexural test,

AV = air-void content in percent,

AC = asphalt content in percent,

ε = flexural strain, and

S = laboratory flexural stiffness in mPa.

For the HVS mix *(2)*, the following expressions were obtained at the 4.8 percent asphalt content:

$$\ln N = -21.9252 - 0.106663AV - 4.14248 \ln \varepsilon$$

and

$$\ln S = 9.5603 - 0.084914AV$$

where S is again expressed in mPa.

Based on these results, the laboratory determined fatigue life of the HVS mix is two to eight times that of the standard mix, depending on strain level, while its stiffness is only 1 to 8 percent larger. Thus, the HVS mix is expected to exhibit improved performance over the standard mix.

These results emphasize the importance of laboratory fatigue testing to assess fatigue performance to insure a realistic estimate of pavement performance and in particular, in insuring proper interpretation of the HVS test results.

Environmental differences also distinguish the HVS test conditions from specific field pavement sites. These include the effects of temperature and moisture differences.

In the 500RF report *(3)*, for example, it was demonstrated that during the period of the test (May to November), the temperature environment of the HVS was slightly more severe than the coastal environment, i.e. the predicted ESALs for the HVS site were about 85 percent of the number that could be sustained in situ.

The second major environmental difference is due to the effects of moisture. The protected HVS environment limits the amount of moisture in the pavement and practically eliminates cyclic wetting and drying. The net effect is expected to be beneficial. Moisture effects are simulated in this analysis by assuming that effective moduli of all supporting layers

(aggregate base, aggregate subbase, and subgrade) under natural conditions are 80 percent of those in Section 501RF. It must be emphasized that the 80 percent is an assumed quantity used for illustration purposes only. It is not a result of detailed scientific inquiry.

Quantification of the effects of these differences, using the fatigue analysis and design system, is the objective of the next section.

4.1.3 General Performance Analysis

For this analysis, the computer code, CIRCLY, was used in computing critical strain levels. The applied load consisted of a 40 kN (9,000-pound) wheel load distributed on dual tires (305 mm [12.0 inches] center-to-center) with a contact pressure of 690 kPa (100 psi). A distinction was made between Section 501RF *design conditions* and the as-built and as-tested *HVS conditions* with respect to layer thicknesses and environmental influences. Quantitatively the differences are as follows in Table 4.2.

Table 4.1 Comparison of Section 501RF design conditions and HVS conditions

	Design conditions	HVS conditions
Thickness of upper asphalt concrete lift (mm)	61	63
Thickness of bottom asphalt concrete lift (mm)	88	76
Thickness of aggregate subbase (mm)	229	215
Moduli of supporting layers (MPa) Aggregate Base Aggregate Subbase Subgrade	240 120 56	300 150 70

Further distinction was made between a *standard mix* and the *HVS mix*. The standard mix was that used in calibrating the fatigue analysis and design system. Components included a Watsonville granite and an AR-4000, apparently from California valley sources. Asphalt and

air-void contents were assumed to be 5 and 8 percent respectively. The HVS test utilized a different aggregate but the grading was similar to that of the standard mix; both gradings conformed to the Caltrans specifications for the Type A, 19-mm-maximum size, coarse gradation. The asphalt was an AR-4000 from California Valley sources, and the asphalt content of the mix was 4.8 percent. Air voids averaged 7.2 percent in the upper lift and 5.6 percent in the lower lift.

The temperature environment was essentially ignored for the General Performance Analysis, with a constant temperature of 20°C assumed for both design conditions and HVS conditions. This assumption results in a TCF of 1.00 because the laboratory test temperature is 20°C. A preliminary comparison of the temperature environments at the HVS site and for the California Coastal environment is included in this chapter.

Five different cases, defined as follows, were analyzed as shown in Table 4.2:

Table 4.2 Definition of five cases

Case	Description	Critical strain location
1	Design conditions with standard mix (8% air void content and 5% asphalt content); full friction interface	Bottom of lower lift
2	HVS conditions with standard mix (8% air void content and 5% asphalt content); full friction interface	Bottom of lower lift
3	HVS conditions with standard mix (4.4% air void content bottom lift, 7.2% air void content top lift and 5% asphalt content); full friction interface	Bottom of lower lift
4	HVS conditions with HVS mix (5.6% air void content bottom lift, 7.2% air void content top lift and 4.8% asphalt content); full friction interface	Bottom of lower lift
5	HVS conditions with HVS mix (5.6% air void content bottom lift, 7.2% air void content top lift and 4.8% asphalt content); frictionless interface	Bottom of upper lift

Elastic parameters used in the CIRCLY computations are identified in Table 4.3. These represent the best estimates of the stiffnesses of the pavement components based on laboratory determined and in-situ measured response characteristics, the latter having been computed from FWD measurements *(2)*.

Table 4.3 Elastic parameters for CIRCLY analyses

Layer	Case				
	1	2	3	4	5
Modulus (MPa)					
Upper Asphalt	6,729	6,729	7,150	7,700	7,700
Lower Asphalt Concrete lift	6,729	6,729	8,071	8,820	8,820
Aggregate Base	240	300	300	300	300
Aggregate Subbase	120	150	150	150	150
Subgrade	56	70	70	70	70
Poisson's ratio					
Upper Asphalt Concrete lift	0.35	0.35	0.35	0.35	0.35
Lower Asphalt Concrete lift	0.35	0.35	0.35	0.35	0.35
Aggregate Base	0.35	0.35	0.35	0.35	0.35
Aggregate Subbase	0.35	0.35	0.35	0.35	0.35
Subgrade	0.45	0.45	0.45	0.45	0.45
Thickness (mm)					
Upper Asphalt Concrete lift	61	63	63	63	63
Lower Asphalt Concrete lift	76	88	88	88	88
Aggregate Base	274	274	274	274	274
Aggregate Subbase	229	215	215	215	215
Subgrade	Semi-infinite	Semi-infinite	Semi-infinite	Semi-infinite	Semi-infinite

The first matter to be addressed includes both the effect of reliability on estimates of design ESALs as well as the fundamental difference between design ESALs (whether from the Caltrans or UCB-ISAP procedures *(14)*),and HVS ESALs (whether measured under HVS loading or simulated using the UCB-ISAP system). In computing HVS ESALs, variances of the several parameters (asphalt content, air-void content, asphalt concrete thickness, foundation support, and traffic) were assumed to be negligible. Computations using the UCB-ISAP system for Case 1 conditions yield the following ESAL estimates:

Table 4.4 Simulated HVS ESALs for Case 1

Simulated HVS ESALs	UCB-ISAP Design ESALs for reliability of:			
	80%	90%	95%	98%
2,446,000	1,030,000	656,000	453,000	297,000

This table shows the influence of reliability on design ESALs, the 2,446,000 simulated HVS ESALs is considerably greater than any of the design ESALs: for a design reliability level of 90 percent, the computed ratio of simulated HVS ESALs to UCB-ISAP design ESALs is approximately 3.7.

The 90 percent design reliability estimate, assuming a constant 20°C asphalt concrete temperature, is 656,000 ESALs, less than the Caltrans design estimate of 1,000,000 ESALs. The UCB-ISAP fatigue analysis and design system estimate of 1,030,000 ESALs at 80 percent reliability is nearly the same as the Caltrans design estimate, again assuming a 20°C asphalt concrete temperature. The preliminary UCB-ISAP design estimates for the California coastal environment are presented later in this chapter.

Next, in order to demonstrate the significant difference between as-built and as-tested HVS conditions and the assumed Caltrans design conditions, the simulated HVS ESALs estimate for Case 2 was compared with that for Case 1. Results in Table 4.5:

Table 4.5 Comparison of simulated HVS ESALs—Case 1 to Case 2

Simulated HVS ESALs for:	
Case 1	Case 2
Design conditions with standard mix (8% air void content and 5% asphalt content): full friction interface	HVS conditions with standard mix (8% air void content and 5% asphalt content): full friction interface
2,446,000	4,760,000

The ratio of HVS ESALs for HVS conditions to that for design conditions is approximately 1.9. The enhanced simulated performance for the HVS environment stems from a combination of thickness differences and the effect of moisture.

To demonstrate the effect of the excellent mix compaction achieved in the construction of Section 501RF, particularly of the lower lift, the simulated HVS ESALs estimate for Case 3 was compared with that for Case 2, Table 4.6:

Table 4.6 Comparison of simulated HVS ESALs—Case 2 to Case 3

Simulated HVS ESALs for:	
Case 2	Case 3
HVS conditions with standard mix (8% air void content and 5% asphalt content): full friction interface	HVS conditions with standard mix (5.6% air void content bottom lift, 7.2% air void content top lift and 5% asphalt content): full friction interface
4,760,000	11,734,000

The very significant effect of air-void content is illustrated by a ratio of approximately 2.5 in the HVS ESALs estimate for a 5.6 percent bottom lift and 7.2 percent top lift compared to that for an 8-percent mix in both lifts. This finding emphasizes the importance of good construction practice and the potential impact of improved compaction above that required in current Caltrans specifications typically require. An even larger improvement in simulated fatigue life than that shown here would have been observed if the 5.6 percent air-void content had been obtained in both lifts. These corroborate similar findings for a variety of typical Caltrans pavement structures reported previously *(8)*.

To demonstrate the effect of the superior fatigue performance of the HVS mix compared to the standard mix, the simulated HVS ESALs estimate for Case 4 was compared with that for Case 3. Results are in Table 4.7:

Table 4.7 Comparison of simulated HVS ESALs—Case 3 to Case 4

Simulated HVS ESALs for:	
Case 3	Case 4
HVS conditions with standard mix (5.6% air void content bottom lift, 7.2% air void content top lift and 5% asphalt content): full friction interface	HVS conditions with HVS mix (5.6% air void content bottom lift, 7.2% air void content top lift and 4.8% asphalt content): full friction interface
11,734,000	66,013,000

The ratio of Simulated HVS ESALs for these two conditions is approximately 5.6. This large difference is not clearly attributable to any one particular component of the two mixes, and is likely due to a combination of potential differences in components including asphalt production and aggregate type and gradation.

It should be noted that the Simulated HVS ESALs for Case 4 (66,013,000) exceeds the measured number of 60,000,000 HVS ESALs (assuming a 4.2 exponent for load equivalency).

A part of this difference may well be due to imprecision of the fatigue analysis and design system, to inappropriate assumptions made for this analysis, and/or to important factors not yet identified and accounted for.

One such factor relates to the lack of bonding at the interface between upper and lower asphalt concrete lifts. CIRCLY allows an examination of the interface condition but, unfortunately, only at the two extremes, full-friction and frictionless interfaces. The interface condition of Section 501RF is likely somewhere between these two extremes: the interface is rough (but unbounded) and the weight of the upper layer combined with vertical compressive stress beneath the load should allow some transfer of stress across the surface. Even though partial friction conditions can not be modeled with available techniques, the notable effect of interface condition can be demonstrated by comparing the HVS ESALs estimate for Case 5 with that for Case 4. Results are shown in Table 4.8:

Table 4.8 Comparison of simulated HVS ESALs—Case 4 to Case 5

Simulated HVS ESALs for:	
Case 4	Case 5
HVS conditions with HVS mix (5.6% air void content bottom lift, 7.2% air void content top lift, and 4.8% asphalt content): full friction interface	HVS conditions with HVS mix (5.6% air void content bottom lift, 7.2% air void content top lift, and 4.8% asphalt content): frictionless interface
66,013,000	6,567,000

This remarkably large effect is due to two factors, one of which is the nature of friction at the interface between lifts. The other results from a shift in the critical strain location from the bottom of the lower lift for the full friction interface to the bottom of the upper lift for the frictionless interface. In the upper lift, the air-void content is greater and load repetitions necessary to propagate cracks to the top surface are expected to be smaller because of the

reduced thickness through which the cracks must penetrate. The combined effect of a larger air-voids content and a reduced overlying thickness results in a significant decrease in simulated fatigue life.

Although this analysis is not definitive because the interface condition cannot be accurately modeled, the estimate of 66,013,000 ESALs seems to be realistically in line with the measurement of 60,000,000 ESALs under HVS loading following qualitative evaluation of interface conditions discussed in Chapter 3. The simulation results indicating that cracking would occur in the upper lift before it occurred in the lower lift for the frictionless interface condition corroborate the cracking observations from Section 501RF cores. Certainly the analysis reported herein is of significant help in reconciling the difference between the Caltrans design estimate of 1,000,000 ESALs and the HVS test measurement of 60,000,000 ESALs. In addition the analysis has highlighted factors such as mix, air-void content and interface condition that can have a significant impact on pavement performance.

4.1.4 Preliminary Estimate of Design ESALs for California Coastal Environment

In Reference *(3)*—the 500RF report—pavement performance in the HVS test was observed during the period May to November 1995. By comparing the performance with that for comparable periods of time in three regions of California for which Temperature Conversion Factors (TCF) had been determined *(8)*, it was demonstrated that the test conducted at the HVS site was more damaging than for comparable traffic conditions at the three in-service sites.

For this report , it was decided to examine an alternative approach and compare, on an annual basis, the performance of the pavement at a constant temperature of 20°C at the HVS site with the variable temperature regime for the California Coastal environment. For Case 1

of the General Performance Analysis (standard mix, design conditions, 8 percent air-voids content, 5 percent asphalt content) the TCF computed for the California Coastal environment is 1.702. The TCF for that case is 1.702. Assuming that the hypothetical mix has temperature susceptibility similar to that of the standard mix, application of the 501RF TCF to Case 1 of the General Performance Analysis results in the following estimates shown in Table 4.9.

Table 4.9 Estimates of design ESALs applying 501RF TCF to Case 1

Simulated HVS ESALs	UCB-ISAP Design ESALs for reliabilities of:			
	80%	90%	95%	98%
1,437,000	605,386	386,000	266,000	175,000

It can be seen that with this assumption the estimated fatigue life for the 90 percent reliability is considerably less than the Caltrans design estimate of 1,000,000 ESALs. The estimated reliability of the Case 1 pavement is 64 percent, indicating a 36 percent probability that the pavement would fail in fatigue cracking before carrying 1,000,000 ESALs. The same analysis applied to Section 500RF indicated a higher level of reliability, i.e. about 90 percent for 1,000,000 ESALs.

4.2 SUBGRADE RUTTING

The Caltrans pavement design procedure is intended to prevent premature failure from subgrade rutting as well as fatigue cracking. The average rut depth at the surface of Section 501RF at the termination of HVS trafficking was approximately 8.4 mm. MDD measurements indicated that about 37 percent, or 3.1 mm, occurred in the base and subbase layers, and about 11 percent, or 0.9 mm, occurred in the subgrade. A comprehensive

procedure for evaluating the potential for rutting in the underlying layers including reliability (like that for fatigue) has not been developed as yet. A cursory evaluation of the Section 501RF pavement with respect to rutting in the underlying layers was performed using criteria developed by the Asphalt Institute for vertical compressive strain at the top of the subgrade to minimize rutting. The subgrade rutting evaluation was performed for the five cases of mix type, site conditions and construction included in the fatigue evaluation.

4.2.1 Subgrade Rutting Criteria

The Asphalt Institute criterion for subgrade strain is:

$$N = 1.05 * 10^{-9} \varepsilon_c^{-4.484}$$

where N = number of load applications, and

ε_c = vertical compressive strain at subgrade surface.

The equation is based on that used by Santucci *(15, 16)* and is based on analyses of pavements designed according to the Caltrans design procedure *(15)*. The authors of the Asphalt Institute methodology using this subgrade stain relation state, "*if good compaction of the pavement components is obtained and the asphalt mix is well designed, rutting should not exceed about 12.7 mm (0.5 in.) at the surface for the design traffic, N.*"

This statement implies some conservatism in the criteria; however it does not include an explicit factor of safety or reliability estimate.

The vertical compressive strain at the top of the subgrade was calculated using the program CIRCLY, for the 40 kN (9,000 lb) dual tire wheel load (305 mm [12.0 in.] center-to-center) and 690 kPa (100 psi) contact pressure, and the pavement structures shown earlier. The difference in thermal environment between the design conditions and HVS

conditions was not addressed in this study. The asphalt concrete stiffness included in the subgrade strain computations is that at 20°C, approximately the temperature maintained at the surface of the Section 501RF pavement. A temperature sensitivity study of the type used to estimate the effects on fatigue life of in-situ temperatures for typical California environments has not been performed for subgrade rutting.

4.2.2 Subgrade Rutting Performance Analysis

The permissible ESALs for the calculated subgrade strain for each of the five cases are compared with the simulated HVS ESALs to fatigue failure in Table 4.10.

Table 4.10 Comparison of permissible ESALs for subgrade strain to simulate HVS ESALs to fatigue failure for five cases

Case	Permissible ESALs by Asphalt Institute Subgrade Strain Criteria	Simulated HVS ESALs to Fatigue Failure
Design conditions with standard mix (8% air void content and 5% asphalt content), full friction interface (Case 1)	14,614,000	2,446,000
HVS conditions with standard mix (8% air void content and 5% asphalt content), full friction interface (Case 2)	36,298,000	4,760,000
HVS conditions with standard mix (5.6% air void content bottom lift, 7.2% air void content top lift and 5% asphalt content), full friction interface (Case 3)	41,390,000	11,734,000
HVS conditions with HVS mix (5.6% air void content bottom lift, 7.2% air void content top lift and 5% asphalt content), full friction interface (Case 4)	45,764,000	66,013,000
HVS conditions with HVS mix (5.6% air void content bottom lift, 7.2% air void content top lift and 5% asphalt content), frictionless interface (Case 5)	9,044,000	6,567,000

The permissible ESALs for subgrade rutting for Case 1 are almost six times greater than the simulated HVS ESALs to fatigue cracking for the same case. This indicates that

fatigue cracking is probably the dominant failure mode for Section 501RF for the design conditions and standard mix, which is the most critical case when a full friction interface between the asphalt concrete layers is assumed.

Comparison of the permissible ESALs for Cases 1 and 2 indicates that the HVS conditions were less critical than the design conditions with respect to subgrade rutting. The differences between the HVS and design conditions for the subgrade strain criteria evaluation consisted of the thicker asphalt concrete layer, slightly thinner aggregate subbase layer, and increased base, subbase and subgrade moduli of the HVS conditions. As for Case 1, fatigue appears to be the dominant failure mode for Case 2, since the permissible ESALs for subgrade strain are approximately 7.6 times greater than the simulated HVS ESALs to fatigue failure.

The beneficial effect of increased compaction of the asphalt concrete on subgrade rutting can be seen from comparison of the results for Case 3 versus Case 2. Reduction of the air-void content in the standard mix from 8 percent to the air-void contents obtained in the Section 501RF pavement increases the permissible ESALs for subgrade rutting by about 14 percent. The increase is the result of the greater protection provided to the subgrade by the increased stiffness of the asphalt concrete at the smaller air-void contents.

Comparison of Case 4 with Case 3 shows that substitution of the HVS mix for the standard mix results in a further 11 percent increase in permissible ESALs for subgrade rutting, due to the larger stiffness of the HVS mix. Despite the increase in permissible ESALs for subgrade rutting, subgrade rutting becomes the presumed dominant failure mode for Case 4 due to the large difference in fatigue resistance between the HVS mix and the standard mix.

Simulation of a frictionless interface between the two asphalt concrete layers results in a significant reduction in the estimate of permissible ESALs for subgrade rutting, as can be seen

from comparison of Case 5 with Case 4. The permissible ESALs for the frictionless interface condition are about 5.1 times less than for the full friction condition. The difference is due to reduction of the ability of the pavement to distribute stresses within the asphalt concrete layer because of the frictionless interface, resulting in increased vertical compressive strain in all underlying layers. The actual interface condition lies in between the full friction and frictionless cases simulated; however, the estimates of permissible ESALs indicate that a reduction in the bonding between the asphalt concrete layers results in increased compressive strains and subgrade rutting in the underlying layers, as well as reduced asphalt concrete fatigue life.

All of the estimates of permissible ESALs for subgrade rutting are less than the 60,000,000 HVS ESALs applied to the section, which suggests that there is some conservatism in the Asphalt Institute criteria. However, it should be noted that the life estimate for Case 4 was very close to the actual ESALs applied. The permissible ESALs estimated from the Asphalt Institute criteria should be considered design estimates which will be lower than measured performance, although the safety factor is unknown.

For all cases, except Case 4, the simulated HVS ESALs to fatigue failure is less than the permissible ESALs for subgrade rutting based on the Asphalt Institute criteria, which strongly indicates that fatigue is the dominant distress mode for the Section 501RF pavement. This is validated by comparison of the 60,000,000 HVS ESALs applied to Section 501RF with the average rut depth in the combined base, subbase and subgrade layers of about 4.0 mm (0.16 in.), and the average maximum rut depth in the combined untreated layers of about 5.0 mm (0.20 in.). The majority of the rutting on Section 501RF occurred in the asphalt concrete layers.

In addition, the results presented in this study provide a strong indication that the air-void content of the asphalt concrete surface and the interface condition between asphalt concrete layers can significantly impact subgrade rutting performance.

4.3 FINDINGS

In general, the analyses reported herein found a rather good correspondence between the Caltrans design estimate of approximately 1,000,000 ESALs and the HVS test measurement of approximately 60,000,000 ESALs. The major impediment to reconciling these two estimates seems to be the inability to accurately quantify effects of the layer interface condition. The following findings of this aspect of the study are considered to have been reasonably well demonstrated and to represent appropriate hypotheses for future inquiry and validation:

1. Fatigue life measurements under full-scale accelerated loading are typically expected to exceed design estimates because design estimates must incorporate a safety factor to minimize the risk of premature failure while accommodating, at the same time, expected variability in testing, in construction, in traffic, and in mix design. For a design reliability level of 90 percent, the computed ratio of simulated HVS ESALs to design ESALs estimated using the fatigue analysis and design system was approximately 3.7.

2. The mixture fatigue analysis and design system proved to be an effective tool for explaining fatigue performance of the HVS pavement. The relatively good agreement between the simulation estimate and actual HVS measurement suggests that the analysis and design system may eventually prove useful for structural design as well as for mixture design.

3. According to the Asphalt Institute's subgrade strain criterion, severe subgrade rutting in the HVS pavement would not be expected. Testing of HVS Section 501RF generally confirmed this.

4. The analysis reported herein corroborates prior work showing the importance of good compaction of the asphalt concrete surface to superior fatigue performance. Good compaction of the mix also reduces the magnitude of subgrade rutting.

5. Loss of bonding at the interface between asphalt-concrete lifts can cause a significant degradation in fatigue life and an increase in subgrade rutting.

6. Different mixes, even with similar binders, can result in significantly different fatigue performance. The importance and effectiveness of laboratory fatigue testing and simulation to quantitatively estimate differences in fatigue performance in situ was demonstrated by the analyses presented in this chapter.

CHAPTER 5

SUMMARY AND CONCLUSIONS

5.1 SUMMARY

This report, the third in a series detailing the results of the CAL/APT program being performed jointly by UCB and Caltrans, describes the results of the second HVS test conducted by the UCB staff on the second of four pavement test sections—501RF, an asphalt concrete section containing only an aggregate base. Also included are: initial analyses of the test section; analyses of the performance of the test section; preliminary comparison of its performance relative to the performance of comparable pavements in the coastal climatic region of California; evaluation of the effect of air-void content on its performance, and implications of these results relative to current Caltrans pavement construction requirements since the test pavements were constructed according to Caltrans's specifications.

HVS trafficking of Section 501RF commenced in November 1996 and was completed in February 1996. A total of 1.43×10^6 load repetitions were applied during this period consisting of 150,000 repetitions of a 40 kN (9000 lb) half axle load, 50,000 repetitions of an 80 kN (18,000 lb) load, and the remainder with a 100 kN (22,500 lb) load.

The first load associated (fatigue) cracks were observed at approximately 550,000 load repetitions. At 1.43×10^6 load repetitions cracking had reached a level which, according to Caltrans pavement management criteria, resembled a newer pavement that had failed by alligator cracking. The average maximum vertical rut depth at the centerline of the test section at this time was 10.5 mm, a significant rut but less than the Caltrans failure criteria of 12.5 mm.

It was noted that the cracks were hairline (less than 1/32 inch) and pumping was not observed in contrast to typical field sections.

Thicknesses for the pavement sections were selected on the basis of a Traffic Index of 9 (800,000 to 1,200,000 ESALs) and a design "R" value for the subgrade of 10 (measured range—4 to 30) *(2)*. The number of ESALs actually carried according to the Caltrans conversion [(actual axle load/18000)$^{4.2}$] is 60 million, which corresponds to a Traffic Index of 14.7.

When the construction of the test pavements had been completed (April 1995), cores and slabs of the asphalt concrete were taken from the pavement for testing. As with 500RF, weakness in the bond (and even a lack thereof) between the two asphalt concrete lifts was observed. At the conclusion of the loading on the test section, a number of cores were taken to check changes in densities of the lifts. When these cores were removed it was noted the two lifts were unbonded and that there was evidence of movement between the lifts resulting from the deflection of the pavement under load. Also, it was observed that the cracking observed at the surface existed only in the top lift; the lower lift was uncracked.

Measurements of densities on cores from the trafficked portion of the pavement indicated that traffic compaction was limited, and probably occurred primarily in the upper lift of the asphalt concrete. In this lift the air void content was reduced by about 0.3 percent (from about 7.2 percent to 6.9 percent).

5.2 CONCLUSIONS

From the results of tests on Section 500RF and associated analyses, the following conclusions appear warranted.

1. The fatigue analysis and design system developed during the SHRP program and refined within the CAL/APT program has been used to explain the difference between the design estimate for Section 501RF of approximately 1×10^6 ESALs and the HVS measurement of approximately 60×10^6 ESALs. Although some of the discrepancy remains unaccounted for (possibly as a result of difficulties in modeling the bonding between the two lifts of asphalt concrete), the overall agreement helps to validate both the analysis and design system as a mechanism for structural design and the current Caltrans design methodology.

2. As with Section 500RF, results of this HVS test suggest that the Asphalt Institute's subgrade strain criterion for controlling subgrade rutting would be a reasonable design parameter. Accordingly, this criterion is suitable for use in mechanistic/empirical analyses of subgrade rutting to supplement routine Caltrans design procedures in special investigations.

3. Results of the 501RF test suggest that the Caltrans structural design procedure may not be sufficiently conservative for pavements with aggregate base, typical compaction, and certain asphalt concrete mixes. The analysis and design system used herein and being refined, in part, through the CAL/APT program, should provide an improved methodology for structural pavement design permitting a higher level of reliability to be obtained for pavements of this type.

4. The recommendations regarding mix compaction and tack coat application resulting from the 500RF test are supported by the results on test 501RF.

REFERENCES

1. California Department of Transportation, *CAL/APT Strategic Plan (July 1995-July 1997)*, adopted by the CAL/APT Steering Committee, May 18, 1995.

2. Harvey, J., L. Du Plessis, F. Long, S. Shatnawi, C. Scheffy, B-W. Tsai, I. Guada, D. Hung, N. Coetzee, M. Riemer, and C. Monismith, *Initial CAL/APT Program: Site Information, Test Pavements Construction, Pavement Materials Characteristics, Initial CAL/HVS Test Results, and Performance Estimates*, Interim Report No. RTA–65W4845–1 for the California Department of Transportation, Institute of Transportation Studies, University of California, Berkeley, April 1996.

3. Harvey, J., L. du Plessis, F. Long, J. Deacon, I. Guada, D. Hung, and C. Scheffy, *CAL/APT Program: Test Results from Accelerated Pavement Test on Pavement Structure Containing Asphalt Treated Permeable Base (ATPB) — Section 500RF*, Report No. RTA–65W4845–3 for the California Department of Transportation, Institute of Transportation Studies, University of California, Berkeley, June 1997.

4. Harvey, J., B. Tsai, F. Long, D. Hung, and C. Monismith, *CAL/APT PROGRAM — Asphalt Treated Permeable Base (ATPB), Laboratory Testing, Performance, Predictions, and Evaluation of the Experience of Caltrans and Other Agencies,* Draft Report for the California Department of Transportation, Institute of Transportation Studies, University of California, Berkeley, June 1997.

5. California Department of Transportation, *Highway Design Manual*, Section 600, Sacramento, 1991.

6. University of California at Berkeley, Institute of Transportation Studies, Pavement Research Center; Division of Roads and Transportation Technology, CSIR, South Africa; and Dynatest, Inc., Test Plan for CAL/APT Goal 3, Prepared for the California Department of Transportation, Institute of Transportation Studies, University of California, Berkeley, March 1997.

7. Transportek, CSIR, *Guideline to the Use and Operation of the Heavy Vehicle Simulator (HVS)*, March 1995.

8. Harvey, J., J. Deacon, B. Tsai, and C. Monismith, *Fatigue Performance of Asphalt Concrete Mixes and Its Relationship to Asphalt Concrete Pavement Performance in California,* Report No. RTA-65W485-2 for the California Department of Transportation, Institute of Transportation Studies, University of California, Berkeley, January 1996.

9. Deacon, J., J. Coplantz, A. Tayebali, and C. Monismith, “Temperature Considerations in the Asphalt-Aggregate Mixture Analysis and Design,” Transportation Research Record 1454, Transportation Research Board, 1994, pp. 97-112.

10. Sousa, J.B., J. Deacon, S. Weissman, J. Harvey, C. Monismith, R. Leahy, G. Paulsen, and J. Coplantz, *Permanent Deformation Response of Asphalt-Aggregate Mixes*, Strategic Highway Research Program Report No. A–414, National Research Council, Washington, D.C., 1994.

11. Optimas Corporation, *Optimas Program Version 5.2*, Bothell, Washington, November 1995.

12. Wardle, L.J., *Program CIRCLY, User’s Manual, Revision 1*, Geomechanics Computer Program No. 2, Division of Applied Geomechanics, Commonwealth Scientific and Industrial Research Organization, Melbourne, Australia, 1976.

13. Reese, R., Faxed results of comparison of Valley binders aging properties with CAL/APT Goal 1 asphalt-concrete properties. Caltrans Engineering Service Center, Sacramento, October 6, 1995.

14. Harvey, J.T., J.A. Deacon, A.A. Tayebali, R.B. Leahy, and C.L. Monismith, *A Reliability-Based Mix Design and Analysis System for Mitigating Fatigue Distress*, Accepted for presentation and publication by the International Society for Asphalt Pavements, 8th International Conference, Seattle, 10–14 August 1997.

15. Santucci, L.E., "Thickness Design Procedure for Asphalt and Emulsified Asphalt Mixes," *Proceedings*, Fourth International Conference on the Structural Design of Asphalt Pavements, University of Michigan, August 1977, pp. 424-456.

16. Shook, J.F., F.N. Finn, M.W. Witczak, and C.L. Monismith, "Thickness Design of Asphalt Pavements — The Asphalt Institute Method," *Proceedings*, Fifth International Conference on the Structural Design of Asphalt Pavements, University of Michigan, August 1982, pp. 17–44.